M-Pos82 **HOW DO PROTONS CROSS THE MEMBRANE-SOLUTION INTERFACE?** John Kasianowicz, Roland Benz and Stuart McLaughlin. Dept. of Physiology and Biophysics, HSC, Stony Brook, NY 11794.

Using a combination of steady state and kinetic (voltage clamp and charge pulse) measurements, we determined that the potent uncoupler S-13 transports protons across the interior of a lipid bilayer membrane by a mechanism similar to FCCP (Benz and McLaughlin, Biophys. J. 41:381-398). We used S-13 to question how protons cross the membrane-solution interface. We assume that protons can be transferred to adsorbed S-13 anions by three mechanisms: 1) a proton in the aqueous phase combines with an adsorbed anion with a rate constant k_R, 2) a buffer molecule in the aqueous phase collides with and transfers a proton to an adsorbed anion, 3) a water molecule donates a proton to an adsorbed anion. Steady state conductance and kinetic experiments demonstrate that the first mechanism cannot account for the voltage-induced flux of protons unless $k_R > 10^{13} M^{-1} s^{-1}$. This value of k_R requires an anomalously large value for the diffusion coefficient of protons in the water adjacent to the bilayer surface. However, Nachliel and Gutman demonstrated that the diffusion coefficient of protons is not anomalously large adjacent to surfaces (Eur. J. Biochem. 143:83-88). To test the second mechanism, we formed membranes from negative lipid and used triphosphate as a buffer. The concentration of this buffer adjacent to the membrane is < 1μM when the bulk aqueous concentration is 1mM. The kinetic parameters did not depend on the concentration of buffer at the membrane-solution interface, which rules out the second mechanism. A simple analysis illustrates that protolysis of water molecules could deliver most of the protons that combine with the anions adsorbed at the membrane-solution interface. Supported by NSF grant PCM 8340253 (S.McL.),by Deutsche Forschungsgemeinschaft grant Be865/3-3 and NATO grant 264/82 (R.B.).

M-Pos83 USE OF $^{14}CO_2$ RATIOS TO ANALYZE ENERGY METABOLISM IN AS-30D HEPATOMA CELLS. J.K. Kelleher, B.M. Bryan III, R.T. Mallet, A.N. Murphy, and G. Fiskum. Departments of Physiology and Biochemistry The George Washington University Medical Center Washington, DC 20037

In metabolic and isotopic steady state the $^{14}CO_2$ production rate from different tracers of the same metabolite indicates the pattern of cellular oxidative metabolism. Specifically, the ratio of $^{14}CO_2$ production with [1,4-^{14}C]succinate as substrate to $^{14}CO_2$ production with [2,3-^{14}C]succinate as substrate indicates the entry of carbon other than acetyl CoA into the TCA cycle. Comparison of this ratio with the ratio of $^{14}CO_2$ production from [2-^{14}C]pyruvate and [3-^{14}C]pyruvate indicates the fraction of pyruvate entering the TCA cycle via carboxylation. Metabolic flux patterns in AS-30D cells were initially examined in media containing either 0 or 5 mM glutamine, 20 μM succinate, 10 mM β-hydroxybutyrate, 10 mM acetoacetate, 50 μM pyruvate, and 50 μM acetate. $^{14}CO_2$ production ratios indicated that, with the addition of glutamine to the medium: (1) Flux of carbon into the TCA cycle increased, supporting the hypothesis that tumor cells have a large capacity for glutamine oxidation; (2) Approximately 30% of pyruvate flux into the TCA cycle occurred via carboxylation, suggesting that either malic enzyme or pyruvate carboxylase is capable of carboxylating pyruvate in this preparation. The flux of carbon to products other than CO_2 was examined in a medium containing 6.0 mM glucose, 0.75 mM glutamine and [2,3-^{14}C]succinate. Significant labeling of aspartate and lactate occurred indicating flux of TCA cycle carbon to these products. This study demonstrates that the $^{14}CO_2$ ratios method, together with measurements of metabolic products, can be used to quantitate metabolic flux patterns in tumor cells. (Supported by USPHS grants CA 32946 to G.F. and GM 33536 to J.K.K.)

M-Pos84 DURAMYCIN DISCRIMINATES AMONG MITOCHONDRIAL CA^{2+} TRANSLOCATION PROCESSES. Patricia M. Sokolove and Roberta G. Shinaberry, Department of Pharmacology & Experimental Therapeutics, University of Maryland Medical School, Baltimore, MD. 21201.

Duramycin has recently been reported to interact with lipids capable of adopting the hexagonal H_{II} phase [Navarro *et al.* (1985) Biochemistry 24:4645]. The antibiotic has the following effects on the energy conservation reactions of isolated rat heart mitochondria: (1) Duramycin is a potent uncoupler, reducing the respiratory control ratio to 1 at ~ 40 μg/mg mitochondrial protein. (2) At the same antibiotic concentration, duramycin has minimal effects on Ca^{2+} uptake. This indicates both that the electrophoretic uniporter is relatively insensitive to duramycin and that, like DNP, duramycin uncouples by dissipating the H^+-gradient across the inner mitochondrial membrane rather than by producing a generalized permeability increase. (3) Duramycin is a potent inhibitor of Ca^{2+} release triggered by palmitoyl-CoA; Ca^{2+} release is eliminated at 40 μg duramycin/mg protein. Inhibition is distinct from the uncoupling effects of duramycin, since DNP speeds palmitoyl-CoA induced Ca^{2+} release. (4) Duramycin (up to 70 μg/mg protein) is without effect on the mitochondrial Na^+/Ca^{2+} exchanger. These observations suggest that of the three Ca^{2+} translocation mechanisms operating across the inner mitochondrial membrane only palmitoyl-CoA induced Ca^{2+} release is sensitive to duramycin. Inverted phase forming lipids, presumably phosphatidylethanolamine and/or cardiolipin, are implicated in palmitoyl-CoA triggered Ca^{2+} release and in the coupling of phosphorylation to electron transport. [Supported by NIH grant HL 32615 and an American Cancer Society Junior Faculty Research Award (#109) to PMS.]

M-Pos85 OUTER MEMBRANE LYSIS INCREASES ACCESSIBILITY OF CATIONIC DRUGS TO THE INNER MITOCHONDRIAL MEMBRANE. J. J. Diwan[1], C. A. Mannella[2], and H. H. Yune[1], [1]Biology Dept., Rensselaer Polytechnic Inst., Troy, NY 12180, and [2]Wadsworth Center for Laboratories and Research, New York State Dept. of Health, Albany, NY 12201.

Susceptibility of rat-liver mitochondria to respiratory inhibition by the polyamines, spermidine and spermine, and the cationic anticancer drugs, methylglyoxal-bis(guanylhydrazone) (MGBG) and adriamycin, increases substantially when the outer membranes are lysed by osmotic shock or digitonin treatment (Mannella et al., 1985, Biophys. J. 47:238a). Such results suggest that the outer mitochondrial membrane may limit access of the organic cations to the inner membrane. Measurements of uptake of radioisotope-labeled daunomycin (a close analog of adriamycin), MGBG, and spermidine indicate varying degrees of adsorption, which in each case is decreased by increasing Mg^{++} concentration in the medium to 24 mM. In experiments carried out at this Mg^{++} concentration, digitonin (0.1 mg/mg protein) causes a rapid antimycin A-insensitive increase in the ^{14}C-spermidine content of mitochondria separated by centrigation through silicone. In one expt. the spermidine distribution space increased from 2.47 to 3.64 ul (1.1 mg protein). This increase is more than can be accounted for by the change in ^3H_2O distribution space from 2.22 to 2.80 ul, due to the increase in entrained water as outer membrane lysis by digitonin alters organelle shape. The digitonin induced jump in spermidine content is followed by a progressive uptake which is blocked by antimycin A. These results suggest respiration dependent transport of spermidine into the mitochondrial matrix, following penetration of the outer membrane barrier. (Supported by NIH Grant GM-20726 & NSF Grant PCM 83-15666)

M-Pos86 CHLORIDE PERMEABILITY OF THE ACIDOPHILE, BACILLUS COAGULANS. D. McLAGGAN and A. MATIN. DEPT. MEDICAL MICROBIOLOGY, STANFORD, CALIFORNIA 94305.

Active cells of Bacillus coagulans, suspended in 0.1M β-alanine buffer pH 3 (+ 2mM $MgSO_4$), maintained an internal pH of 6.25 and a membrane potential ($\Delta\Psi$) of +55 mV, giving a protonmotive force of -145 mV. In the presence of NaCl (100mM), the $\Delta\psi$ was consistently less positive. The kinetics of change in $\Delta\psi$ upon Cl^- addition were measured using the technique of rapid centrifugation and [^{14}C]-$KSCN^-$ distribution. Within 15s after Cl^- addition, the $\Delta\psi$ decreased to +15 mV. It then increased to +35 mV over the next 4 minutes and remained at this value. The transient collapse of the $\Delta\psi$ was probably due to the influx of Cl^- down its electrochemical gradient and the partial recovery to the influx of H^+ reequilibrating with the lowered $\Delta\psi$. If this is so, the results suggest that Cl^- is a relatively permeant ion in this organism. To test this possibility, everted vesicles were prepared containing 0.1M β-alanine buffer pH 5, 2mM $MgSO_4$ and 0.5M K_2SO_4 in the intravesicular space. The vesicles were suspended in a series of external K^+ concentrations and K^+ diffusion potentials were induced with valinomycin (8μM) in the presence of the potential sensitive dye $diSC_3$ (10μM). The absorbance changes were related to the K^+ equilibrium potential given by the Nernst equation. The degree of quenching of the dye increased linearly over the range of 30 to 120 mV. Replacing SO_4^- by Cl^- in the intravesicular space diminished the response of the dye to the K^+ diffusion potential in a manner which was linearly dependent on the K^+ concentration gradient. Thus, compensatory movement of Cl^- probably occurred concomitantly with valinomycin induced K^+ efflux, which is consistent with the predicted Cl^- permeability of B.coagulans. These findings may have a bearing on the current controversy concerning the effect of ProtonoPhores on the ΔpH in acidophilic bacteria.

M-Pos87 CYTOSOLIC FREE Ca^{2+} CONCENTRATION AND ITS RELATION TO PYRUVATE DEHYDROGENASE INTERCONVERSION IN ISOLATED CARDIAC MYOCYTES. Richard G. Hansford, Gerontology Research Center, National Institute on Aging, Baltimore, MD 21224.

We have measured the concentration of cytosolic free Ca^{2+} ($[Ca^{2+}]_c$) in suspensions of myocytes isolated from rat hearts, using the fluorescent indicator Quin-2. Further, we have measured the proportion of total pyruvate dehydrogenase which exists in the active form (PDH_A) by a rapid quenching of interconversion followed by spectrophotometric assay. The response of $[Ca^{2+}]_c$ and PDH_A to agents affecting plasma membrane, sarcoplasmic reticulum (SR) and mitochondrial ion transport has been studied. The "resting" value of $[Ca^{2+}]_c$ was 78 + 9 (10) nM in cells incubated in media containing 1 mM $CaCl_2$, rising to 142 + 26 (8) nM 10 min after partial depolarization with 25 mM KCl. Higher concentrations of KCl, up to 80 mM, gave higher values of $[Ca^{2+}]_c$. Calibration of the Quin-2 signal was achieved by sequential additions of gramicidin, $MnCl_2$ and digitonin. PDH_A was found to be 45 + 5% of PDH_{TOTAL} under "resting" conditions (5 mM KCl), rising to 61, 70 + 2, 84 + 5 and 98 + 10% at KCl concentrations of 20, 40, 55 and 80 mM, respectively. Caffeine (10 mM) and ouabain (0.2 mM) were unsucessful in raising either $[Ca^{2+}]_c$ or PDH_A in cell preparations of high integrity. However, 50 μM veratridine, which opens Na^+ channels, increased PDH_A to 77 + 5% and this effect was potentiated by ouabain (98 + 5%). The increase in PDH_A due to KCl was abolished by ruthenium red (12 μM) which inhibits mitochondrial Ca^{2+} uptake, and was unaffected by ryanodine (1 μM), which inhibits SR Ca^{2+} transport. Thus, it is concluded that net Ca^{2+} transport into the mitochondria is important in increasing PDH_A, and that ADP generated in response to increased SR Ca^{2+} cycling and increased actomyosin ATPase is relatively unimportant, under these conditions.

M-Pos88 A Kinetic Description of the Na^+-Independent Ca^{2+}Efflux Mechanism of Liver Mitochondria. D.E. Wingrove and T.E. Gunter, Dept. Rad. Biol. and Biophys., Univ. of Rochester, Roch., NY 14642.

Na^+-independent Ca^{2+} efflux from liver mitochondria has been studied using the arsenazo III technique over the range of Ca^{2+} loads from 2 to 60 nmol/mg with emphasis on the lower (more physiological) part of this range. Endogenous Ca^{2+} has been depleted using a new procedure which avoids both substrate depletion and de-energization and thereby leaves the mitochondria less sensitive to the membrane permeability transformation. The results of this study may be fit to the equation:

$$V/V_{max} = ([Ca]^2 + a[Ca])/(K_m^2 + [Ca]^2 + 2a[Ca]),$$

where V_{max} = 1.2 ± 0.1 nmol/mg·min, K_m = 8.4 ± 0.6 nmol/mg and a = 0.9 ± 0.2 nmol/mg (X ± SE). This equation is representative of either a nonessential activation mechanism with a single transport site or of an Adair-Pauling mechanism with two transport sites. Failure of the maximum transport velocity to decrease with increasing Pi suggests that the extreme flatness of the saturation characteristics of Na^+-independent transport is a property of the mechanism itself and not the result of precipitation of Ca^{2+} with Pi. Where other forms of mitochondrial Ca^{2+} efflux are low then, characteristics of the second order kinetics of the Na^+-independent Ca^{2+} efflux mechanism can provide a means for maintaining a significant Ca^{2+} load in the mitochondrial matrix at low Ca^{2+} levels and can provide a mechanism for maintaining an intermediate "quasi steady state" level of cytosolic Ca^{2+} for a period following a hormonally induced pulse of Ca^{2+}. Supported by PHS RR05403, GM35550, and 5T32 GM07356.

M-Pos89 THE BEHAVIOR OF POTENTIAL-SENSITIVE MOLECULAR PROBES IN THE EXPOSED CEREBRAL CORTEX OF THE GERBIL, J.C. Smith and Diane Evans*, Dept. of Chemistry and LMBS, Georgia State Univ., Atlanta, GA. Using the technique of surface fluorescence, we tested the ability of a number of potential-sensitive molecular probes to respond to electrical activity changes that accompany normoxic/anoxic transitions and spreading depression episodes in the exposed cerebral cortex of the gerbil. The response of the pyridine nucleotide fluorescence signal has been compared to that of the various probes using a time-sharing instrument configured as a dual channel fluorimeter. The administration of nitrogen through a tube inserted in the trachae caused a ΔF/F change as large as 17% with oxonol V; somewhat smaller changes were observed with diS-C_3-(5) and M540. These changes were closely followed by an increase in the pyridine nucleotide signal of 5 to 30%. Both signals developed within nominally 1 minute after the administration of nitrogen at low flow rates. An irreversible increase in the pyridine nucleotide signal that was closely followed by an oxonol V fluorescence yield increase was observed upon injection of rotenone into the cortex tissue; this observation suggests that the signals arise at least in part from the cortex mitochondria. Topical application of 1 M KCl at a remote skull opening induced oscillations in the oxonol V, diS-C_3-(5), and pyridine nucleotide fluorescence signals characteristic of spreading depression that could be reversed by washing the tissue at the remote skull opening with physiological saline. Much larger singals could be obtained by injecting KCl into the lateral ventricle. Picrotoxin and bicuculline when injected in the ventricles also induced ΔF/F periodic oxonol V increases of nominally 15% that persisted over time periods of 20-30 minutes. Additional work with a number of other optical probes is in progress. Support: GSU Research Fund; NIH grant GM 30552.

M-Pos90 **FREE FATTY ACIDS' INTERACTIONS WITH THE MITOCHONDRIAL INNER MEMBRANE PROTEINS: STUDIES WITH FLUORESCENT AND SPIN-LABELED STEARIC ACID ANALOGS** HAGAI ROTTENBERG, Pathology Department, Hahnemann University, Philadelphia, PA

Free fatty acid (FFA) uncouple oxidative phosphorylation in mitochondria without significant reduction of the proton electrochemical potential. Our investigation of the mechanism of uncoupling by FFA suggest a specific interaction with one or more of the mitochondrial proton pumps which result in intrinsic uncoupling. We used the fluorescent stearic acid analogs, 2-Antroyloxystearate (2AS) and 12-Antroyloxystearate (12AS), and the spin labeled ɔ-doxylstearate (5DS) and 12-doxylstearate (12DS) to characterize these interactions in rat liver submitochondrial particles (SMP). The fluorescent membrane probes, diphenylhextriene and 9-Vinylanthracene were used as controls to characterize the responses of membrane imbedded dyes not attached to FFA. Phospholipid vesicles prepared from dioleylphosphatidylcholine (PL) were used as controls to characterize dye responses in the absence of membrane proteins. The effects of dyes' concentrations, FFA, 5DS, 12DS general anesthetics, and various quenchers on fluorescence intensity, anisotropy and fluorescent energy transfer from membrane protein were investigated and analyzed.

The results confirm the suggestion that FFA interacts specifically with a mitochondrial membrane protein complexes or aggregates. The identity of this complex is under investigation. Supported by PHS Grant GM-28173

M-Pos91 ORIENTATIONAL ORDERING OF UBIQUINONE-10 AND UBIQUINONE ANALOGS IN MODEL AND BIOLOGICAL MEMBRANES: A ^2H NMR STUDY. P.W. Westerman#, M.A. Keniry*, R.N. Robertson¶ and B.A. Cornell§. #Northeastern Ohio Univs. College of Medicine, Rootstown, OH 44272. *Dept. of Pharmaceutical Chemistry. Univ. of California, San Francisco, CA 94143. ¶School of Biological Sciences, Univ. of Sydney, Sydney, N.S.W. 2006. §CSIRO Division of Food Research, P.O. Box 52, North Ryde, N.S.W. 2113 Australia.

^2H NMR of aqueous dispersions of dimyristoylphosphatidylcholine (DMPC) containing 3 mole% of selectively ^2H-labelled ubiquinone (Q) analog, have been recorded in the L_α phase. The analog has a saturated straight chain of 13 carbons and is ^2H-labelled at each chain position. Results show the Q analog is dispersed in the bilayer with its long molecular axis parallel to the long axis of the lipid molecules. Reduction of the analog gives the ubiquinol, which ^2H NMR shows is still intercalated in the lipid bilayer. Corresponding ^2H-sites on the hydrocarbon chains are more ordered implying that reduction of the ubiquinone ring decreases the penetration of the chain in the bilayer. Similar experiments with Q_{10}, deuterated on the chain and methoxyl groups, show a single isotropic peak in the ^2H NMR spectrum. No ordered component could be detected at levels of 3 mole% Q_{10} in DMPC, egg yolk lecithin or asolectin bilayers. Thus, Q_{10} does not readily dissolve in these lipids. These results support the view that Q_{10} performs its role in mitochondrial electron transport in association with specific binding proteins and not as a free molecule dissolved in the bilayer. (PWW and MAK supported by CSIRO visiting scientist awards.) [Supported in part by NIH Grant #GM27127 to PWW.]

M-Pos92 INVOLVEMENT OF A SPECIFIC PHOSPHOLIPID IN THE OXIDATION OF UBIQUINOL IN THE CYTOCHROME $\underline{b}$-$\underline{c}_1$ COMPLEX. F-D Yang, L. Yu, and C. A. Yu, Dept. of Biochem., Oklahoma State Univ., Stillwater, OK 74078.

A quinone-like inhibitor, 5-undecyl-6-hydroxy-4,7-dioxobenzothiazol (UHDBT), has been shown to inhibit ubiquinol oxidation and to alter the EPR characteristics of reduced iron sulfur protein (ISP) in the mitochondrial cytochrome $\underline{b}$-$\underline{c}_1$ complex, and thus it implies that there is a specific interaction between ubiquinone (Q) and ISP. However, the inhibitory effect of UHDBT is not reversible by Q and the incorporation of azido-Q to the cytochrome $\underline{b}$-$\underline{c}_1$ complex is not affected by UHDBT indicating that UHDBT is not bound to the same site as that of Q. Recently, we have synthesized a series of UHDBT derivatives and studied their inhibitory properties. The incorporation of azido-UHDBT to the cytochrome $\underline{b}$-$\underline{c}_1$ complex after photolysis is also examined. The results are summarized in the Table. From these results we conclude that the inhibition of UHDBT is due to the perturbation of a specific phospholipid which is closely associated with ISP or other quinol oxidizing components. (supported by NIH grant GM 30721)

R_2	R_6	Inhibition Act.	$\underline{b}$	$\underline{c}_1$	EPR (ISP) g_x (G)	Incorporate Prot.	PL
N_3	OH	+++	+	-	→ (50)	-	+
N_3	OCH_3	+	+	-	nd	-	+
H	N_3	-	-	-	→ (40)	?	+
H	OH	++	+	-	→ (20)		
H	OCH_3	++	-	-	nd		
Br	OH	++	+	-	→ (60)		
Br	OCH_3	±	+	-	→ (30)		
H	Br	+	-	±	→ (25)		

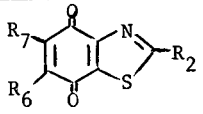

M-Pos93 STRUCTURE OF THE ACTIVE SITE OF MEMBRANE BOUND CYTOCHROME OXIDASE. L. Powers,* B., Chance A. Naqui, I-Y Ching* and C.P. Lee+, *AT&T Bell Laboratories, Murray Hill, NJ 1797; Dept. Biochem. Biophys, Univ.of Penna.,Phila., PA 19104; and +Dept.Biochem.,Wayne State Med.Sch., Detroit, MI 48201

Use of a structural study for the determination of enzyme integrity is afforded here by a comparson of the Cu edge and EXAFS of cytochrome oxidase in the native membrane of submitochondrial particles (SMP) as compared with various purified preparations. SMP contained 2.76 nmoles of Cu/mgm protein and 18.5 nmoles iron/mgm protein. The protein was used at 200- 300 uM copper (2 sites). The X-ray data were obtained at SSRL at 3.0 GeV, 20-50 mA on Beamline I-5. The results are most simply summarized by no detectable difference of the edge and EXAFS of the Yonetani purified preparation and the membrane bound oxidase. All parameters are identical to within the error. At the same time, highly significant differences in both these properties are observed with respect to authentic and modified Hartzell-Beinert preparations. In fact, comparison of the edge and EXAFS data suggests that the edge spectrum itself can be used as diagnostic of the authenticity of the cytochrome oxidase preparation. These results set standards for the use of cytochrome oxidase preparations in EXAFS studies, and at the same time to indicate the feasibility of EXAFS study of this important membrane bound protein in its natural state. SUPPORTED in part by NIH Grants HL 31909, GM 31992 & RR 01633; and SSRL Project 632B (supported by DOE,OBES;NSF,DMR & NIH,BRP,DRR).

M-Pos94 BEEF HEART MITOCHONDRIA CYTOCHROME c_1 IS A MIXTURE OF TWO NERNSTIAN COMPONENTS WITH n = 2 VALUES RATHER THAN A SINGLE n = 1 SPECIES. Richard W. Hendler and K.V. Subba Reddy, Laboratory of Cell Biology, National Heart, Lung, and Blood Institute, NIH, Bethesda, MD 20892.

When a potentiometric titration of intact beef heart mitochondria is analyzed by the use of the ΔA (553-540 nm) followed by plotting and graphic resolution of E vs log ([OX]/[RED]) plots, cytochrome c_1 appears to be a single entity with n = 1 and E_m = 230 mV. However, when the entire α peak from 545 to 560 nm is analyzed using the magnitude of the second derivative at 553 nm, the titration is resolved into two n = 2 species with E_m values near 200 and 250 mV. The same result is obtained using a totally different method of analysis. Complete optical spectra from 525 to 650 nm are accumulated for each of about 100 voltages and analyzed by singular value decomposition. This procedure yields n values, E_m's, and unique optical difference spectra. The species with E_m near 200 mV and n = 2 has its peak at 555 nm and the species with E_m near 255 mV and n = 2 has its peak at 553 nm. For a single heme group to display a potentiometric n value of 2, requires a strong coupling with another redox group so that 2 electrons are needed to reduce both centers in a concerted manner. The appearance of two separate species with n = 2 values suggests a difference in environment of the c_1 heme centers. Recently published evidence for the existence and functionality of the bc_1 segment as well as cytochrome oxidase as dimers may be relevant to the findings reported here.

M-Pos95 DOES PURPLE MEMBRANE HAVE A Q-CYCLE? A. Hollub, L. Brogley and R. Renthal, Univ. of Texas at San Antonio, San Antonio, Texas 78285

It has been assumed that proton pumps such as purple membrane lack redox loops. Surprisingly, purple membrane contains an electron carrier. Kushwaha et al. (Can. J. Biochem. 53, 284, 1975) reported the presence of 0.14 moles of vitamin MK-8 per mole of bacteriorhodopsin among the non-polar lipids. Is this quinone functionally important in the proton pump mechanism? It is possible to write a Q-cycle mechanism for purple membrane in which the MK-8 could cyclically exchange electrons with bacteriorhodopsin while transporting protons. Since the pump stoichiometry may be as high as 2 H^+/cycle, a Q-cycle could account for some of the translocated protons. However, many experiments seem to rule this out. For example, it is possible to reconstitute the proton pump from apparently lipid-free bacteriorhodopsin (Huang et al., PNAS 77, 323, 1980). A loophole in this experiment is that the pump stoichiometry was not reported. If MK-8 accounts for only some of the H^+ pumped, it would be necessary to measure the stoichiometry with and without added MK-8 to assess the contribution from a Q-cycle. We report here the results of proton pumping experiments with lipid-free bacteriorhodopsin reconstituted in vesicles of soybean or H. halobium lipids to which varying amounts of vitamin K_1 were added. With soybean lipids, in the presence of TPB^-, the pump stoichiometry was 0.5 H^+/cycle. This result was independent of the amount of vitamin K_1 added over a range of 0 to a 30-fold mole ratio to bacteriorhodopsin. A similar result was obtained with H. halobium lipids. Although the pump stoichiometry of our vesicles is less than that reported for membrane sheets and whole cells, our results support the conclusion that a vitamin K Q-cycle is not involved in the purple membrane proton pump. (Supported by NIH GM 25483 and RR 08194)

M-Pos96 RESPIRATION IN METHYLOTROPHIC BACTERIA. V.L. Davidson & M. Husain, Molecular Biology Division, VA Medical Center, San Francisco, CA 94121 and Dept. of Biochemistry & Biophysics, UCSF

Methylophilus methylotrophus, an obligate methylotroph, bacterium W3A1, a facultative methylotroph, and Paracoccus denitrificans, a facultative autotroph, are each capable of using methanol or methylated amines as a sole source of carbon and energy. Many of the proteins involved in the primary oxidation pathways for these substrates are inducible and synthesized at high levels. Some function in the periplasm of these gram negative bacteria. In the first 2 bacteria, trimethylamine induces the expression of a trimethylamine dehydrogenase and an electron transfer flavoprotein to which it donates electrons, neither of which are expressed during growth on methanol or methylamine. In each bacterium, methylamine dehydrogenase is induced only during growth on methylamines. In Paracoccus, a blue copper protein, also specifically induced by methylamine, has been shown to mediate electron transfer from methylamine dehydrogenase to cytochrome c. In each bacterium, the soluble proteins involved in methylamine- and methanol-dependent respiration function in the periplasmic space, and subunits of the periplasmic methanol and methylamine dehydrogenases from bacterium W3A1 have been synthesized in vitro as larger precursor forms. Enzymatic and immunological cross-reactivities have been demonstrated for some of the individual components of the analogous respiratory chains of these 3 bacteria. As many of these oxidoreductases and electron carrier proteins are syntheiszed to high levels, coordinately expressed, and translocated across biological membranes, these bacteria can provide an excellent system in which to study the kinetic mechanisms, genetic regulation and biosynthesis of proteins involved in electron transport and energy transduction. Supported by NIH grant HL-16251 and the Veterans Administration.

M-Pos97 KINETICS OF ELECTRON TRANSFER IN REACTION CENTER-CYTOCHROME o PROTEOLIPOSOMES.

C.C. Moser, K. Matsushita‡ D.E. Robertson, H.R. Kaback‡ and P.L. Dutton. Department of Biochemistry and Biophysics, University of Pennsylvania and *Roche Institute of Molecular Biology, Nutley, New Jersey.

A proteoliposome hybrid protein system consisting of photosynthetic reaction centers (RC) from Rhodopseudomonas sphaeroides, ubiquinol-O_2-oxidoreductase (cyt o) from E. coli and ubiquinone-8 was reconstituted to study the mechanism of O_2 reduction and the generation of $\Delta\mu_H+$ by cyt o. Steady-state illumination of proteoliposomes leads to an O_2 uptake rate of 4.15 µatom O/min/mg protein. This uptake is inhibited by 5-n-undecyl-6-hydroxy-4,7-dioxobenzothiazole (UHDBT) or 2-heptyl-4-hydroxyquinonoline-N-oxide (HQNO). Illumination also leads to the generation of an interior negative $\Delta\psi$ of -115 mV as measured by ^{3}H-TPP distribution. The advantage of the RC-cyt o hybrid system lies in the ability of the RC to deliver reduced ubiquinol following absorption of a photon. A rapid flash of actinic light (5µsec) induces a single turnover of the RC and the resultant pulse of ubiquinol leads to millisecond reduction of b-type heme with a broad α-band maximum between 558 and 565 nm. Reduction is sensitive to UHDBT and HQNO and occurs with a halftime ($t_{1/2}$) of 4 ms. Subsequent cyanide-sensitive reoxidation occurs in the presence of minimal quantities of O_2. The extent of b-heme reduction by ubiquinol at pH 7.4 decreases steeply with redox potential around 185 mV. The two reported b-hemes of cyt o are similar on a kinetic, redox and α-band spectral basis.

Supported by NIH GM 27309-06.

M-Pos98 A LOW POTENTIAL INTEGRAL MEMBRANE c CYTOCHROME FROM DESULFOVIBRIO DESULFURICANS.

J.F. Kramer, D.H. Pope and J. C. Salerno, Biology Department, Rensselaer Polytechnic Institute, Troy, NY 12180

The cytoplasmic membrane of the sulfate reducing bacterium Desulfovibrio desulfricans contains a cytochrome system with absorption maxima at 421, 524, 554 and 631 nm after reduction with dithionite. Potentiometric titration of the membranes using optical monitoring revealed two c-type components with potentials of approximately -230 and -100 mV; no ascorbate reducible c cytochrome was observed. The two components were responsible for roughly equal absorbance of the α band. Extraction of the membranes with 1% Triton X-100 solubilized a c cytochrome with bands at 421, 524 and 554 nm; the 631 nm band was absent. Electron paramagnetic resonance spectra of the membrane fraction showed an asymmetric peak near g=3, indicative of a low spin ferriheme. The solubilized fraction contains a heme protein with a molecular weight of 30 KD. The potentials of the c type components suggest that they might function as a transmembrane electron transferring arm between periplasmic components (hydrogenase, c cytochromes and/or ferredoxins) and the sulfate reducing cytoplasmic components.

M-Pos99 ASYMMETRIC INCORPORATION OF METALLOPORPHYRINS INTO PLANAR LIPID BILAYERS.

Martin C. Woodle, Eishun Tsuchida and David Mauzerall, The Rockefeller University, New York, NY 10021 and Waseda University, Tokyo, JAPAN.

Porphyrin containing lipid bilayers typically have been prepared from a lipid porphyrin solution which results in a symmetrical distribution of the porphyrin in the bilayer. However, asymmetry is essential for electrical measurements of charge transfer reactions across the bilayer or the lipid-water interface. Previously the asymmetry has been achieved by varying the components of the aqueous phases on either side of the bilayer. We have now incorporated charged porphyrins asymmetrically into planar lipid bilayers by absorption from the aqueous phase. Absorption of zn-tetraphenyl-phosphocholine-porphyrins or chlorophyll b-cholylhydrazone produces an interfacial photovoltage resulting from electron transfer when the aqueous acceptor is symmetrically distributed. The asymmetrical distribution of the porphyrin in the bilayer persists for the life of the membrane, typically 1 to 2 hr., showing that the cross membrane transit time is very slow because of the charged nature of the porphyrins used. The incorporation of the porphyrins into the bilayer appears to reach equilibrium in less than 5 min. The asymmetrical distribution of the porphyrin in the bilayer not only allows electrical measurements of the interfacial charge transfer without asymmetrical aqueous phases, but also makes possible measurements of other cross bilayer process such as the porphyrin transit time and construction of asymmetric bilayer systems.

This work was supported by NIH-PHS Grant 25693-07.

M-Pos100 EXTRAGRANULAR ASCORBATE AS THE SOURCE OF REDUCING EQUIVALENTS DURING NOREPINEPHRINE SYNTHESIS IN CHROMAFFIN GRANULES. Michael F. Beers*, Robert G. Johnson+, and Antonio Scarpa*, U. of Pa. School of Medicine, Dept. Biochem. & Biophys.*, Phila., PA 19104, and Mass. Gen. Hospital, Div. of Endocrinology+, Boston, MA 02114.

A transmembrane electron shuttle between external (cytosolic) and intragranular ascorbate pools was demonstrated in vitro in intact bovine chromaffin granules undergoing tyramine- or dopamine-stimulated DβH turnover. Incubation of intact chromaffin granules with external tyramine shows a time- and dose-dependent decrease in reduced intragranular ascorbate and production of octopamine, with a stoichiometry approaching unity. Tyramine induced oxidation of intragranular ascorbate is almost completely inhibited by addition of disulfuriam. Extragranular dopamine also induces oxidation of intragranular ascorbate which is inhibited by reserpine. On the other hand, incubation with octopamine causes no net decrease in reduced ascorbate. The presence of extragranular ascorbate abolishes the observed tyramine-induced intragranular ascorbate consumption. The addition of ascorbate 30 min after addition of tyramine produces a net increase in the concentration of intravesicular reduced ascorbate. The use of ^{14}C-ascorbate distribution ratios in granule pellets and supernatants indicates that there is no transmembrane transport of ascorbate. Extravesicular NADH had no significant effect on matrix ascorbate levels during ß-hydroxylation. These data provide new in vitro evidence that chromaffin granules shuttle reducing equivalents inwardly from an extra- to an intravesicular ascorbate pool, and strongly indicate that cytosolic ascorbate is the source of intragranular reducing equivalents required during norepinephrine biosynthesis. Supported by NIH grant AM-33928.

M-Pos101 THE ABSENCE OF MITOCHONDRIAL ATPase INHIBITOR PROTEIN IN CARDIAC MUSCLE MITOCHONDRIA FROM THE RAPIDLY BEATING HEARTS OF RATS AND OTHER SMALL MAMMALS. William Rouslin, Department of Pharmacology and Cell Biophysics, University of Cincinnati Coll. of Med., Cincinnati, Ohio 45267.

A cross-species study has demonstrated that the cardiac muscle mitochondrial ATPase from rabbits and from several larger mammalian species examined exibits the reversible, ischemia-induced or protonic ATPase inhibition described by us earlier (Rouslin, W. (1983) J. Biol. Chem. 258: 9657-9661). Analyses showed the cardiac muscle mitochondria of rabbits and of the larger mammalian species studied to contain a normal complement of ATPase inhibitor protein.

In contrast, the cardiac muscle mitochondrial ATPase from rats and from all other small mammals examined showed no ischemia-induced inhibition. Moreover, and consistent with this lack of ATPase inhibition, analyses of extracts prepared from these cardiac muscle mitochondria showed them to contain very little or no ATPase inhibitor protein. Briefly, we found that mammals with heart rates in excess of approx. 220 beats/min lacked both the reversible ATPase inhibition and ATPase inhibitor protein.

Our results thus far suggest to us that, in that the function of the mitochondrial ATPase inhibitor protein is primarily the regulation of the enzyme's back reaction rate, i.e., the rate of ATP hydrolysis, that this back reaction rate is probably very low in the rapidly beating hearts of rats and other small mammals and, therefore, does not require the presence of a regulatory protein. In rabbits and in larger mammals including humans, however, the back reaction rate may contribute significantly to the net rate of ATP synthesis and thus requires modulation by the inhibitor protein. (Supported by NIH grant HL-30926).

M-Pos102 EXPLORATION OF THE TIGHT BINDING OF 2-AZIDO-ATP TO CF_1 AND ECF_1 ATPase. T. Melese, Z. Xue, K. Guerrero and P.D. Boyer, Dept. of Chem. and Biochem., UCLA, L.A., CA 90024

The photoaffinity analogues 2-azido-ADP and 2-azido-ATP bind tightly to the β subunits of the ATP synthase on chloroplast thylakoids (Abbott, Czarnecki, and Selman, JBC, 1984 259, 12271), and the soluble chloroplast ATPase (CF_1) (Melese and Boyer, JBC, in press). This binding is analogous to the tight binding reported for [^{3}H]ATP and thus we favor the interpretation that it represents binding at a catalytically competent site (Feldman and Boyer, JBC, in press).

In the binding change mechanism for the multisubunit ATP synthase, all the catalytic β subunits participate equally in sequence during the catalytic cycle. To test this hypothesis we have examined 2-azido-ATP-binding to both CF_1 and the Escherichia coli F_1 ATPase (ECF_1). CF_1 has only one tight nucleotide site. This is on the beta subunit and can be covalently labeled with up to 2 moles of azido nucleotide per mole CF_1, suggesting that at least two catalytic sites are functioning. No binding to other subunits is detected. The effect of catalysis on the labeling and the kinetic properties of labeled enzyme are being investigated.

We have also shown that both 2-azido-ATP and [^{3}H]ATP bind to ECF_1 and that most of the bound nucleotide can be chased off the enzyme in the presence of ATP and Mg^{++}. However, 10% still remains tightly bound as the ATP form to beta subunits. Other results in our laboratory have shown that ECF_1 that has been precipitated with ammonium sulfate shows considerable amounts of "free" beta subunits when migrated in a non-denaturing polyacrylamide gel. Moreover, the equilibrium between associated and free beta subunits is affected by prior exposure to either ATP or Mg^{2+}. Comparisons of nucleotide binding by the free beta and intact ECF_1 are underway.

M-Pos103 ^{18}O PROBES OF REACTION PATHWAYS IN PHOTOPHOSPYORYLATION. S.D. Stroop and P.D. Boyer, Dept. of Chem. and Biochem., UCLA, Los Angeles, CA 90024 (Intr. by W.F. Mommaerts)

The distribution of ^{18}O in P_i from the ATP formed by photophosphorylation can give useful information about the nature and number of pathways involved. The extent of water oxygen incorporation into the γ-phosphoryl of ATP increases as ADP concentration is lowered (Hackney and Boyer, PNAS, 1979, 76, 3646). The extent of replacement and the statistical distribution of ^{18}O in the γ-P of ATP as analyzed by mass spectrometry allows deductions about the reversals of bound-ATP formation and whether a single pathway (homogeneous ^{18}O distribution) or more than one pathway (heterogeneous ^{18}O distribution) is involved. A study of the limits of ADP modulation (Stroop and Boyer, Biochem. 1985, 24, 2304) indicated an upper limit of about 50 reversals and a suggestion that more than one pathway operates for ATP synthesis. We have now investigated ^{18}O distributions at low light intensity and find interesting deviations from the statistically homogeneous distribution. Sufficient decrease in the light intensity to reduce photophosphorylation by 98% increases the number of reversals of bound-ATP synthesis to about 4, even in the presence of 40 μM ADP and 1.5 mM P_i. Some heterogeneity in ATP formation by submitochondrial particles, together with a theoretical explanation, has been reported by Sines and Hackney (submitted). Our results show that a significant number of reversals of bound-ATP formation still occurs when P_i and ADP sites are occupied, but there is inadequate protonmotive force for ATP release. The heterogeneity observed may be explained by a hindered rotation of phosphate at the active site. Other possible explanations are being investigated further.

M-Pos104 NUCLEOTIDE ANALOGUES AND THE MITOCHONDRIAL OXYGEN EXCHANGE REACTIONS. Robert A. Mitchell, Department of Biochemistry, Wayne State University School of Medicine, Detroit, MI 48201.

The intermediate Pi-HOH oxygen exygen reaction accompanying ATP hydrolysis catalyzed by soluble or vesicular mitochondrial ATPase systems results from the reversible hydrolysis of ATP on the enzyme, with Pi free to tumble. Uncoupler stimulates vesicular ATPase activity (presumably due to increased proton pumping) but does not alter the exchange, as if increased proton pumping was due to recruitment of more pumping units. By contrast, higher concentrations of ATP decrease the exchange as if binding of a second (or third) ATP facilitated product release (for review see Curr. Topics. Bioenergetics 13 203-255, 1984). We report that the fluorescent ATP analog epsilon-ATP (eATP) shows the same exchange properties as ATP, indicating that addition of a second eATP mimics the effect of a second ATP. This is compatible with the idea that ATP and eATP can act as competing substrates for ATP-driven reverse electron flow. The ATP analogue, AMP-PNP which competes with ATP but is not hydrolyzed by the ATPase also decreases the intermediate exchange. This suggests that the second binding site is not ATP specific and that substrate binding alone is sufficient to drive product release.

M-Pos105 **COUPLING OF CREATINE KINASE (CK) AND OXIDATIVE PHOSPHORYLATION IN THE GENERATION OF PHYSIOLOGICAL PHOSPHOCREATINE LEVELS: A THERMODYNAMIC APPROACH.** C. Andrew Bergman, Marc R. Litt, William E. Jacobus, Departments of Medicine and Biological Chemistry, The Johns Hopkins Medical Institutions, Baltimore, MD. 21205.

A major controversy exists concerning the thermodynamic aspects of the myocardial CK reaction. Under physiological conditions, the free energy of the reaction, ATP + Cr <---> PCr + ADP, favors the production of ATP and Cr. Previous experiments suggested that in respiring mitochondria the apparent mass action ratio does not predict the direction of the reaction, possibly resulting from a microcompartmentation of CK, or because the reaction is in a nonequilibrium steady-state. We studied the reaction at equilibrium with rabbit muscle CK compared to isolated rat heart mitochondria under coupled respiring conditions. At pH 7.2 and 37° C the apparent Keq =[ADP] x [PCr] x [H+]/[ATP] x [Cr] was 2.82×10^{-9} (M) for rabbit muscle CK and 2.55×10^{-9} (M) for the mitochondrial CK. However, the mitochondrial reaction generated a 30 fold higher [PCr]. At equilibrium [PCr]/[Cr] = [ATP]/[ADP] x Keq/[H+], suggesting the mitochondrial generation of a high [ATP]/[ADP] ratio as the driving force behind this high [PCr]. The [ATP]/[ADP] ratio generated by isolated mitochondria was related linearly to the initial [ADP]. With 30mM Cr and under conditions of varying [ATP]/[ADP] ratios mitochondria produced a linear relationship between [ATP]/[ADP] and [PCr]/[Cr] at equilibrium, throughout a physiological range. Rabbit muscle CK produced a similar relationship, however, 50mM phosphoenolpyruvate was required to generate a physiological [ATP]/[ADP] ratio. Thus, although both CK reactions reach the same equilibrium, only the mitochondrial reaction coupled to oxidative phosphorylation translates a high [ATP]/[ADP] ratio into a physiological [PCr]/[Cr] ratio.

M-Pos106 GRADED METABOLIC IMPAIRMENT OF SMOOTH MUSCLE. M.J. Fisher & P.F. Dillon (Intr. by R. Wagner), Depts. of Physiol. & Radiol., Michigan State U., East Lansing, MI 48824.

^{31}P-NMR was used to define the effects of graded ischemia and reperfusion on intracellular (IC) phosphagens and their chemical environment. Isolated rabbit bladders were perfused with Ringer's/blood solution containing carbachol (10^{-6} M) and 12 mM phenylphosphonate (PPA). PPA was used as an NMR-detectable extracellular (EC) pH-sensitive marker. Perfusion flow was fixed, in turn, at .500 (control), .300, .100, .050, .025 and .500 ml/min. Six collections of 900 1 sec free induction decays were performed at each flow except for .025 ml/min when only 3 were made. Identifiable spectral peaks included PPA, phosphoethanolamine (PE), Pi, glycerolphosphorylcholine (GPC), PCr, ATP, and at low flows, ADP. EC and IC pH were determined from chemical shifts of PPA and Pi, resp.. When flow increased to .100 ml/min, PCr fell to 57±13% (x±SD;n=3) of control and remained stable during further flow reductions. Further, an ADP peak became resolvable permitting direct quantification of IC free ADP (approx. 300 μM; see spectrum). EC (7.06±.09;n=7) and IC(7.15±.15;n=7) pH and ATP gradually decreased to 6.50±.35(n=3), 6.62±.03(n=3), and 56±12%(n=3) of control, resp., when flow decreased to .025 ml/min. Reperfusion restored EC and IC pH within 15 min and PCr to 85%±3%(n=3) of control. ATP remained depressed. The PPA peak, stable during graded ischemia, increased 78±7%(n=3) during reperfusion indicating that PPA may be entering cells. These results define steady-state metabolite levels in flow compromised smooth muscle. They reveal that ADP levels may be directly assessed during controlled ischemia and that pH recovery may not reflect phosphagen recovery. (Supp. by NIH AM34885 & Whitaker Fdn.)

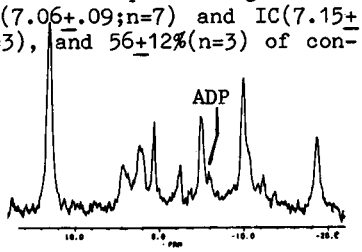

M-Pos107 DOUBLE SATURATION TRANSFER MEASUREMENTS OF ATP SYNTHESIS AND DEGRADATION IN THE PERFUSED RAT HEART AT HIGH WORKLOAD. R.S. Spencer, J.S. Leigh, J.A. Balschi, J.S. Ingwall, Harvard Medical School NMR Lab, Boston, MA and Univ. of Penn., Phila., PA.

Fluxes for phosphate exchange among ATP, phosphocreatine (PCr), and P_i were measured in the intact heart using double and single magnetization transfer NMR methods. Single saturation with 2-site exchange analysis provides information about creatine kinase (CK) flux but not overall ATP balance; double saturation with 3-site exchange analysis provides information about both.

$$PCr \underset{k_r}{\overset{k_f}{\rightleftharpoons}} \gamma\text{-ATP} \underset{k_r'}{\overset{k_f'}{\rightleftharpoons}} P_i$$

Multiple saturation was achieved through use of amplitude modulated rf and yielded the quantities $T_1(\gamma\text{-ATP})$ and $(k_r + k_r')$(n=7). We obtained T_1(PCr), $T_1(P_i)$, k_f, and k_f' using single-peak irradiation (n=6). For high workload hearts we found k_f = .82 ± .05, k_f' = .65 ± .25, $(k_r + k_r')$ = 1.09 ± .11, T_1(PCr) = 2.16 ± .20, $T_1(P_i)$ = 1.05 ± .55, and $T_1(\gamma\text{-ATP})$ = .96 ± .14 . Combining rate constants with tissue contents of PCr, ATP, and P_i we may then assess the equality of the fluxes into and out of ATP: the ratio of flux in (= k_f[PCr] + k_f'[P_i]) to flux out (= $(k_r + k_r')$[ATP]) is 1.2±0.2. Analysis using a single saturation at PCr or at [γ-P]-ATP and 2-site model yields similar values for T_1's of the metabolites and for k_f, but the ratio of fluxes for ATP synthesis to ATP degradation is 1.6, showing the inadequacy of this model. We conclude that 1) values for T_1's and k_f are similar for single saturation within a 2-site exchange model and double saturation within a 3-site exchange model, 2) flux through CK is at least 5 times greater than ATP synthesis, and 3) the balance between fluxes for ATP synthesis and degradation can be shown by adding a third site for P-exchange.

M-Pos108 INTRACELLULAR PH AND THE POSITION OF EQUILIBRIUM OF THE CREATINE KINASE REACTION. M.J. Kushmerick and J.M. Krisanda, Dept. of Radiology, Brigham & Women's Hospital, Boston, Mass. 02115.

The forward and reverse fluxes of the CK reaction:

$$H^+ + PCr + ADP \leftrightarrow ATP + Cr$$

measured in skeletal cardiac muscle indicate that this reaction is close to local equilibrium. If this reaction was not coupled to any other, intracellular acidification should decrease PCr and ADP levels, and increase ATP in Cr. This hypothesis was tested in the isolated, unstimulated cat soleus muscles, perfused as previously described (Meyer, Brown & Kushmerick, *Am. J. Physiol.* 248:C279-C287, 1985). Intracellular pH was measured by the chemical shift of the Pi peak, and was altered over the range of pH 6.2-7.4 by equilibrating the perfusate with different partial pressures of CO_2. ^{31}P-NMR spectra were obtained at 109.3 MHz, using a 90° pulse and a recycle delay of 15 s.

Acidification to pH 6.5 increased PCr content and decreased Pi content by approximately 2 μmol/g/pH unit. The effect was reversible. No change in the steady-state oxygen consumption was detected during the pH shift. Because of the changes in Pi content, at least one other reaction is involved, most probably the ATPase and synthetase reaction. The size and sign of the observed changes are inconsistent with proton stoichiometries measured *in vitro*. These results could be explained if the CK ATPase and ATP synthetase reactions were in local equilibrium with a third reaction, which has a large free-energy drop and whose chemical potential is influenced by intracellular pH.

Supported by NIH grant AM-14485 and a grant from the Muscular Dystrophy Association.

M-Pos109 RESPIRATORY IMPAIRMENT AND CYTOCHROME OXIDASE DEFICIENCY ASSOCIATED WITH CONGENITAL FATTY METAMORPHOSIS OF THE VISCERA. M. E. Martens[b], P. L. Peterson[b] & C. P. Lee[a], Depts. of Biochemistry[a] and Neurology [b], Wayne State University School of Medicine, Detroit, MI 48201; and M. Weisenfeld & S. S. Yang, Dept. of Anatomic Pathology, William Beaumont Hosp., Royal Oak, MI 48072

A 6-1/2 month old female presented with profound hypotonia, hepatomegaly and cardiomegaly. Cardiac arrest occurred and autopsy revealed an enlarged liver and massive accumulation of fat in the heart, liver, skeletal muscle and renal tubules. Two sisters previously died in infancy, at ages 2 days and 4 months; both possessed an enlarged liver. Ultrastructural studies showed fatty infiltration, especially near the mitochondria, and swollen mitochondria of bizarre shape. Mitochondrial fractions were isolated and characterized from frozen autopsy specimens of heart, liver and skeletal muscle. Spectrophotometric analyses revealed that substrate (NADH & succinate) and chemically (dithionite) reducible amounts of cytochrome oxidase were <50% of those in controls in heart and skeletal muscle, and <10% of that in control in liver mitochondria, whereas the cyt. b & c contents were comparable to those in controls in all cases. The mitochondrial preparations exhibited very poor NADH, succinate, and cyt. c oxidase activities. They were 13, 58, 160; 7, 27, 370; and 4, ND, 320 natoms O/min/mg protein for liver, skeletal muscle and heart mitochondrial preparations respectively. These data together with those for NADH-ferricyanide reductase and succinate-PMS reductase activities revealed that in all 3 tissues, the rate-limiting step of NADH and succinate oxidase was not associated with the flavoprotein of NADH dehydrogenase or with cytochrome oxidase, nor with succinate dehydrogenase in skeletal muscle. In liver, succinate oxidase was limited by succinate dehydrogenase. Our data provide the first instance of cytochrome oxidase deficiency and impaired electron transfer of the respiratory chain associated with this disease.

M-Pos110 REYE'S SYNDROME: MITOCHONDRIAL FUNCTIONS OF LIVER AND SKELETAL MUSCLE OF REYE'S SYNDROME PATIENTS. C. P. Lee[a], M. E. Martens[b], G. Kucyj[a] and E. Arcinue[c], Depts. of Biochemistry[a], Neurology[b] & Pediatrics[c], Wayne State University School of Medicine, Detroit, MI 48201

Reye's syndrome (RS) is a grave and often fatal illness of children characterized by encephalopathy and fatty degeneration of the viscera, especially the liver. RS has been classified clinically into 5 stages with Stages I & II fully recoverable & Stage V terminal. Mitochondrial preparations have been isolated and characterized from liver and skeletal muscle biopsy specimens of 3 Stage V patients. In all cases, the skeletal muscle mitochondria (HSM) were tightly coupled with both pyruvate + malate (RCI = 5.1-9.0) & succinate (RCI = 2.4-5.1) as substrates. The respiratory rates and their accompanying phosphorylation efficiencies were normal with both types of substrates. A 4-9 fold stimulation of HSM-ATPase by DNP was also seen. In contrast, the liver mitochondria (HLM) showed poor respiratory rates and respiratory controls with both pyruvate + malate and succinate as substrates, though the phosphorylation efficiencies approached normal (P/O = 2.3-2.7 with pyr. + mal.; and 1.8 with succ.). No DNP stimulated ATPase of HLM was seen. These data are in line with our studies on the effects of RS-plasma, allantoin + Ca^{+2} and salicylate + Ca^{+2} on isolated rat liver (RLM) and rat heart (RHM) mitochondrial preparations. With RLM we have shown that RS-plasma, allantoin + Ca^{+2} and salicylate + Ca^{+2} can cause respiratory inhibition with NAD-linked substrates which results from the increase of permeability of the mitochondrial inner membrane and loss of endogenous pyridine nucleotides (Arch. Biochem. Biophys. 214: 522, 1982; Biochem. Pharm. 33: 2869, 1984, & Arch. Biochem. Biophys. In Press). More recent studies with RHM have shown that under conditions in which RS-plasma and salicylate +Ca^{+2} gave optimal effects on RLM there was no effect on RHM, even when the salicylate was elevated by 80-fold (270 nmoles/mg protein).

M-Pos111 PHOTO-INDUCED NICKING OF DEOXYRIBONUCLEIC ACID BY RUTHENIUM(II)-BLEOMYCIN IN THE PRESENCE OF AIR. R. Subramanian and C. F. Meares, Department of Chemistry, University of California, Davis, CA 95616.

Bleomycin, a glycopeptide derived anticancer drug, causes strand scission of DNA both *in vivo* and *in vitro*. Cleavage of DNA by bleomycin has been extensively studied *in vitro*, with the findings that ferrous ion and molecular oxygen must be present and that addition of reducing agents greatly enhances the reaction (1). Also, light induced nicking of DNA by Co(III)-Bleomycin complex and the sequence-dependent interactions between DNA and Co(III)-Bleomycin have been investigated earlier (2). Here it is reported that a Ruthenium(II) complex of Bleomycin is strikingly effective in causing single strand breaks in supercoiled DNA (ϕX174) in presence of light. In contrast to Co(III)-Bleomycin, Ru(II)-Bleomycin required oxygen for efficient nicking of DNA in presence of light. By use of ^{32}P-end-labeled DNA restriction fragments as the substrates for cleavage, products have been analyzed on high-resolution polyacrylamide gels and compared to those produced by Iron and Cobalt Bleomycins. The results indicate that the sites of damage to DNA are similar in all the three cases: pyrimidine residues located at the 3' side of guanine are preferentially attacked.

1. E. A. Sausville, J. Peisach and S. B. Horwitz, Biochemistry 17, 2740-2746 (1978).
2. C.-H. Chang and C. F. Meares, Biochemistry 23, 2268-2274 (1984).

M-Pos112 ^{31}P NMR SPECTROSCOPIC CHARACTERIZATION OF RADIATION MUTANT STRAINS OF SACCHAROMYCES CEREVISIAE S.A. Knizner, C.E. Swenberg, P.K. Holahan, A.E.Lunsford, Radiation Sciences Dept., Armed Forces Radiobiology Research Institute, Bethesda, MD 20814-5145. Phosphorus NMR spectra of perchloric acid (PCA) extracts and viable cells perfused in agarose threads were obtained for wild type (wt) and three repair deficient mutants of the yeast S. cerevisiae. The repair deficient mutants differ in their ability to repair DNA damage caused by ultraviolet light and ionizing radiation: (1) rad3 is deficient in the excision repair pathway, (2) rad6 is deficient in recombination repair, and (3) rad52 is incapable of repairing DNA double strand breaks induced by ionizing radiation. Both haploid (a or α mating loci) and diploid (a α crosses) wt and rad mutants were examined. In spectra obtained on perchloric acid extracts, resonances could be assigned to sugar phosphates (SP), inorganic phosphate, the α , β , γ phosphates of ATP, NAD, and the end and middle phosphates of polyphosphates. Haploid and diploid rad6 mutants exhibited the highest concentrations of polyphosphates, whereas in rad52 mutants polyphosphates were virtually undetectable. In all of the α mating type rad mutants sugar phosphates predominated the spectra. This was not the case for the α wt mating strain. Diploid crosses of rad mutants also exhibited high concentrations of SP, but again this was not apparent in diploid wt cells. A correlation may exist between the high concentration of sugar phosphates α rad mutant strains and their increased radiation sensitivity.

M-Pos113 USE OF ORTHOGONAL FIELD ALTERNATING GEL ELECTROPHORESIS (OFAGE) FOR STUDYING DNA DOUBLE BREAKS AND REPAIR. Robert Mortimer, Rebecca Contopoulou and Vince Cook. Department of Biophysics and Medical Physics, University of California, Berkeley, CA 94720.

The study of DNA double strand breakage and repair has normally been carried out by using neutral sucrose gradient or neutral elution techniques. We have applied OFAGE procedures, which can resolve individual yeast chromosomes (200kb to 2,000kb), to study x-ray induced double strand breaks and repair. Breakage of chromosomes is seen by a decrease in intensity of individual chromosome bands; as expected, this decrease becomes more pronounced as chromosome size increases. The fragments of chromosomes appear as a broad smear in the size range 100kb to $\sim$ 1,000kb. Following repair in wild type, these fragments disappear and chromosome bands return to their original intensity. In three repair deficient mutants, rad51, rad52 and rad54, no double strand break repair was seen. In fact, degradation of fragments was observed and this could appear as partial repair using other techniques.

M-Pos114 CLASSICAL VIRAL MULTIPLICITY REACTIVATION CAN BE QUANTITATIVELY EXPLAINED BY RECOMBINATIONAL DNA DOUBLE-STRAND BREAK REPAIR.

C.S. Lange, J. DeLeon and E. Perlmutter
SUNY Downstate Medical Center, Brooklyn, New York 11203

One double-strand break (DSB) per genome has been shown to explain ca. 76% of T4 loss of plaque-forming ability (Lange et al., 1984 Rad. Res. 100:1). Infectious Center Assays were performed, at various multiplicities of infection, and their results compared with predictions based on the proportion of cells expected to be infected by: a) undamaged T4; b) ≥2 T4 containing a non-DSB potentially lethal lesion (PLL, lethal in singlet infection); c) ≥2 T4 both containing ≥1 DSB; or d) 1 T4 containing ≥1 DSB or a non-DSB PLL. The number of Infectious Centers was found to be consistent with a+b+c, at low dose (ca. 1 DSB/genome), but decreased, consistent with a lower DSB repair efficiency (ca. 1 DSB repaired/genome), at higher dose (ca. 2, 3.5, 5.5 DSB/genome). Therefore, DSB repair takes place during multiplicity reactivation (MR) and is quantitatively consistent with being the only significant cause of MR. Experiments with genetically identical recA⁻ and recF⁻ deletion mutant hosts showed that the MR observed is independent of the lost recA and recF systems and may depend only on phage-coded enzymes.

This work is supported by grants from USDOE (AC0280EV10503) and the Mathers Charitable Foundation.

M-Pos115 FLUORESCENCE AS A PROBE TO MELANIN PHOTOPROTECTION MECHANISMS J.M.Gallas*, M. Eisner**, (Intr. by Andrew Tsin). U of Texas at San Antonio* and U of Houston**

Physical and chemical characteristics of the recently discovered melanin fluorescence have been explored and analyzed. Some interesting features of the biopolymeric pigment have emerged through fluorescence analysis. Of particular importance is the demonstration of optical bands in the emission spectra in contrast to the structureless optical absorption spectrum long associated with melanin. The overlapping emission bands are shown to originate from at least two distinct fluorophores. Parameters which have been found to affect the fluorescence are discussed. The fluorescence intensity is affected by pH, temperature and metal ions. It is also affected by the manner in which the melanin is prepared. Heat treating the melanin increases the fluorescence significantly. The same physical and chemical parameters which are known to affect the melanin ESR signal are also found to affect the fluorescence signal. The experimental results suggest that the fluorescence originates from sites of the polymer associated with free radicals which have been long associated with the melanin radiation protection mechanism. The results further suggest that the melanin fluorophores are engaged in a reaction equilibrium with the free radicals. Because of the close proximity of the fluorophores with the free radicals, fluorescence analysis allows examination of the role played by the light induced free radicals in the malanin photoprotection mechanism.

M-Pos116 THE DNA SYNTHETIC RESPONSE OF PRIMARY AND TRANSFORMED CELLS TO PULSED ELECTROMAGNETIC FIELDS. W. C. Parkinson, Department of Physics and C. T. Hanks, School of Dentistry. University of Michigan, Ann Arbor, Michigan 48109. It has been reported that dc electric fields (Brighton, 1977) and appropriately pulsed electromagnetic fields (Bassett, 1981) promote osteogenesis and wound healing. There is also a report that pulsed electromagnetic fields stimulate DNA synthesis in fetal rat calvarial osteoblasts grown in culture (Hanley, 1981). There is to our knowledge only one report in a refereed journal of a response by transformed cells (Colacicco, 1983). We report here results on a series of studies of the DNA synthetic response to pulsed electromagnetic fields (PEMF) on finite cell lines (quail somite fibroblasts and periosteal cells from fetal rat calvarium) and continuous cell lines (L-929, Balb/c3T3, Chinese hamster ovary, and rat osteosarcoma [ROS 17/2.8]).

The apparatus for generating the pulsed electrical field consists of a pair of coils each of four turns of formvar-covered #12 wire wound at a mean diameter of 17 cm, and accurately coaxial and parallel, and separated by only 3.2 cm. They are connected via a 3-ohm strip line to an externally triggered 2 kw pulse generator. Contrary to an earlier report (Hanks, 1985), we find no evidence that the pulse electromagnetic field alters the rate of DNA synthesis of either the fetal rat calvarial osteoblasts or Balb/c3T3 cells grown in culture.

Brighton CT, Friedenberg ZB, Mitchell EI, Booth RE (1977). Clin. Orthp. 124:106-123.
Colacicco G, Pill AA (1983). Z Naturforsch 38C, 468-470.
Hanks CT, Parkinson WC (1985). Biophys J 47:149a.
Hanley K, Norton LA, Rodan GA (1981). J Dent Res 60(a):402.

M-Pos117 TIME-RESOLVED FLUORESCENCE ANISOTROPY STUDIES OF INTERNAL MOTIONS IN MULTI-TRYPTOPHAN CONTAINING PROTEINS P.M. Bayley, Division of Physical Biochemistry, National Institute for Medical Research, Mill Hill, London NW7 1AA

Fluorescence anisotropy from tryptophan has been measured for several native and denatured proteins, on a double-beam spectrometer, using a pulsed UV laser and channel place detector, with time resolution (FWHM) 250ps, following Wijnaendts van Resandt et al., Rev. Sci. Instr. (1982) 53:1392-7. Fully orthogonal geometry for the excitation and two emission directions permits cancellation of time-correlated effects between the two detected signals and gives significant advantages in signal/noise. Subtilisin Carlsberg shows rapid internal depolarisation (ϕ < 0.3 ns) of the emission from the single Trp, consistent with a rapid segmental motion of the residue. Subtilisin BPN (3Trp) shows a similar effect superimposed on the global motion of the protein. This rapid motion is not affected by external viscosity changes. Denaturation (8M urea; 6M guanidine HCl) produces characteristically different behaviour in the motions of analogous Trp residues in lysozyme (6Trp) and α lactalalbumin (4Trp), the latter showing potentially greater dynamic freedom upon loss of secondary and tertiary structure.

(Supported by EMBO Short-term Fellowship : ASTF:4798).

M-Pos118 STRUCTURE - CONFORMATION - ACTIVITY RELATIONSHIPS OF "TRANSITION STATE" SUBSTITUTED RENIN INHIBITORY PEPTIDES STUDIED BY RESONANCE ENERGY TRANSFER

Dennis, E. Epps[1], Boryeu Mao[2], David Duchamp[1], and Tomi K. Sawyer[3], [1]Physical and Analytical Chemistry, [2]Computational Chemistry, and [3]Biotechnology, The Upjohn Company, Kalamazoo, Michigan.

Renin, the rate limiting step of the renin-angiotensin converting enzyme cascade, is important pharmacologically in that interference in the biosynthesis of angiotensin II may result in the lowering of blood pressure. The substrate based competitive inhibitor synthesized by Burton and coworkers was a moderately potent ($IC_{50} = 10^{-5}$-10^{-6}M) decapeptide, H-Pro-His-Pro-Phe-His-Phe-Phe-Val-Tyr-Lys-OH (RIP). Further work by others and ourselves involved the incorporation of "transition state" dipeptide isosteres (e.g. Phe_{ψ} [CH_2NH_2] Phe) at the clevage site (P_1-P_1') of human substrate resulting in greatly enhanced potency. We also found considerable differences in potency between N^{IN}-formyl Trp and Trp modified cogeners, with compounds containing the former modification being more efficacious. This led us to hypothesize that introduction of the formyl group (CHO) into the indole ring may have effected an altered conformation in the peptide which could more favorably bind to the active site.

Forster energy transfer has previously been used by Schiller and others to demonstrate conformation-activity differences in enkephalins, somatostatin and other peptides. In the present work, octapeptide RIP analogs containing the dipeptide isostere Phe_{ψ} (CH_2NH) Phe and tyrosine at the C-terminus were studied. Peptide sequences were identical except for the substitutions at the N-terminal end. A donor fluorescent (tyrosine) reference peptide of similar sequence was also synthesized. We then measured end-to-end peptide distances using the tyrosine quenching procedure in distilled water, and in increasing concentrations of trifluoroethanol.U-70,714E (Acetyl-N^{IN} CHO Trp-Pro-Phe-His-Phe_{ψ} (CH_2NH) Phe-Val-Tyr-NH_2, $IC_{50} = 3X10^{-9}$M) was found to have an average end to end distance of 14.11 ± .27 A°,whereas U-71,590E (acetyl Trp-Pro-Phe-His-Phe_{ψ}[CH_2NH] Phe Val Tyr, $IC_{50} = 1.5x10^{-8}$M) had a distance of 11.26 ± .07 Å in distilled H_2O. The secondary structure-inducing solvent trifluoroethanol affected the two analogs differently.

M-Pos119 **INTRAMOLECULAR DISTANCES IN HUMAN PLASMA FIBRONECTIN DETERMINED BY FLUORESCENCE ENERGY TRANSFER.** Hilda Forastieri.
American Red Cross; Biomedical Research and Development Laboratories;
9312 Old Georgetown Road; Bethesda, MD 20814

The intramolecular distance between the N-termini of plasma fibronectin (Fn) chains at low ionic strength and pH 7.5 was determined by non-radiative energy transfer. Using coagulation factor XIIIa, equimolar amounts of monofluorescein-cadaverine (donor) and monoeosin-cadaverine (acceptor) were enzymatically attached to the GLN-3 residue of each Fn chain. Based on a transfer efficiency of approximately 59% (R_o=42Å), the average distance between donor and acceptor is approximately 40Å. Increasing the ionic strength reversed quenching of donor fluorescence at 520 nm (λ E_x=490 nm), 50% of the reversal occurring near physiological salt concentration and complete reversal occurring near 0.3M NaCl. High concentration of denaturants such as guanidine HCl and urea also reversed the quenching. Increasing the ionic strength did not affect the fluorescence intensity of monolabeled control samples, monofluorescein-cadaverine-Fn (FCFn) and monoeosin-cadaverine-Fn (ECFn). However, their fluorescence polarization decreased with increasing ionic strength suggesting an enhancement of flexibility in the N-terminal region of the Fn chains. FCFn and EFFN also underwent a temperature and salt dependent reversible transition whose midpoint occurred near 50°, about 10° less than the melting T of the protein. A corresponding transition is observed in the differential calorimetry scan of the unlabeled Fn molecule. These data are consistent with a model in which, under physiological conditions, extended fibronectin molecules occur in equilibrium with more compact pretzel-like ones.

M-Pos120 THE DISTRIBUTION OF DONOR-TO-ACCEPTOR DISTANCES IN TROPONIC C FROM FREQUENCY-DOMAIN FLUOROMETRY. Joseph R. Lakowicz, Robert F. Steiner and Ignacy Gryczynski, University of Maryland, School of Medicine, Department of Biological Chemistry, Baltimore, Maryland 21201 and Michael L. Johnson, University of Virginia, School of Medicine, Department of Pharmacology, Charlottesville, Virginia 22908.

Fluorescence energy transfer is often used to measure distances between donors (D) and acceptors (A). Typically, this method is used to find a single distance. However, macromolecules can exist in random coil states, for which a single D-A distance does not exist. We generalized the use of energy transfer and frequency-domain fluorometry to recover the distance distribution between D-A pairs. As a model system we chose troponin C. The donor was dansyl azridine on methionine-25 and the acceptor was eosin on cysteine-98. The existence of a range of D-to-A distances results in a more heterogeneous decay of the donor fluorescence. The data were fit assuming a range of D-A distances. Typically, the half widths of the distance distributions were near 10 A°, depending upon temperature and ionic strength. These techniques and analysis procedures are also useful for the resolution of lipid distributions in bilayers and ion distributions around double helical DNA. Simulations indicate that the frequency-domain method provides good resolution of the distance distribution functions.

M-Pos121 LIGAND-INDUCED ASSYMETRY AS OBSERVED THROUGH FLUOROPHORE ROTATIONS AND FREE ENERGY COUPLINGS: APPLICATION TO NEUROPHYSIN. Suzanne F. Scarlata* and Catherine A. Royer+, *AT&T, Princeton, N. J. 08540, +U. E. R. de Biochemie, Univ. de Paris VII, Paris 75005, France.

Changes that occur in subunit neurophysin structure upon ligand binding were explored by two methods. 1) The monitoring of the thermal coefficient of the viscosity around the subunit tyrosine by fluorescence polarization which yields information on the environmental flexibility and free rotational space of the fluorophore. Initially, it was determined that the environmental flexibility and the free space around each subunit tyrosine are unperturbed upon dimerization. Ligand binding causes these once homologous environments to become drastically different such that one moves onto a closely-packed environment whereas the other moves into a region of large free space. Even though the subunits as seen by each tyrosine are very different, the binding sites as seen by the ligands are similar. It was also found that ligand binding is stabilized by ring stacking and that energy transfer occurs between the tyrosine of the ligand and the neurophysin subunit tyrosine. 2) Changes in subunit structure upon ligation were also followed by the determination of the order of free energy coupling between ligand binding and oligomerization which tells how each ligand affects the subunit affinity. Since the binding of ligand is cooperative and induces dimer formation, the order of couplings between ligand binding and dimerization is second. Therefore, the binding of the second ligand is responsible for the increase in subunit affinity. This work was supported by U.S.P.H.S. grant (GM 11223) to Gregorio Weber.

M-Pos122 INTERACTION OF FATTY ACID BINDING PROTEIN (FABP) WITH FLUORESCENT ANALOGUES OF FREE FATTY ACIDS. *J. Storch, *A.M. Kleinfeld, ‡N. M. Bass and ‡‡H. Shields, *Harvard Medical School, ‡‡ Beth Israel Hospital, Boston, MA 02115, and Univ. Calif. San Francisco, CA 94143.

Spectral properties of the series of n-9-anthroyloxy-stearate derivatives (AOffa) were used to investigate the interaction of long chain ffa with hepatic FABP, a 14,000 m.w. cytoplasmic protein, and to compare such interactions with ffa-phospholipid bilayer interactions. The fluorescence quantum yield (Q) was found to increase as AO attachment site increases from the carboxy terminal: Q(2AS)=0.28, Q(9AS)=0.34 and Q(12AS)=0.44, a trend similar to that found for AO in egg phosphatidylcholine. In contrast to the uniform decrease in steady state polarization with attachment site observed in membranes, the P values of the protein-bound AOffa increase with AO position, achieving a maximum at C7. P values were significantly higher for FABP-bound (e.g., 0.11 for 12AS) than lipid-bound probe (0.06 for 12AS). Excited state lifetimes of FABP-bound AOffa were determined by the phase-modulation technique and showed a mirror image trend compared to P, i.e., τ decreased with distance from the carboxy terminal, with an absolute minimum value at C7. τ_{mod} values were 12, 9, and 11.5 ns for 2AS, 7AS and 12AS respectively. The relative FABP vs. membrane affinity of the AOffa was determined using small unilamellar vesicles (SUV). For all probes examined, the affinity for FABP was about an order of magnitude greater, on a molar basis, than for the SUV. These data suggest that FABP-bound AOffa are tightly buried within a hydrophobic pocket and their motion is most restricted at the center of the fatty acyl chain. Supported by a grant-in-aid and done during an Established Investigatorship (AMK) and a research fellowship (JS) from the American Heart Association and the Massachusetts Affiliate, Inc.

M-Pos123 PHOTOINDUCED CHANGES OF LENS CRYSTALLINS IN RELATION TO THEIR TERTIARY STRUCTURE. B. Chakrabarti, K. Mandal, and S.K. Bose, Eye Research Institute, Boston, MA 02114.

The possible role of light in the etiology of human cataract is of intense research interest. Recently we have shown that sensitized photooxidation causes a major change in the tertiary structure of α-crystallin, but the nature of the changes varies for different sensitizer molecules, namely methylene blue (MB) or riboflavin (RF). Studies have now been extended to β- and γ-crystallin using MB as a sensitizer. Fluorescence and near-UV CD of the proteins were monitored to probe the change in secondary and tertiary structure. For β-, a red shift (4-5 nm) in Trp emission as well as a major change in near-UV CD (but no change in far-UV) can be observed following the MB-sensitized reaction. However, the change in fluorescence and CD parameters are very different from that of α-crystallin. γ-crystallin, on the other hand, becomes turbid upon irradiation, unless SH groups are protected by labeling with iodoacetamide, and even then irradiation needs to be done in the dilute solution. This indicates that both disulfide and non-disulfide type crosslinks or aggregations are involved in this photoreaction. The variations in the nature of the photoinduced changes in conformation among lens crystallins are attributed to differences in their tertiary structure.

M-Pos124 INFLUENCE OF pH ON "STEADY STATE" AND "DYNAMIC" FLUORESCENCE PROPERTIES OF CHOLERA TOXIN. M. DE WOLF[1], G. VAN DESSEL[2], A. LAGROU[1], H.J. HILDERSON[1] and W. DIERICK[1,2].
[1]RUCA-Laboratory for Human Biochemistry and [2]UIA-Laboratory for Pathological Biochemistry, University of Antwerp, Groenenborgerlaan 171, B2020 Antwerp (Belgium)

The fluorescence intensity of cholera toxin is highly pH-dependent. In the pH range 7-9.5 it reaches a maximum corresponding to a quantum yield of 0.076. In the pH range 4 to 7 a strong increase in fluorescence intensity is observed ($\Delta Q/Q_{max}$ = 0.64). Evaluation of the pH sensitivity of the fluorescence intensity of the A and B subunits reveals that the B subunit is mainly responsible for the observed pH effect ($\Delta Q/Q_{max}$ for B subunit = 0.64). The intensity changes are paralleled by similar although less pronounced changes in the average fluorescence excited state lifetime τ ($\Delta\tau/\tau_{max}$ = 0.44 for CT). Fluorimetric titration of the B subunit which is related to the indole fluorescence of the lone Trp 88 reveals that the fluorescence intensity changes in the pH range 4-7 are due to reaction of two types of ionizable quenchers displaying apparent pK_a values of 4.4 and 6.2 respectively. It is suggested that the increase in fluorescence intensity with a midpoint at pH 6.2 is the result of deionization of the imidazolium side chain of one or two out of the four histidine residues present in each β-polypeptide chain whereas a deionized carboxyl group is responsible for the quenching with midpoint at pH 4.4. Complex formation of CT or B with GM_1 completely prevents the quenching and dissociation of B in its constituent monomers at low pH. Our data indicate that binding to the receptor prevents protonation of certain amino acid side chains committed to β-polypeptide association leading to a preservation of the multimeric nature of CT which is essential for binding.

M-Pos125 CHANGES IN TRYPTOPHAN FLUORESCENCE OF EEL TROPONIN-C MEDIATED BY BINDING OF Ca^{2+} AND LANTHANIDES. F. G. Prendergast, J. M. Francois*, R. Alcalat, E. Grattont, and C. Gerday*. Department of Biochemistry, Mayo Foundation, Rochester, MN 55905; *University of Liege, Belgium; †Department of Biophysics, University of Illinois, Urbana, IL 61801.

The aminoacid sequence of eel troponin-C (TnC) is homologous with TnC from rabbit skeletal muscle but has a tryptophan substituted for a phenylalanine residue at a single location, and is devoid of tyrosine residues. The absence of tyrosine reduces the ambiguity in interpretation of the fluorescence emission properties of tryptophan in this protein. The protein binds Ca^{2+} and lanthanide ions with high affinity. Metal ion binding causes a 20 nm blue shift in the tryptophan emission spectrum, a decrease in the apparent accessibility of the fluorophore to water soluble quenchers, a marked increase in fluorescence anisotropy and a change in the near UV CD spectrum which is attributable to the tryptophan residue. We have used multifrequency phase fluorometry (with a laser excitation source) to examine the dynamics of the tryptophan moiety in the presence and absence of Ca^{++} as determined by time resolved intensity and anisotropy decays. Supported by GM34847.

M-Pos126 FLUORESCENCE LIFETIME DISTRIBUTIONS IN SINGLE TRYPTOPHAN PROTEINS. J. R. Alcala (*), G. Marriott (**), E. Gratton (*) and F. G. Prendergast (***). (*) Department of Physics, and (**) Department of Biochemistry, University of Illinois, Urbana, IL 61801. (***) Department of Pharmacology, Mayo Foundation, Rochester, MN 55905.

The conventional analysis of the fluorescence decay curve consists of determining the number and relative amplitude of exponential components. Our studies suggest that for some proteins this is not the case and the resolution of the decay curve using two or more exponentials is an approximation. Using our high resolution technique based on frequency domain fluorometry we show that the decay is better described by a continuous distribution of decay times. We have analyzed the observed decay using different distributions of lifetime values. The Lorentzian distribution function better described the data. We have also used the superposition of two and three different Lorentzians to better account for the real shape of the lifetime distribution. Furthermore, using this approach it is possible to determine if a distribution is unimodal or multimodal. We have studied the evolution of the lifetime distribution over a temperature range from 4C to 33C for a series of proteins (RNAse T1, Scorpion NTV3 and PLA2) and down to -48C for azurin in 80% glycerol. Our results indicate that an increase in temperature causes a shift of the average value of the distribution to shorter lifetime and also causes a narrowing of the distribution. We interpret these observations as an evidence that the dynamics of the protein is involved in the generation of the lifetime distribution. Alternative explanations will be presented. Supported in part by the National Science Foundation grant NSF PCM84-03107 and the Department of the Navy grant MDA903-85-K-0027.

M-Pos127 FLUORESCENCE LIFETIME STUDIES ON THE SULFHYDRYL GROUPS OF BOVINE LENS CRYSTALLINS IN A PHOTODYNAMIC SYSTEM Usha Andley and Jack Liang, Howe Laboratory, Harvard Medical School, Boston, Massachusetts.

Photochemical mechanisms have been implicated in the changes in lens proteins observed in the aging and cataractous human lenses. In this study, the effect of light and photosensitizers on the conformation of isolated lens crystallins was investigated. Fluorescence lifetime measurements were used to study the change in microenvironment of sulfhydryl (SH) groups of bovine lens crystallins in a photodynamic system generating singlet oxygen. α, β and γ-crystallins were irradiated with visible light in the presence of the photosensitizers methylene blue or riboflavin. The proteins were labeled with N-iodoacetyl-N'-(5-sulfo-1-naphthyl)ethylenediamine (IAEDANS) before and after irradiation. The major component of the lifetime of AEDANS-α-crystallin decreased from 15 ns for the control to 6 ns for the irradiated protein, indicating a change in the microenvironment of SH groups to a more exposed one. In the case of β-crystallin, no change in the lifetime was found, which remained at 14.5 ns for both control and irradiated samples. The lifetime of AEDANS-γ-crystallin decreased from 14 ns for the control to 11.6 ns for the irradiated protein. The total SH content of the proteins was measured by titration with 5-5'dithiobis (2-nitrobenzoic acid) (DTNB). β-crystallin showed the largest decrease in total SH by irradiation. A decrease of 27 %, 50% and 37% in the number of SH of α-, β- and γ-crystallins, respectively, was observed after 5 h of irradiation. These results are consistent with the exposed position of SH groups of β-crystallin, and suggest that the rapid crosslinking and change in tertiary structure by singlet oxygen, observed previously for β-crystallin, might be due to oxidation of its exposed SH to S-S.

M-Pos128 CALORIMETRIC AND SPECTROSCOPIC INVESTIGATION OF THE STABILITY OF PHENYLMETHYLSULFONYL-CHYMOTRYPSIN. Marcelo M. Santoro and David W. Bolen, Department of Chemistry and Biochemistry, Southern Illinois University, Carbondale, Illinois 62901.

We have initiated spectrophotometric and differential scanning calorimetric studies of some derivatives of α-chymotrypsin (α-CT) in an attempt to delineate the number of cooperative units(domains) within them as well as evaluate the thermodynamic parameters associated with these transitions.Due to its reported chemical stability we have started with phenylmethylsulfonyl--chymotrypsin(PMSCT) and we present here preliminary DSC results for the denaturation of this protein.The data were collected on a Microcal MC-2 calorimeter at a scan rate of 1°C/min and at a protein concentration of 0.5-0.8 mg/ml.Glycine 0.01 M buffers in the pH range of 3.0-4.0 were used and aggregation of the denatured protein was avoided by lowering the protein concentration employed,as well as the ionic strength of the buffer.The denaturation profile showed a single endothermic peak in all cases and the ratio calorimetric to van't Hoff ΔH is equal to unity within 10% error.The mean molar enthalpy change is a linear function of temperature of denaturation(Tm) and the estimated value at 25°C is 77 Kcal/mole.Evaluation of denaturation free energy at pH 4.0 and 25°C for this protein was done by ultraviolet difference spectroscopy at 293 nm, using urea and guanidine hydrochloride as denaturants.A single transition was observed and linear extrapolation to zero denaturant concentration of a ΔG versus denaturant concentration plot gives,within experimental error,the same result with both denaturants,the mean value being 9.0 Kcal/mole.Similar to α-Ct, this protein undergoes a single denaturing cooperative conformational change in the acid pH range which is well described by a one-step model of transition between two macroscopic states.

M-Pos129 THERMODYNAMICS OF THERMAL DENATURATION OF VARIANTS OF T4 LYSOZYME CONTAINING DUAL AMINO ACID REPLACEMENTS EACH OF WHICH INDIVIDUALLY LOWERS THE STABILITY OF THE FOLDED PROTEIN

W.A. Baase, D.C. Muchmore and W.J. Becktel Inst. of Mol. Biol., Univ. of Oregon, Eugene, OR 97403

The thermodynamics of thermal denaturation of wild-type bacteriophage T4 lysozyme and four temperature sensitive variants have been determined as a function of pH over the range 2 to 6.5 using circular dichroism spectroscopy at 223nm. Variants of T4 lysozyme containing pairs of these substitutions were constructed and the thermodynamics of unfolding of the dual variants were also determined as a function of pH over this range.

All T4 lysozymes containing single and dual temperature sensitive substitutions were found to have essentially the same difference in heat capacity of unfolding. To a first approximation, the temperatures of melting (Tm) of the dual variants were lowered as a simple sum of the melting temperature depressions taken relative to the wild type enzyme of the single point variants from which they are constructed. A concomitant decrease in the enthalpy and entropy of unfolding was also found. Calculated free energies of unfolding at a given temperature were found to be additive. The approximate additivity of melting temperatures can be explained most easily by the observed additivity of the free energies. For these examples, at least, it is clear that the contributions from each amino acid substitution to the overall stability of the variant proteins were transferable from variant to variant and hence were unique.

This study has been extended to amino acid substitutions can which thermally stabilize T4 lysozyme (see Becktel, Baase, Wetzel and Perry, these abstracts) where a similar additivity of thermal effects is seen.

M-Pos130 THERMODYNAMICS OF THERMAL DENATURATION OF VARIANTS OF T4 LYSOZYME WHICH ALL CONTAIN THE ILE 3 -> CYS SUBSTITUTION IN THE PRESENCE AND ABSENCE OF THE C3-C97 DISULFIDE BRIDGE

W.J. Becktel and W.A. Baase Institute of Molecular Biology, Univ. of Oregon, Eugene, OR 97403
R. Wetzel and L.J. Perry Genentech, Inc., 460 Pt. San Bruno Blvd., S. San Francisco, CA 94080

Gentle oxidation of bacteriophage T4 lysozyme where isoleucine 3 has been replaced by cysteine (I3C) results in the formation of a disulfide bridge between C3 and C97 [L.J. Perry & R. Wetzel (1984) Science 226,555-557]. Circular dichroism at 223 nm has been used to follow the thermal denaturation of this protein in both the oxidized and reduced forms from pH 1 to 7, a range over which the denaturation can be made reversible. Variants of the IC3 protein containing additional amino acid replacements which independently reduce the thermal stability of T4 lysozyme to different extents have also been studied in both the oxidized and reduced forms.

We find that the formation of the C3 to C97 disulfide bridge results in an increased temperature of thermal denaturation. Moreover, oxidized IC3 is, itself, clearly thermally stable relative to the wild type enzyme. The entropy and enthalpy of denaturation as well as the difference in the heat capacity of the folded and denatured states changes dramatically upon formation of this single, covalent bond. Finally, for all substitutions investigated to date, the thermal behavior of the amino acid substitutions is additive; i.e., the behavior of variants with multiple amino acid replacements is the simple sum of that of the individual parental variants (see also Baase, Muchmore and Becktel, these abstracts). Stabilizing and destabilizing amino acid replacements compensate for one another in the determination of the overall thermal stability of each variant.

M-Pos131 EQUILIBRIUM UNFOLDING STUDIES OF BOVINE GROWTH HORMONE: A REVERSIBLY SELF-ASSOCIATING INTERMEDIATE H.A. Havel, E.W. Kauffman, D.N. Brems and S.M. Plaisted, Control Analytical R&D, The Upjohn Company, Kalamazoo, MI 49001

One approach to studying the forces which stabilize the three-dimensional structure of native proteins is to use physicochemical methods to characterize the structural rearrangements of a protein as the protein chain folds or unfolds. We have previously reported that bovine growth hormone (somatotropin, bGH)unfolds in guanidine hydrochloride through a reversible multi-state process with stable equilibrium intermediates (D.N. Brems et.al. 1985. Biochemistry 24: in press). Recently, we have obtained similar results for bGH unfolding in urea. One of the intermediate structures, observed with both chemical denaturants, has been identified as a self-associated form of bGH by measuring the bGH concentration dependence of optical probes and by hydrodynamic measurements (size exclusion HPLC, static and dynamic light scattering). The apparent maximum concentration of the self-associated intermediate occurs when bGH is partially denatured, i.e. at 3.7 M Gdn HCl or 8.5 M urea. The self-associated species is characterized by a) quenched tryptophan fluorescence, b) increased tryptophan CD intensity, c) a weight-average radius of about 5 nm, d) reversible formation and e) no further increase in size once the bGH concentration exceeds 2 mg/mL. We have also obtained evidence that α-helix regions of bGH are involved in the self-association and that this type of self-association occurs for all denaturing conditions investigated.

M-Pos132 ORIGIN OF THE SLOW PHASE IN THIOREDOXIN REFOLDING. Robert F. Kelley and F.M. Richards, Yale University, New Haven, CT 06511.

Refolding of guanidine hydrochloride (Gu) denatured E. coli thioredoxin (trx) in 2 M [Gu], pH 7 at 25°C detected by trp fluorescence measurements is dominated by a slow kinetic phase (τ=560 s, α=0.79) that has features characteristic of proline peptide bond isomerization. Kelley and Stellwagen (Biochemistry (1984) 23, 5095) have proposed that the slow phase can be accounted for solely by the isomerization of pro-76; of the five proline residues in trx only pro-76 has the cis configuration in the native protein. We are testing this hypothesis by examining the folding kinetics of trx mutants with single amino acid replacements of the proline residues. TrxA76, a proline to alanine change at position 76, displays 5% of the specific activity and a 6-fold greater trp fluorescence emission spectrum relative to wild type. TrxA76 unfolds in a cooperative and reversible equilibrium transition centered at 1.0 M [Gu] as determined by trp fluorescence measurements. The slowest kinetic phase observed for refolding of trxA76 in 0.7 M [Gu] has a time constant of 30 s and accounts for 50% of the equilibrium increase in fluorescence intensity accompanying refolding. In contrast, trxS34, a proline to serine change at position 34, has a specific activity, trp fluorescence emission spectrum and equilibrium midpoint for Gu induced unfolding (2.4 M) almost identical to wild type. A slow phase (τ=500 s, α=0.83) is detected for refolding trxS34 in 2 M [Gu]. As determined for the wild type protein, multimixing experiments indicate this phase results from an equilibration between fast and slow folding denatured states. We conclude that assignment of the slow phase in thioredoxin refolding to the isomerization of only pro-76 is consistent with these data. (Supported by NIH Program Project Grant GM22778.)

M-Pos133 GUANIDINE DENATURATION OF BOVINE HEART CYTOCHROME C OXIDASE.
Bruce C. Hill & Neal C. Robinson, Department of Biochemistry, The University of Texas Health Science Center, San Antonio, TX 78284.

The denaturation of isolated cytochrome c oxidase as a function of guanidineHCl concentration occurs in two phases. This biphasic denaturation pattern was observed by UV and Soret circular dichroism, Soret absorbance and intrinsic tryptophan fluorescence spectral measurements. The CD signal at 220 nm of cytochrome oxidase decreases in intensity as the gdnHCl concentration is raised: one phase occurs between 0 and 2 M and the second phase between 2 and 7 M gdnHCl. In contrast, the Soret CD signal at 426 nm is completely lost at 2 M gdnHCl. Between 0 and 2 M gdnHCl the Soret absorbance spectrum shifts from 419 to 423 nm with little change in intensity, and from 2 to 7 M gdnHCl the intensity declines by 30% while the spectrum remains at 423 nm. Changes in the tryptophan fluorescence signal are also indicative of a biphasic denaturation process. The intensity of fluorescence emission increases from 32.5% in the native enzyme to about 90% at 2 M gdnHCl, relative to a tryptophan analog. Above 2 M gdnHCl the fluorescence intensity decreases to about 40% at 7M gdnHCl. This data indicates that in the cytochrome c oxidase complex there are regions of different guanidine sensitivity and that the heme containing portion of the protein is more sensitive to denaturation than the rest of the protein. Supported by NIH Grant GM 24795.

M-Pos134 UREA AND THERMAL STABILITY OF THIOREDOXIN VARIANTS ALTERED IN THE ACTIVE SITE AMINO ACID SEQUENCE by Knut Langsetmo, Geoffery Hahn, James Fuchs and Clare Woodward, Department of Biochemistry, University of Minnesota, St. Paul, MN 55108.

E. coli thioredoxin is a small, stable globular protein containing one disulfide bond. The reduced form of the protein $(SH)_2$ acts as a hydrogen donor in the enzymatic reduction of ribonucleotides to deoxyribonucleotides. The redox-active disulfide bond is formed by Cys32-Cys35, in the highly conserved active site sequence Cys-Gly-Pro-Cys. Unlike many proteins, the disulfide form of thioredoxin is markedly less stable to urea and temperature denaturation than the dithiol form. It is generally expected that the introduction of a disulfide bond will stabilize protein structure. The reason for the difference in stability of reduced and oxidized thioredoxin may be a strain in the Cys-Gly-Pro-Cys ring. To test this we have constructed plasmids with two variants of the active site sequence, one with a Ser for Pro substitution, and one with an Arg insertion between Gly and Pro. The Ser substitution is obtained from the temperature sensitive $fip^-, ^{TS}$ chromosomal gene cloned into M13 mp13 after digestion of the chromosomal DNA with restriction enzymes Pst and Kpn. The Arg insertion was constructed from the plasmid carrying the cloned thioredoxin gene (Lim et al., J. Bact. 163, 311-316) by AvaII digestion, followed by treatment with DNA polymerase I to fill in the single strands and then by ligation of the blunt ends. The Ser substitution produces a protein that is more stable than the wild type, but which still retains the large difference in stability of the oxidized and reduced forms.

M-Pos135 CHARACTERIZATION OF BETA-LACTAMASE FOLDING

Linda J. Calciano, Anthony L. Fink, and Debbie J. Joy, Department of Chemistry, University of California, Santa Cruz, CA 95064

The reversible unfolding and refolding of beta-lactamase I from B.cereus was investigated as a function of urea, pH and temperature. The folding process was monitored by fluorescence, absorbance, circular dichroism (cd) and catalytic activity. The major conclusions are as follows. Low pH induces a reversible isomerization in the enzyme involving substantial unfolding and loss of catalytic activity. The mid-point of the transition is solute-dependent. At low ionic strength it is at pH 3.0, increasing to pH 4.0 at 0.5M. The mid-point of the transition in urea is 4M, as measured by fluorescence. The kinetics of unfolding in urea are unusually slow when measured by fluorescence (1.7×10^{-5} s^{-1} at 25°C), and are somewhat faster if measured by loss of catalytic activity. Refolding kinetics in urea are faster when measured with cd and fluorescence than by return of catalytic activity. The mid-points of the urea-induced unfolding transition are not superimposable when measured with fluorescence, cd and loss of catalytic activity. These observations are consistent with the existence of populated intermediate states in the unfolding and refolding of beta-lactamase.

M-Pos136 CYSTEINE RESIDUES IN γ-CRYSTALLINS: DIFFERENCES IN ARRANGEMENT AND ACCESSIBILITY.

K. Mandal, S.K. Bose, B. Chakrabarti, Eye Research Institute, Boston, MA 02114, and R. Siezen, Dept. of Physics, M.I.T., Cambridge, MA

The three major bovine γ-crystallin fractions (γ-II, γ-III, and γ-IV) are known to have closely related amino acid sequences and three-dimensional folding of the polypeptide backbone. The emission properties of theses crystallins labeled with the sulfhydryl-specific probe, 2-(4'-maleimidyl-anilino)naphthalene 6-sulfonic acid (MIANS) are now shown to differ distinctly. The fluorescence maximum (λ_{ex} = 328 nm) of the probe attached to the sulfhydryl group of the protein appears at 430, 433, and 435 nm for γ-II, γ-III, and γ-IV, respectively. The maximum for γ-III and γ-IV does not shift with varying concentration of the probe, whereas for γ-II crystallin it shifts from 430 to 420 nm with increasing concentration of the probe, suggesting that the microenvironments of the sulfhydryl groups are different. Analysis of the time and concentration (dye)-dependent fluorescence of the labeled protein further indicates that at least more than one class of SH groups exists in each crystallin and the accessibility of each class of thiols is different. Measurements of possible Forster-type energy transfer from tryptophan (Trp) to the MIANS-labeled cysteine (Cys) residues show energy transfer with a distinct isoemissive point in the case of γ-II and γ-III, whereas in γ-IV, no such transfer takes place.

M-Pos137 INTRAMOLECULAR DISULFIDE LOOP FORMATION IN A PEPTIDE CONTAINING TWO CYSTEINES

G.H. Snyder , Dept. of Biological Sciences, State Univ. of N.Y., Buffalo, N.Y. 14260

Each of the six rate constants has been determined for the disulfide exchange reaction between oxidized N-acetylcysteine methyl ester (○-SS-○) and a peptide containing two cysteines. The cysteines are separated by eight amino acids in the primary sequence. In concentrated guanidine hydrochloride, k-LOOP = 0.35 events/sec for a fully ionized thiolate group. This provides a frame of reference for loop formation in a sterically unrestricted peptide. This value is easier to interpret than published rate constants for steps in the oxidation of reduced proteins containing six or eight cysteines. These results also demonstrate the feasibility of using a linear disulfide reagent (○-SS-○) to investigate factors affecting loop formation in a series of small synthetic peptides.

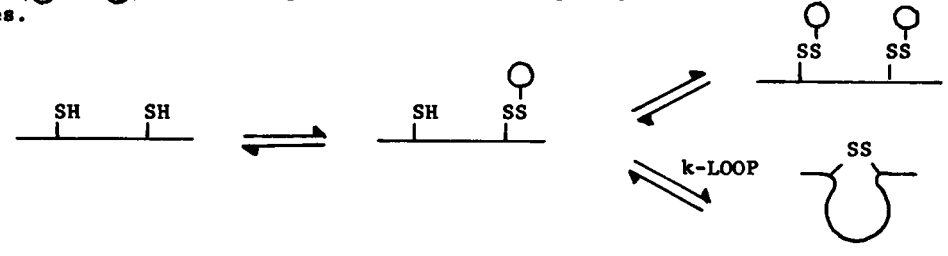

M-Pos138 THE KINETICS OF HUMAN APOLIPOPROTEIN A-I FOLDING REACTIONS. William W. Mantulin, Roger D. Knapp and Henry J. Pownall. Baylor College of Medicine and The Methodist Hospital, Department of Medicine, Houston, TX 77030

Apolipoprotein A-I (apo A-I), the major protein constituent of human plasma high density lipoprotein (HDL), is a surface active, conformationally adaptive protein. Examples of structural adaptability include a low free energy of denaturation (2-4 kcal/mol) and labile displacement of apoA-I from the HDL surface. Apo A-I activates lecithin:cholesterol acyltransferase, the major cholesteryl ester forming enzyme in plasma, through a protein-protein interaction on the HDL surface. Thus, the structure-function relationship in apoA-I centers on structural dynamics. We have measured the kinetics of apoA-I folding reactions, both denaturation and refolding, by fluorescence detected stopped flow. The guanidinium chloride (GdmCl) induced equilibrium curve for apoA-I shows a midpoint at 1.1 M GdmCl. Concentration jumps in GdmCl, corresponding to apoA-I denaturation, reveal a single kinetic phase (1-3 sec at 20°C) throughout the entire equilibrium curve. Dilution of GdmCl results in apo A-I refolding and yields bi-exponential decay curves. A computer generated stripping function separates a small amplitude long phase (5-12 sec) from a large amplitude short phase (0.5-1.5 sec). These data are consistent with a refolding scheme for unfolded (U) apoA-I, involving slow and rapid conformational changes, finally resulting in a native conformation (N). $U_s \longleftrightarrow U_r \longleftrightarrow N$. We tentatively assign the slow kinetic phase to a rate limiting proline cis-trans isomerization reaction. The rates of apoA-I folding may thus govern its functional efficacy and transfer rates between HDL. (HL27104).

M-Pos139 KINETIC MEASUREMENTS OF THE VOLUME CHANGE ASSOCIATED WITH THE FOLDING OF DENATURED THIOREDOXIN. William Shalongo, Jane Wilson and Earle Stellwagen, Department of Biochemistry, University of Iowa, Iowa City, IA 52242

E. coli thioredoxin is a globular protein containing 108 residues in a single polypeptide chain. The polypeptide is folded into a compact native structure containing a central twisted sheet with flanking helices. The native protein is reversibly unfolded in a single cooperative transition centered at 5 M urea at 2 degrees. The unfolding of the native protein occurs in a single kinetic phase while the refolding of the denatured protein occurs in three kinetic phases as detected by tryptophan fluorescence emission measurements. The compact native protein and the unfolded denatured protein can be resolved in less than 10 minutes by exclusion chromatographic measurements at 40 bars pressure. Equilibrium and kinetic exclusion chromatographic measurements indicate that each of the two faster refolding phases generates a compact folding intermediate and that the slow refolding phase represents the conversion of the compact intermediates into the native conformation. Supported by Public Health Service research grant GM22109 and program project grant HL14388.

M-Pos140 LYSOZYME SECONDARY STRUCTURE FOLDING KINETICS BY CONSTANT FLOW RAMAN SPECTROSCOPY Robert W. Williams and Sheila Loughran, Department of Biochemistry, Uniformed Services University of the Health Sciences, Bethesda, MD 20814-4799.

Lysozyme, 32% (0.022 M), in 4.8 M guanidine HCl (GnHCl) was diluted with water in a rapid mixing constant flow apparatus to 1.2 M GnHCl. Time for the folding reaction was varied from 5 milliseconds (ms) to 500 ms by changing the length of capillary tubing between the mixing cell and the measuring cell. The Raman spectrum in the region between 1170 and 1500 wavenumbers was measured with a diode array detector.

This region is free of intense GnHCl bands. At 22° C and 5 ms the amide III Raman spectrum is that of folded lysozyme. At 5° C the 5 ms spectrum is similar to that of unfolded lysozyme and spectra collected at 40 ms show that helical secondary structure is forming. Several bands appear to change, including the secondary structure sensitive amide III band and the 1360 wavenumber tryptophan band, giving a simultaneous measurement of different structural probes. The fluorescence background is very high in these experiments. A single time point is the average of many days experiments.

M-Pos141 NON-ENZYMATIC GLYCOSYLATION IN HUMAN DIABETIC LENS PROTEINS. Jack Liang and Usha Andley Howe Lab, MEEI, Harvard Medical School, Boston, MA

Lens proteins have been found glycosylated in aged and diabetic lenses. The site of glycosylation has been determined primarily in lysine residues. We have isolated glycosylated α-crystallin from senile human diabetic lenses and studied its conformation by physicochemical measurements. It appears that glycosylated proteins become more unfolded and undergo further secondary changes. There is an increased blue fluorescence and a decrease of sulfhydryl groups. The different tertiary structure is manifested in the change of the near ultraviolet circular dichroism, a shift of emission maxima in tryptophan and covalently labelled extrinsic fluorescent probes. We also have used induced glycosylated poly-L-lysine and other proteins to see what kind of effect the glycosylation is on conformation. There is controversy whether glycosylation plays any major role in diabetic cataract. The differences in conformation observed in glycosylated proteins suggest that glycosylation may have some contribution in the altered conformation and possibly function.

M-Pos142 POLYPEPTIDE-GLYCAN CHAIN INTERACTIONS IN OROSOMUCOID. K.T. Schlueter, M.L. Friedman, H.B. Halsall, Dept. of Chemistry, Univ. of Cincinnati, Cinti., OH 45221-0172.

Orosomucoid (OMD) is a heavily glycosylated human serum glycoprotein containing ~40% carbohydrate. It contains five complex-type glycan chains which can be bi-, tri-, and/or tetraantennary. We are using this as a model system to examine the role(s) of glycan chains in glycoproteins. In this work we have prepared biantennary OMD using lectin affinity chromatography, and compared the accessibility to its surface with the tri-/tetra-antennary form. The efficiencies (K_Q) and fractional (fa) quenching of the intrinsic fluorescence of the OMD by chlorpromazine (CPZ), Cs^+, I^- and acrylamide were used for these comparisons. In addition, the thermal stabilities of the antennary forms have been compared. Essentially no differences in accessibility were seen. This is somewhat unexpected since the surface occlusion by the chains has been reduced by some 40%, and would suggest therefore that a rather asymmetric chain dispersal exists on the surface. It does, however, indicate that the putative negatively charged NeuNAc residue proximal to the CPZ binding site (Biophys. J. 47 (1985) 409) originates from a biantennary chain. This would further imply the existence of a glycosylation site restricted for the biantennary glycan chain. No differences were seen in thermal stability, indicating that the primary function of the glycan chains is not the conferral of protein core integrity.

M-Pos143 FUNCTIONAL OCTOPUS HEMOCYANIN MOLECULES ARE ASSEMBLED FROM A SINGLE TYPE OF SUBUNIT. K.I. Miller and K.E. van Holde, Dept. Biochemistry-Biophysics, Oregon State University, Corvallis, OR 97331, J. Lamy and J. Lamy, Francois Rabelais University, Tours, France

Hemocyanin of Octopus dofleini consists of 51S decameric molecules ($M \approx 3.5 \times 10^6$). It can be dissociated into 11S subunits by removing divalent cations. The subunit has been shown to be a single immunologically distinct polypeptide chain, ($M = 3.5 \times 10^5$), containing seven oxygen binding domains. Seven globular regions are clearly seen in the electron microscope, and limited proteolysis reveals seven immunologically different domains. A tentative sequence for these domains within the polypeptide chain has been determined, and initial N terminal sequences for purified domains are underway. The subunits can be quantitatively reassembled to decamers, upon the addition of divalent cations, with the uptake of 3-4 cations per subunit. The kinetics of this reaction have been studied by light scattering. After an initial lag phase, the association accurately follows second order reaction equations. The proposed mechanism involves an initial pseudo-first order isomerization reaction involving divalent ions, followed by a rate limiting dimerization process. Subsequent steps are very fast. Evidence for the isomerization can also be obtained from stopped flow fluorescence experiments. Reassociated molecules bind oxygen almost identically with native hemocyanin. Oxygen binding by subunits indicates heterogeneity of function among the domains. This observation, combined with immunological and sequence differences, and the observed uptake of only 3-4 divalent cations during association, leads us to propose considerable heterogeneity of structure and function among domains.

Supported in part by NSF Grant #PCM82-12347.

M-Pos144 ISOLATION AND PHYSICO-CHEMICAL CHARACTERIZATION OF α-SUBUNIT OF BOVINE BRAIN S-100a PROTEIN. I. Leung, R.S. Mani, C.M. Kay, MRC Group in Protein Structure and Function, University of Alberta, Edmonton, Alberta, T6G 2H7 Canada.

Bovine brain S-100 is a mixture of 2 predominant isomers, S-100a and S-100b, with a subunit composition of αβ and ββ respectively. The α-subunit has been isolated from S-100a using a DEAE Sephadex A-25 column in the presence of 8 M urea. The α-subunit undergoes a conformational change upon binding Ca^{2+} and Zn^{2+}, as revealed by UV difference spectroscopy and CD studies in the aromatic and far UV range. In the presence of Ca^{2+}, the $[\theta]_{222}$ value decreased by 1700 deg.cm^2 dmole^{-1} and this was further reduced by 700 deg.cm^2 dmole^{-1} when Zn^{2+} was subsequently added to the same sample, suggesting that Ca^{2+} and Zn^{2+} bind at different sites on the α-subunit. Aromatic CD studies revealed that Ca^{2+} and Zn^{2+} induced different environments near the aromatic residues. UV difference spectroscopy showed that the tryptophan and tyrosine residues became more exposed to solvent on the addition of Ca^{2+}. Zn^{2+}, on the other hand, resulted in a small blue shift of these residues.

Fluorescence titration of the α-subunit with Ca^{2+} gave a K_d value of 1.26×10^{-4} M. In the presence of 90 mM KCl, the affinity for Ca^{2+} was lowered to 5×10^{-4} M. Sedimentation equilibrium studies showed that the α-subunit aggregates in the presence of Ca^{2+} and Zn^{2+}. The Ca^{2+} binding properties of the α-subunit are similar to that of S-100a, suggesting the Ca^{2+} binding sites are similar on both proteins.

(Supported by Alberta Heritage Foundation for Medical Research)

M-Pos145 KINETICS AND THERMODYNAMICS OF Zn^{2+}-INDUCED STACKING OF GLUTAMINE SYNTHETASE DODECAMERS Ann Ginsburg, John B. Hunt, Michael R. Maurizi, Philip G. Kasprzyk, and Marlana B. Blackburn, NHLBI, NIH, Bethesda, MD 20892

Glutamine synthetase (GS) from E. coli contains 12 identical subunits arranged in 2 superimposed hexagonal rings ~ 140 Å in diameter. Zn^{2+} binds at a site distinct from the active site of each subunit with $K_A' = 5 \times 10^6$ M^{-1} at pH 7.0 and with a concomitant release of one proton per Zn^{2+} bound. The binding of Zn^{2+} deforms the enzyme in such a way that when 50 mM $MgCl_2$ also is present, spontaneous face-to-face aggregation of GS dodecamers and later side-to-side interactions between twisted single strands occur. Fluorescence energy transfer measurements have shown that active-site nucleotide probes on layered dodecamers are ~ 36 Å apart. Kinetic studies of Zn^{2+}-induced stacking of GS dodecamers along the 6-fold axes of symmetry at pH 7.0 indicate that the initial process has a second-order rate constant of 5×10^4 M^{-1}s^{-1} at 25°C and an Arrhenius activation energy of 22.3 ± 0.2 kcal/mol. Enthalpy changes (ΔH) for (1) the binding of Zn^{2+} to GS with accompanying proton release and protein conformational changes and (2) the Zn^{2+}-induced aggregation of GS dodecamers and, as confirmation, (3) the reversal of reactions in (1) and (2) by addition of the Zn^{2+} chelator pyridine-2,6-dicarboxylate were measured by calorimetry at pH 7.0 and 30°C. In the absence of $MgCl_2$ at pH 7.0, the addition of 0.66 eq of Zn^{2+}/subunit produces no aggregation of GS (as monitored by light scattering) and ΔH = +80 ± 10 kcal/mol of GS for (1) at 30°C after correcting for buffer protonation. Essentially the same ΔH value was measured in the presence of 50 mM $MgCl_2$ at pH 7.0 and 30°C, indicating that ΔH ≈ 0 at 30°C for protein-protein interactions in (2). Thus, Zn^{2+}-induced stacking of GS dodecamers is entropically controlled at 30°C.

M-Pos146 CA(II) BINDING BY AEQUORIN. M. D. Kemple, M. L. Lovejoy, B. D. Ray, B. D. Nageswara Rao, Physics Dept., IUPUI, Indpls., IN 46223, and F. G. Prendergast, Dept. of Pharmacology, Mayo Medical School, Rochester, MN 55901

Aequorin is a bioluminescent protein of molecular weight 21,000 isolated from the jellyfish *Aequorea victoria*. Light is emitted from the excited state of a substituted pyrazine derived from oxidation of a noncovalently bound chromophore. The bioluminescent reaction is triggered by the binding of Ca(II) and Ln(III) ions, and is inhibited by Mn(II) and Mg(II). The Ca(II) concentration effect curves for the bioluminescence of aequorin, and an analysis of the amino-acid sequence of aequorin indicate that there are three Ca(II) binding sites on native aequorin. The competition of Ca(II) for the single Mn(II) site on aequorin as measured by EPR was used to probe the details of Ca(II) binding to aequorin. Ca(II) shows approximately half of the affinity of Mn(II) for that site which in turn is the strongest of the Ca(II) binding sites. The experiments are performed at 5°C to minimize the effects of Ca(II)-independent discharge of the protein. Competition of other ions with Mn(II) for the metal sites on aequorin will also be described.

(Acknowledgment is made to the donors of the Petroleum Research Fund, administered by the American Chemical Society. The work is supported in part by the grant NIH GM 30178.)

M-Pos147 LONG RANGE CONFORMATIONAL CHANGES INDUCED BY Na IN THE INTESTINAL Na/GLUCOSE COTRANSPORTER. B.E. PEERCE AND E.M. WRIGHT. DEPT OF PHYSIOLOGY UCLA, LOS ANGELES, CA 90024.

The Na-induced conformational change in the region immediately surrounding the glucose site (approximately 25Å) was examined using fluorescence energy transfer from tryptophans to anthracene isothioyanate bound to the glucose site. Those trp near the glucose site were selected by monitoring sensitized anthracene emission following trp excitation in the presence of trp quench reagents. Compared to the average brush border trp, those groups near the glucose site are in a more positively charged, less hydrophobic environment. The fraction of trp near the glucose site (f_a) accessible to acrylamide decreases from 45% to 23% and the Quench constant increases from $26M^{-1}$ to $79M^{-1}$ in the presence of Na. Cs-susceptible trp decrease from 16% to 10% and the Quench constant decreases from $157M^{-1}$ to $76M^{-1}$ with Na, in contrast to I where f_a increases from 28% to 48%. These results indicate that the Na-induced conformational change extends as far as 25Å away from the glucose site and results in increased solvent exposure, altered charge distribution and increased order around the site. Changes in Quench constants suggest a single class of surface accessible trp and at least 2 classes of hydrophobic trp near the glucose site. 53% are in a very hydrophobic environment and do not respond to Na. 47% are in a less hydrophobic region and respond to Na by moving into a more hydrophilic environment. (Supported by AM 19567, AM 34807 and AM 17328)

M-Pos148 CHARACTERIZATION OF A PHOSPHORYLATION AND CALMODULIN BINDING SITE FROM CHICKEN GIZZARD MYOSIN LIGHT CHAIN KINASE. T.J. Lukas, W. Lau, and F.G. Prendergast*. (Intr. by D. Martin Watterson) Dept. of Pharmacology, Vanderbilt Univ., Howard Hughes Medical Inst., Nashville, TN and *Dept. of Pharmacology, Mayo Clinic, Rochester, MN.

A cAMP-dependent protein kinase phosphorylation site in chicken gizzard myosin light chain kinase (MLCK) has been identified. The phosphorylation of this site in MLCK is diminished when reactions are done in the presence of calmodulin. A fragment of MLCK containing the phosphorylation site had the amino acid sequence: A-R-R-K-W-Q-K-T-G-H-A-V-R-A-I-G-R-L-S-S-S. The interaction of calmodulin with a synthetic peptide based on this sequence was characterized by using circular dichroism and fluorescence spectroscopies and by inhibition of the calmodulin activation of MLCK. The peptide had an estimated dissociation constant of 1 nM based upon inhibition kinetics and exhibited spectroscopic changes in the presence of calmodulin which are consistent with the induction of an alpha helical structure and apparent 1:1 stoichiometry. Additional peptides based upon the MLCK sequence and from a homologous region of the γ-subunit of phosphorylase kinase were also synthesized and tested as calmodulin inhibitors. These studies provide a model for calmodulin binding domains in structurally diverse calmodulin binding proteins.

Supported in part by National Institutes of Health Grants GM30861 (DMW) and GM31241 (FGP)

M-Pos149 CALCIUM-DEPENDENT THERMAL TRANSITIONS IN COMPLEMENT SUBCOMPONENTS $C1\bar{r}$ AND $C1\bar{s}$. T.F. Busby, S.A. Brew, M. Lennick, & K.C. Ingham. Biochemistry Laboratory, American Red Cross Biomedical R & D Labs, Bethesda, MD 20814

The first component of complement, C1, is a large multiprotein complex comprised of 3 subcomponents, C1q, r, and s, each containing multiple domains. Some domains are responsible for the Ca^{2+}-dependent associations which hold the complex together while others mediate the interaction with immune complexes or cellular receptors. Still others are responsible for the proteolytic action of C1 and for its reaction with C1-Inhibitor. We have initiated a study of the stability of C1 with initial emphasis on the activated forms of C1r and C1s. These homologous enzymes both melt irreversibly above 50°. The transitions are relatively insensitive to Ca^{2+} and produce a loss of esterolytic activity and ability to react with C1-Inh. In the presence of EDTA, both proteins exhibit an additional transition at lower temperature with no loss of activity or reaction with C1-Inh. The transitions are detected by increase in the fluorescence intensity of 1,8-anilinonaphthalene sulfonate (ANS), by changes in the fluorescence polarization of fluorescein-labeled derivatives, by light scattering, and by differential scanning calorimetry. The low-temp transition for $C1\bar{r}$ occurs with a midpoint near 32°C and is accompanied by the formation of soluble aggregates. The corresponding transition for $C1\bar{s}$ occurs near 42°C with no aggregation. It appears that the transitions above 50°C correspond to unfolding of the catalytic domains while those at lower temperature involve the Ca-binding regions. Studies are in progress to further characterize the effects of the low-temp transitions on protein-protein interactions between the subcomponents of C1.

M-Pos150 THE ROLE OF CALCIUM IN THE STRUCTURE OF CHONDROCALCIN.

S.S. Margossian, H.U. Choi, L.C. Rosenberg and H.S. Slayter, Montefiore Medical Center, Bronx, NY 10467 and Dana-Farber Cancer Institute, Boston, MA 02115

Chondrocalcin, a calcium-binding extracellular matrix protein was purified from epiphyseal cartilage (Choi, *et al.* (1983) J. Biol. Chem. 258, 655), and immunoelectron microscopy revealed it to be distributed in fetal epiphyseal cartilage. High speed sedimentation equilibrium analysis in H_2O/D_2O buffers gave a value of 0.714 cc/g for the partial specific volume and a molecular weight of 79,000 d. Inclusion of 1-10 mM $CaCl_2$ in the buffer (0.15 M NaCl, 0.05 M Tris, pH 7.4) did not result in any change in the molecular weight suggesting the absence of calcium-induced self-association. When the equilibrium centrifugation was performed in the presence of 2 mM DTT and 1 mM EGTA, the molecule dissociated into a single component with a molecular weight of 39 KDa which was identical to that obtained in 5 M GdmCl and DTT. Moreover, when the analysis was done in the presence of DTT, but not EGTA, the calculated molecular weight was 78 KDa, suggesting that the molecule was held together through calcium bridges in spite of the reduction of disulfide bonds. Electron microscopy of tungsten-shadowed molecules revealed a spherical molecule with two subunits clearly discernible. The individual subunits could be seen to be dissociated when prepared for electron microscopy in a buffer containing DTT and EGTA. Thus, both hydrodynamic and electron microscopic analyses reveal that calcium appears to play a central role in maintaining the proper conformation of chondrocalcin. (Supported in part by NIH grant HL 26569).

M-Pos151 Ca-BINDING SITE ON A NEUROFILAMENT PROTEIN OF THE MYXICOLA GIANT AXON. R. Abercrombie, K. Gammeltoft and L. Young, Department of Physiology, Emory University School of Medicine, Atlanta, Georgia 30322.

The buffering of calcium by cytoplasmic constituents of neurons has been recognized for some time. Of the suggested intraneuronal Ca buffers--i.e., mitochondria, endoplasmic reticulum, and cytoplasmic proteins--probably least is known about the cytoplasmic proteins. We report evidence that a protein associated with the neurofilament gel of the Myxicola giant axon contains a Ca-binding site, which has an affinity for Ca of ~0.2 μM, a capacity of ~200 μmoles/kg gel, and which binds Ca with positive cooperativity. These conclusions are based on Ca titration studies of solutions containing the axoplasmic proteins. The normal axoplasmic gel was changed to a liquid by dialyzing this material against a high ionic strength medium. The soluble axoplasmic proteins (those in the supernatant after ultracentrifugation of the sample) remained soluble even when the ionic strength was returned to normal, but could be converted back to a gel by freezing and thawing the sample. Calcium titrations of these proteins before gel formation were compared to titrations of the supernatant after removal of the gel. At pCa = 6.2, 78% + 6% (N=6) of the Ca-binding capacity departed the supernatant with the gel, yet only 40% +~6% (N=6) of the protein was lost. This suggests that the Ca-binding sites are located mainly on the gel-forming proteins. Polyacrylamide gel electrophoresis showed that three components of approximate molecular weight, 191 Kd, 169 Kd, and 155 Kd, departed the solution with the gel. From measurements of the protein concentration of the neurofilament gel and the concentration of Ca-binding sites in the gel, we calculate one site for 1,000 amino acid residues. (Supported by USPHS NS1919404.)

M-Pos152 **PHYSICAL DEMONSTRATION OF MULTIENZYME COMPLEX FORMATION BETWEEN SOLUBLE, INDEPENDENT, METABOLIC ENZYMES: THE YEAST ORNITHINE TRANSCARBAMOYLASE-ARGINASE REGULATORY COMPLEX.** Edward Eisenstein, Le T. Duong, Susan M. Green, James C. Osborne, Jr., Richard J. Feldmann, and Preston Hensley* (Dept. of Biochem., Georgetown U., Wash., D.C., Lab. of Cell Biol. and Genetics and Computer Center Branch, NIH, Bethesda, MD., and Beckman Instruments, Inc., Palo Alto, CA.)

To uncouple a potential futile urea cycle in *Saccharomyces cerevisiae*, a regulatory multienzyme complex forms between ornithine transcarbamoylase (OTCase) and arginase. Using purified proteins from yeast enzyme overproducing strains, we have confirmed that OTCase is 100% inhibited as a result of complex formation with arginase. This dramatic modulation of enzyme activity results from a one to one association of the two enzymes. This was demonstrated by analytical ultracentrifugation and electron microscopy. Equilibrium sedimentation of OTCase, arginase and the complex yields molecular weights of 110,000, 110,000 and 220,000, respectively. The latter data were analyzed in terms of an enzyme-enzyme dissociation constant of 6×10^{-8} M.

Electron microscopy demonstrates that the free enzymes are trimers with subunits which are oblate ellipsoids of revolution. The dimensions of the arginase subunit are 42 x 56 x 56 A (p=1.33), and those of the OTCase subunit are 39 x 59 x 59 A (p=1.51). Again, the enzymes were visualized in a one to one complex. The dimensions of the complex are 85 x 101 x 101 A. The frictional ratios due to shape for the free enzymes were calculated from these dimensions (1.02 for OTCase and 1.007 for arginase). Hydrodynamic frictional ratios for the two enzymes may be calculated from sedimentation velocity experiments (1.13 for OTCase and 1.06 for arginase). These results predict waters of hydration for OTCase and arginase of 0.26 and 0.12 gm H_2O/gm protein, respectively. These values are reasonable and suggest that the dimensions of the molecules determined from electron microscopy are similar to those of the molecules in solution.

M-Pos153 INTERACTION OF FIBRONECTIN WITH ISOLATED FLUORESCENT-LABELED CHAINS OF COLLAGEN AND COMPLEMENT Clq. B.S. Isaacs & K.C. Ingham, Biochemistry Laboratory, American Red Cross Biomedical R & D Labs, Bethesda, MD 20814

Fibronectin is a large multidomain protein which mediates the attachment of cells to collagen-coated surfaces. Clq, a subcomponent of the first component of complement, is also a large protein which contains a collagen like domain. Previous studies indicate that strong fibronectin-binding sites on solid-phase Clq and collagen become exposed only after the later are denatured. The resulting complexes are stable in 1 M NaCl but dissociate in urea. The present study aims to characterize the interaction of fibronectin with isolated chains of these molecules using fluorescein isothiocyanate (FITC) as a covalent probe. SDS-PAGE of reduced samples of FITC-labeled Clq and collagen produced well-resolved fluorescent bands which were excised from the gel, extracted into SDS-containing buffer, and dialysed against 6 M urea followed by distilled water and PBS (0.01 M Phosphate, 0.135M NaCl, pH 7.3). The C-chain of Clq was consistently less fluorescent than A or B suggesting less efficient labeling in the native molecule. In preliminary titrations with fibronectin in PBS at 25°, all three chains gave dose-dependent changes in fluorescence polarization with half-maximal responses between 0.5 and 1.0 x 10^{-7}M, close to that obtained with the FITC-α_1 chain of type I collagen. In all cases, the response was unaffected by 1M NaCl but could be reversed by 6 M urea. These studies, in addition to providing the first direct observation of a fluid-phase interaction between fibronectin and Clq, demonstrate the feasibility of isolating fluorescent-labeled chains by SDS-PAGE in sufficient quantitiy for fluorescent titration.

M-Pos154 RAMAN STUDIES ON METALLOTHIONEIN - A UNIQUE, PREDOMINANTLY 'TURN' CONTAINING PROTEIN. [1]J. Pande, [2]C. Pande, [1]M. Vašák, [2]R.H. Callender and [1]J.H.R. Kägi. [1]Biochemisches Institut der Universität Zürich, 8057-Zürich, Switzerland, and [2]Dept. of Physics, City College of New York, New York 110031, U.S.A.

Secondary structure prediction calculations have indicated a high potential for β-turns in metallothioneins (MTs). Raman spectroscopic studies on Zn(II) and Cd(II) substituted MT-1 between 1000 - 1800 cm^{-1} reveal high lying, intense amide III bands (1284 - 1310 cm^{-1}), suggesting the presence of a large number of β-turns. The sensitivity of these bands to deuteration, and the correspondence between the observed frequencies and those predicted for model compounds, lend strong support to this assignment. Metal incorporation into thionein (apo MT), results in changes in the 1000 - 1800 cm^{-1} region signalling an increase in turns, and marked alterations in the skeletal stretching and bending region below 1000 cm^{-1}. In view of the near-absence of helical or β-sheet segments, and the presence of unique metal-thiolate clusters in MT, the latter Raman spectral features most likely originate from turns consequent to cluster formation. Such a spectral pattern could thus serve as a model for turn like regions in proteins with similar structural constraints. The relevance of the unique structure of MT to some of its proposed functions will be discussed.

3. Gilg, D. cited in Vašák and Kägi, in 'Metal ions in Biological systems' 15, 213, (1983).
4. Boulanger et al., Proc. Natl. Acad. Sci., U.S.A. 80, 1501, (1983).
5. Krimm and Bandekar, Biopolymers, 19, 1, (1980).
6. Lagant et al., Eur. J. Biochem. 139, 137, (1984).

M-Pos155 BIOPHYSICAL PROPERTIES OF MELITTIN-INDUCED LYSIS OF MURINE SPLEEN CELLS. Jerald J. Killion and Jon Dunn, Departments of Physiology and Anatomy, Oral Roberts University School of Medicine, Tulsa, Oklahoma 74171.

Melittin, a 26-amino acid peptide, is the major toxic component of bee venom, and presumably lyses mammalian cells by disruption of the cell lipid bilayer in a fashion analagous to complement-mediated destruction of membrane integrity. Therefore, we designed experiments to further define the biophysical characteristics of melittin-induced lysis of DBA/2 strain mouse spleen cells. These cells were lysed within 5 minutes when incubated with melittin concentrations of 6-20 micrograms/ml; the lysis being independent of both temperature (4, 22 and 35^0 C) and the presence of the metabolic inhibitor sodium azide. However, lysis of the cells was totally blocked by addition of 0.33% β-lactoglobulin, whole DBA/2 serum (at a dilution of 1:500) or the carbohydrates D-glucosamine and D-galactosamine (but not the analogs D-glucose, D-galactose or lactose). Gel chromatography and immunoelectrophoresis confirmed that melittin did not form complexes with serum components. Hence, the inhibition of melittin-induced lysis by β-lactoglobulin and serum albumin was likely due to competition between melittin and these molecules for common binding sites within the membrane structure of DBA/2 cells. Further studies showed that reduction of neuraminidase treatment did not alter cell lysis by melittin. Phosphotidylcholine (but not phosphotidylserine or phosphotidylethanolamine) and gangliosides also blocked the lytic effects of melittin. Together, these data suggest that melittin disrupts the mammalian cell lipid bilayer through low affinity interactions with carbohydrate-binding structures.

M-Pos156 AGGREGATION OF HAPTEN-BEARING LIPOSOMES BY ANTIBODIES. Aaron B. Kantor, Susan G. Stanton and John C. Owicki, Department of Biophysics and Medical Physics, Univ. of CA and Division of Biology and Medicine, Lawrence Berkeley Laboratory, Univ. of CA, Berkeley CA 94720.

We have developed a model system for analyzing the interactions of antibodies with antigenic membranes [Petrossian and Owicki (1984) *Biochem. Biophys. Acta* **776**:217; Stanton *et al. ibid.* **776**:228] A hapten, fluorescein, is covalently linked to a lipid and incorporated into liposomes. Antibody binding occurs in seconds to minutes, as monitored by the resulting quenching of the hapten's fluorescence. Aggregation occurs more slowly, as assayed by centrifugal separation of aggregates of radiolabeled liposomes. Initial flocculation is also monitored by light scattering. Fundamental parameters, such as hapten lateral density, are readily controlled. For a variety of murine monoclonal antibodies (MAB's) [courtesy E.W. Voss, Jr.] we find pronounced differences in aggregation behavior at a constant extent of antibody binding. For example, MAB 4-4-20 (IgG_{2a}, K_a=500/μM) does not readily flocculate or precipitate liposomes; however, MAB 6-19-1 (IgG_{2b}, K_a=4/μM) does. Aggregation by 6-19-1 resembles the classical precipitin reaction; it is least effective with either little or excess antibody. The aggregation behavior of the various MAB's reflects differences in competition for inter- and intra- vesicle bivalent binding. The system should prove valuable for analyzing structure-function relationships for MAB's of varying affinities and isotypes. Supported by N.I.H. grants AI19605-02 and 5T32GM07379-07.

M-Pos157 INTERACTIONS OF ANTIBODY STABILIZED PHOSPHATIDYLETHANOLAMINE LIPOSOMES WITH HERPES SIMPLEX VIRUS: A NOVEL IMMUNOLIPOSOME ASSAY FOR HSV ANTIGEN, GLYCOPROTEIN D. R. J. Y. Ho, B. T. Rouse and L. Huang, University of Tennessee, Knoxville, TN 37996-0840.

Native IgG does not bind to liposomes under physiologic conditions. However, when the monoclonal IgG against Herpes Simplex virus (HSV) surface antigen glycoprotein D (gD) was derivitized with N-hydroxysuccinimide ester of palmitic acid, the increased hydrophobicity of the antibody enabled the antibody to incorporate into the lipid bilayer. In addition, we have found that the palmitoyl antibody is capable of stabilizing the bilayer of dioleoyl phosphatidylethanolamine (DOPE) which does not form bilayer by itself at neutral pH. Mixing of palmitoyl-anti-HSV-gD IgG with DOPE at 1:4000 molar ratio was sufficient to form stable liposomes by sonication, as judged by the entrapment of 50mM self quenching dye, calcein. When the antibody stabilized DOPE immunoliposomes were incubated with intact HSV, lysis of liposomes occurred with the release of calcein into the medium as detected by the enhancement of calcein fluorescence. Since no lysis activity was observed with other viruses such as Sendai, Semliki Forest and Sindbis, this direct fluid-phase assay is specific for HSV. A likely mechanism for liposome lysis is the aggregation (contact capping) of antibody at the contact area between the virus and liposome due to multiple immune complex formation. As a result of lateral phase separation in the immunoliposome membrane, DOPE may undergo the bilayer-to-hexagonal phase transition, causing the release of the entrapped dye. Furthermore, the HSV specific liposome lysis could be inhibited by free antibody, but not by other IgG's. Using this principle, we have shown that this novel fluid-phase immunoliposome assay is sensitive to 50,000 plaque forming units of HSV and the inhibition assay is sensitive to ng quantity of the free antibody in 5μl incubation medium. (Supported by NIH Grants EY 05093 and CA 24553).

M-Pos158 Collisional Quenching of Xanthene Dyes Applied to Study the Mechanism of Complement-Mediated Lysis of Lipid Vesicles. Anne L. Plant,Naval Research Laboratory,Washington,D.C.

The concentration-dependent quenching of xanthene dyes has been shown to occur in part by a collisional mechanism (Plant et.al.,Biophys.J. 47(2),1985). Collisional quenching of dye encapsulated in vesicles is determined by a decrease in the fluorescence lifetime. For sulforhodamine 101,the lifetime decreases from an unquenched value of 4.5 nsec to 0.7 nsec at an encapsulated concentration of 33 mM. The Stern-Volmer plot of τ_0/τ vs. dye concentration is linear, and provides a standard curve for determining intravesicular dye concentration. Vesicles containing dinitrophenyl-conjugated phosphatidylethanolamine in their bilayer matrix are useful models for serum complement activity in the presence of anti-DNP antibodies. A xanthene such as 5-carboxyfluorescein or sulforhodamine 101 is entrapped in the aqueous cavity of vesicles and its fluorescence is quenched until the vesicles are disrupted and dye is released. Under most assay conditions, complement activity results in less than 100% vesicle lysis as determined by incomplete recovery of available fluorescence. Either some vesicles are not lysed at all, or complement attack results in a temporary lesion in the bilayer from which only a portion of the contents escape. The measurement of fluorescence lifetimes of marker dye after complement activity has taken place is used to discern which of these alternatives occurs. The presence of trapped dye plus free dye yields 2 lifetimes: an unquenched lifetime plus a quenched lifetime which is proportional to microscopic dye concentration. The presence of a fully quenched lifetime indicates that some vesicles are not lysed by complement; the presence of an intermediate lifetime indicates the partial release of dye and supports the concept of a temporary complement lesion.

M-Pos159 THE INTERACTION OF SENDAI VIRUS WITH TARGET CELLS: BASIS OF NOVEL HOMOGENEOUS IMMUNOASSAY. Brenda P. Heath, Francis Martin and Anthony Huang. Liposome Technology, Inc. 1050 Hamilton Court, Menlo Park, CA 94025.

We have developed a homogeneous immunoassay based on the lytic activity of Sendai Virus. In this system, analyte-specific antibodies are first introduced into the virus envelope. The virus is allowed to react with modified human erythrocytes (RBC) bearing analyte molecules on their surface. The virus-target cell interaction results in specific lysis of the RBC and the release of reporter molecules encapsulated in the target cells. The inhibition of this reaction is used to quantitate the presence of soluble analyte in the reaction medium. Modified virus was prepared by incubating the virus with an antibody-palmitate conjugate in the presence of sodium deoxycholate. 40-50% of the added antibody was incorporated into the viral particle with initial antibody to virus input ratios of 50-200 ug antibody/mg viral protein. To prepare analyte-specific RBC targets, analyte molecules were incorporated into desialylated RBC membrane using an analyte-ganglioside conjugate. Using this procedure, between $3{\cdot}9 \times 10^4$ and $2{\cdot}6 \times 10^5$ copies of hIgG could be introduced into each RBC.

Three different assay configurations were studied: a sandwich system in which the analyte was an antibody recognizing an endogenous RBC surface antigen; a direct system in which a high molecule weight analyte (hIgG) was directly attached to the cell surface and a direct hapten system, in which 4-amino-phthalate was incorporated into the RBC membrane. Using hemoglobin as the lysis reporter, we were able to detect soluble hIgG, and phthalate in uM range. Two other reporter systems, beta-galactosidase and calcein, were also examined in the sandwich configuration. Results showed that all three reporter systems behaved similarly. [This work was performed by Cooper-Lipotech, Inc., a Joint Venture between CooperBiomedical, Inc. and Liposome Technology, Inc.]

M-Pos160 THE CRYSTAL AND MOLECULAR STRUCTURE OF DIBENZOYL DISULFIDE.
Chitta R. Paul, T. Srikrishnan, Edwin E. Budzinski, and Harold C. Box, Biophysics Department, Roswell Park Memorial Institute, Buffalo, New York 14263.

Sulfur containing compounds play an important role in the chemistry of biomolecules. The (S-S) bond is an important linkage binding large biomolecules together. The disulfide bonds are radiation sensitive, have potential scavenging activity and are used as radiation protectors. Crystals of dibenzoyl disulfide are obtained by slow evaporation at room temperature of a saturated solution in toluene. The crystals are monoclinic, space group $P2_1/c$ with the cell constants a = 12.356(1), b = 12.071(1), c = 9.071(2)Å, β = 107.15(1)°, V = 1292Å^3, D_o = 1.42 gm/cc, D_c = 1.411 gm/cc and Z = 4. Complete three dimensional data was collected on a CAD-4 diffractometer using the $\omega/2\theta$ scan and the crystal structure was solved using the Heavy Atom technique and refined by full-matrix least squares method to a final R value of 0.036 for 2738 observed reflections. The (S-S) bond distance is 2.021Å, has a partial double bond character and the dihedral angle around the disulfide bond is 80.8°. The two (S-C) distances are 1.805 and 1.823Å. The central part of the molecule C-S-S-C adopts a skewed nonplanar configuration and the planes of the benzene rings are inclined at an angle of 93.7°. The S-S bond direction from the X-ray structure is compared with the directions of g_{min} for (S-S) anion and g_{max} for (S-S) cation from electron spin resonance spectroscopy. The former makes an angular separation of 4.6° whereas the latter 18.1° with the (S-S) bond direction.

(Supported by grants CA-25027 and GM-24864 from the National Institutes of Health.)

M-Pos161 CRYSTAL STRUCTURE AND CONFORMATION OF AZIMEXON, AN IMMUNOSTIMULANT AND AN ANTITUMOR AGENT.
T. Srikrishnan, Center for Crystallographic Research, Roswell Park Memorial Institute, Buffalo, NY 14263.

Azimexon[2-cyanaziridinyl-2-carbamoyl-aziridinyl-1-propane] is an immunostimulant which shows therapeutic effects in tumor models and experimental infections in mice in vitro, enhances human T-lymphocyte transformation in vitro and increases phagocytosis of latex particles by mouse peritoneal cells. In cancer patients it increases blood active T-rosettes, increases T4/T8 ratio and is used in the treatment of melanomas. Crystal structure of azimexon has been undertaken to study the conformation of the molecule in the solid state as a first step in the investigation of structure-function relationship of immunomodulators. Crystals of azimexon (from methanol/water) are triclinic, space group P1, with a=6.342(2), b=6.804(1), c=13.106(2)Å, α=75.17(1), β=89.17(2), γ=83.26(2)°, V=542.8Å^3, Z=2, D_o=1.18g/cc and D_c=1.189g/cc. The structure was solved with CAD-4 data (2227 reflections, $1615>3\sigma$) by multi-solution techniques and refined to a final R value of 0.057. The mean lengths of C-N and C-C in the aziridine rings are 1.461 and 1.494Å and the configuration of the ring nitrogen is pyramidal. The mean C-C-N and C-N-C bond angles in the ring are 59.2° and 60.6° respectively. The two molecules, which differ significantly in the relative orientation of their aziridine rings, are linked by hydrogen bonds involving the amino group of one as the donor and the cyano nitrogen and carbonyl oxygen of the other molecule as acceptor respectively. There are a number of C-H...O and C-H...N interactions in the structure. Thanks are due to Boehringer Mannheim for a gift of the sample, and to Mr. Christopher Wood for technical assistance. Work supported by ACS IN 54W8 and in part by NIH GM-24864.

M-Pos162 ION SELECTIVITY IN MONENSIN.
W. A. Pangborn, W. L. Duax and D. A. Langs (Intr. by D. L. Dorset). Molecular Biophysics Department, Medical Foundation of Buffalo, Inc., Buffalo New York, 14203

Monensin, a member of the family of monocarboxylic acid, polycyclic, polether antibiotics which induces monovalent cation permeability, exhibits selectivity for Na^+ over K^+. Structures of free acid, the anhydrous and hydrated Na^+ complexes, the complex of the acid form with NaBr and the hydrated Ag^+ complex have been reported. The similarity of all these complexes with each other and the consistent manner in which they differ from the free acid, indicate that the determining factor in the conformation of the ionophore is the rearrangement required to accommodate the ion and successfully coordinate it. Single crystals of the hydrated K^+ complex of monensin have been grown from aqueous ethanol. These crystals are isomorphous with the hydrated Na^+ complex, orthorhombic, space group $P2_12_12_1$, a = 16.484Å, b = 19.189Å, c = 12.661Å. The structure has been determined and refined to a residual of 0.046. Empirical calculations of the bond strength on the basis of the coordination bond lengths would indicate a stronger binding for K^+ than Na^+, in contrast to the observed selectivity sequence and stability constants. An examination of the torsion angles reveals that the K^+ complex is unique in one respect. The torsion angles of the fused spiro ring system, which one would expect to be the least flexible portion of the molecule, are highly conserved in all the complexes except the K^+ complex. It is reasonable to conclude that the introduction of the K^+ ion into the coordination site of the ionophore is done at the cost of significantly distorting a constrained portion of the molecule from its low energy conformation. Supported by grant GM321812 from NIH, DHHS.

M-Pos163 THE SHORT RANGE ORDER IN TMV LIQUID CRYSTALS MEASURED BY LOW ANGLE X-RAY SCATTERING

R. Oldenbourg, B.B. Brodsky, D.L.D. Caspar and D. Schneider, Physics Department and Rosenstiel Center, Brandeis University, Waltham, MA 02254.

We have recorded low angle X-ray patterns from uniaxially aligned nematic liquid crystals of the Tobacco Mosaic Virus (TMV). The uniaxial alignment of the sample solutions filled in a thin quarz capillary was accomplished by means of a magnetic field of 1.5 Tesla produced by a small permanent magnet mounted together with the capillary. The recorded X-ray patterns show that the equatorial scattering in the plane perpendicular to the rod axis is sampled by a short range liquid like order between the rods. The sampling of the single particle scattering function is observed out to wave vectors about three times the reciprocal distance 1/d between adjacent rods in the solution ($d \sim 300$ Å). At high particle concentration (30% volume fraction) the sampling is observed further out, whereas for concentrations as low as the critical density for the formation of the nematic phase (5% volume fraction) the sampling extends only out to a second shell of next neighbours. We have developed a computer program to separate the sampling function (structure factor) from the single particle scattering function. The single particle scattering function was obtained by computing the Fourier transform of a simple cylindrical layer model for the TMV particle. We recover the structure factor for TMV solutions of different ionic strength and particle concentration to map out the typical distances over which interactions are strong between TMV particles.

M-Pos164 Conformational flexibility of dinucleoside monophosphates with cyclobutane type pyrimidine dimers and 6-4 photoadducts. Shashidhar N.Rao and Peter A. Kollman (Intr. by V.N. Balaji), Department of Pharmaceutical Chemistry, University of California, San Francisco CA 94143.

Conformational analysis of deoxydinucleoside monophosphates with the sequences TT, CT, TC and CC have been carried out with the incorporation of both cyclobutane type pyrimidine dimers and 6-4 photoadducts using the methods of molecular mechanics. The effect of flexibility with respect to a few typical conformational parameters such as sugar geometries, phosphodiester and glycosidic torsions has been studied and the relative energies of a large variety of structures have been compared. The sensitivity of structural features such as deviations from planarity of the glycosidic nitrogen in the pyrimidines to the above mentioned flexibility, has been examined, particularly in the light of currently available models for the repair of pyrimidine dimers. The salient features obtained from these calculations have been compared with very recent spectroscopic data on pyrimidine dimer incorporated dinucleoside monophosphates. The effect of "inserting" minimum energy conformations of such structures into B-DNA helices will be discussed in terms of the distortions in helical structures.

M-Pos165 CONFORMATIONS OF THE SIXTEEN DEOXYDINUCLEOSIDE MONOPHOSPHATES BY MINIMIZED SEMI-EMPIRICAL POTENTIAL ENERGY CALCULATIONS. B.E. Hingerty,Health and Safety Research Division, Oak Ridge National Lab., Oak Ridge, TN 37830, T.L. Hayden, S. Figueroa, Dept. of Mathematics, University of Kentucky, Lexington, KY 40506, and S. Broyde, Biology Dept., New York University, NY, NY 10003.

With a view to devising a rational strategy for searching the conformation space of single stranded nucleic acid oligomers, we have computed the minimum energy conformations of the sixteen deoxydinucleoside monophosphates, searching all combinations of staggered rotamers for the O3'-P, O5'-P and C4'-C5' torsion angles, C2'-endo and C3'endo deoxyribose puckers, and syn and anti glycosidic bonds, with all torsion angles and the sugar puckers flexible. These calculations were carried out on a Cray-XMP with optimized code, using a new program that can compute minimum energy conformations of any number of residues to 12, and of any desired base sequence. The low energy forms of the deoxydinucleoside monophosphate conformational building blocks are to be employed in combination, in a build-up strategy to generate larger polymers.

This work was supported jointly by PHS Grant #1R01 CA28038-05(SB), DOE Contract #DE-AC02-81ER60015(SB), and by the Office of Health and Environmental Research, U.S. Dept. of Energy, under Contract #DE-AC05-840R21400 with Martin-Marietta Energy Systems, Inc. (BH).

M-Pos166 SPERMINE/DNA INTERACTIONS IN OLIGOMERS Burt Feuerstein, Nagarajan Pattabiraman, Laurence Marton; Brain Tumor Research Center (BF, LM), Department of Laboratory Medicine (LM), Computer Graphics Laboratory (NP), University of California, San Francisco; Intr. by Richard Shafer

In order to study the interaction of polyamines and DNA, we have carried out conformational energy calculations on spermine and molecular mechanics calculations on the spermine/DNA complex. From these calculations, it appears that spermine's central diaminobutane moiety maintains the trans configuration. By searching for the distance defined by the diaminobutane as a fixed distance between proton acceptors in B DNA, we found the N7 positions of purines in the major groove of alternating purine/pyrimidine sequences to be likely sites of spermine binding. We compared this model to that of Liquori, where spermine bridges the minor groove, by constructing $d(GC)_5.d(GC)_5$ and $d(AT)_5.d(AT)_5$, docking the spermine to DNA with the MIDAS program, and carrying out molecular mechanics calculations using AMBER on both complexed and uncomplexed polymers.

When docked into the major groove, spermine stabilizes the energy of both oligomers by maximizing interactions between proton acceptors in DNA and proton donors in spermine. Maximum interaction is achieved by bending the major groove over spermine and altering the sugar puckering from C3' endo to C2' endo. Interactions of spermine with sugar/phosphates and bases in the major groove of both oligomers show several patterns. Our comparison with Liquori's minor groove model shows it to be significantly less stable than the major groove model. We are presently investigating other base sequences and interaction positions in order to better characterize spermine's interaction with DNA. These will be presented.

M-Pos167 CONFORMATIONAL AND NORMAL MODES ANALYSES OF OLIGONUCLEOTIDE-DRUG COMPLEXES. Barbara R. Rudolph, Dzung T. Nguyen, and David A. Case. Department of Chemistry, University of California, Davis, CA 95616.

Two studies describe the effects of intercalated drugs on the dynamics of double-stranded DNA: A. More than a dozen local minima on the $d(CpG)_2$ proflavine potential energy surface are identified using quenched molecular dynamics. This procedure uses points along a high-temperature simulation trajectory as starting points for energy minimization. These conformers have a wide range of backbone torsional angles. B. Normal mode calculations have been performed on the ethidium and proflavine complexes with the $d(CGCGCG)_2$ hexanucleotide. The vibrational motions are described by projecting the eigenvectors onto rigid groups and by analysing movies generated by computer graphics. For both the DNA and DNA-drug complexes, most of the lowest modes involve deformations of the two terminal base-pairs. Other low-frequency modes describe the motion of the drug in the intercalation space.

M-Pos168 **LOW FREQUENCY COLLECTIVE MOTIONS OF DNA DOBLE HELICES -A REDUCED SET OF COORDINATES APPROACH**

A. E. Garcia*†, Chang-Shung Tung† and J. A. Krumhansl*
*Laboratory of Atomic and Solid State Physics
Cornell University, Ithaca, NY 14850 USA. and
†Los Alamos National Laboratory , T10- MS K710 , Los Alamos, NM 87545. USA

By using Metropolis Algorithm (Monte Carlo Method) and energy minimization, we have studied the geometry of short DNA double helices with a set of reduced coordinates. In this set of reduced coordinates, each base is treated as a rigid body rolled with respect to the long axis. Base pairs are alloved to translate along the helix axis, the long axis , and rotate with respect to the helix axis. All degrees of freedom within the sugar - phosphate backbone are included.

Pair correlations between the sugar pseudorotational angle, glycosidic and backbone torsional angles [$c(w,\delta)$;$c(w,\epsilon)$;$c(w,\chi)$] have been found. These correlations are used to get a reduced set of coordinates which describes low frequency collective motions. A non-linear analytical model involving the reduced set of coordinates will be presented, and their relevance to the B to A DNA transition will be discussed.

M-Pos169 THEORETICAL COMPARISON OF SUPERCOILED DNA STRUCTURES. Janet Cicariello and Wilma K. Olson, Department of Chemistry, Rutgers University, New Brunswick, New Jersey 08903.

Three-dimensional models of closed circular B-DNA supercoiled along a variety of trajectories have been constructued using differential geometric methods. Bases are confined to their normal stacking distances of 3-4Å with their relative orientations (i.e., twist, roll, and tilt) as dependent variables. The extent of helix bending and twisting has been monitored using standard semi-empirical energy calculations. Previous studies comparing the relative stabilities of the various structures have been limited to GC base pairs in B-DNA. However, the different side groups of an AT base pair (especially the bulky methyl group of thymine) can be expected to have an effect on the stacking and electrostatic interactions between adjacent base pairs as compared to the same interactions for a GC pair. Also, alternate helical geometries (i.e., A- and Z-DNA) will have an effect on these interactions and on the local geometric orientations of the bases. The relative stabilities of the various supercoiled structures are compared using several sequence variations and helical types. (Supported by U.S.P.H.S. Grant GM-34809).

M-Pos170 NEAR AND VACUUM ULTRAVIOLET THEORETICAL CIRCULAR DICHROISM CALCULATIONS OF RIGHT- AND LEFT-HANDED NUCLEIC ACIDS. Arthur L. Williams, Jr. Department of Physiology and Biophysics, Mount Sinai School of Medicine, New York, NY 10029; Chaejoon Cheong and Ignacio Tinoco, Jr., Department of Chemistry and Laboratory of Chemical Biodynamics, University of California, Berkeley, CA 94720.

Theoretical circular dichroism (CD) calculations are presented for oligo- and polynucleotides of regular and random sequences. A set of parameters that describe the pi-pi* transitions of the nucleic acid bases were used in matrix method calculations of the near and vacuum uc CD. In the near uv, calculated CD spectra using the coordinates of right- and left-handed structures derived from x-ray studies on fibers agreed qualitatively with experimental solution CD spectra, believed to be in those conformations. However, the calculated CD compared nearly quantitatively with the same experimental spectra in the far and vacuum uv. The calculated results add further evidence to the experimental observation that a large positive maximum ($\Delta E > 40$) located to the red of 180 nm in the observed spectra of low-salt right-handed alternating guanine cytosine polynucleotides is shifted to the blue of 180 nm for high-salt left-handed Z-form conformations. The large negative maximum ($\Delta E < -30$) located near 195 nm in the experimental Z-form spectra is also found in the calculated spectra. The large positive maximum to the red of 180 nm is also found to be characteristic of all sequences calculated in right-handed conformations, while the large positive maximum to the blue of 180 nm as well as the large negative maximum near 195 nm were found to be characteristic of all alternating purine pyrimidine sequences in left-handed conformations. Thus the calculations indicate that the vacuum uv CD, in contrast to the near uv CD, is a better indicator of the helical-handedness of double-stranded nucleic acids.

M-Pos171 THEORETICAL STUDIES ON B-DNA DIMENSIONS AND FLEXIBILITY - THEIR BASE SEQUENCE AND CHAIN LENGTH DEPENDENCE. R. C. Maroun and W. K. Olson. Wright Chemistry Laboratory, Rutgers University, New Brunswick, New Jersey 08903.

Computations have been carried out to assess the variations of local base pair geometry and base pair sequence in B-DNA. Appropriate values of the ω', ω phosphodiester angles that keep base rolling and tilting motions within narrow ranges and appropriate separations of parallel bases have been selected for statistical mechanical calculations of average configuration-dependent properties including the mean square unperturbed end-to-end distance, higher moments of the displacement vector, and the spatial density distribution W(r). The computed dimensions and distribution functions are used to estimate overall chain stiffness/flexibility as well as the chain length and base sequence dependence of loop/circle formation. (Supported by U.S.P.H.S. Grant GM-20861).

M-Pos172 CAN THE DOUBLE HELIX BE PARALLEL? N. Pattabiraman, School of Pharmacy, University of California, San Francisco, CA 94143. A parallel righthanded double helical structure for poly d(A).poly d(T) with the reverse Watson and Crick AT base pairing scheme is proposed. A parallel righthanded double helical structure for poly d(A). poly d(T) from the coordinates of the 5′ nucleotide (monomer) of B-DNA antiparallel righthanded double helix was model built by using the helix axis as a dyad axis instead of the perpendicular dyad axis in the case of antiparallel chain used to generate the double helical structure. In our model one of the chains was rotated about the helix axis one of the chains, say poly d(T) such that thymine bases form reasonable hydrogen bonds with the corresponding adenine bases. In the case of the antiparallel structure, the atom N6 of adenine forms a hydrogen bond with the carboxyl oxygen O4 and with the carboxyl oxygen O2 in the parallel structure. The other hydrogen bond between A and T (N1... N3) is the same for both the structures. In the parallel double helical structure, the number and the nature of hydrogen bonds are the same as that of antiparallel double helix. Another difference between the parallel and antiparallel double helix is that the grooves are of equal sizes for parallel structure due to the diad along the helix axis; in other words there are no major and minor grooves. Molecular mechanics calculations were carried out using AMBER to compare the stability of both parallel and antiparallel right handed double helical structures. It is found that the parallel structure is energetically as favourable as that of the antiparallel

M-Pos173 STATISTICAL ANALYSIS FOR THE PREDICTION OF PROTEIN CODING REGIONS IN DNA SEQUENCES II. Kotoko Nakata, Minoru Kanehisa and Jacob V. Maizel Jr. Laboratory of Mathematical Biology, NCI - FCRF, Frederick, Maryland 21701

A general method based on the statistical technique of discriminant analysis was developed to distinguish boundaries of coding and non-coding regions in DNA (Nakata, Kanehisa and DeLisi, Nucleic Acids Research 13, 5327-5340, 1985). In this study, more characteristic patterns including consensus sequences of promoters in DNA (e.g. TATAATG) are used in conjunction with a pattern recognition algorithm called the perceptron method. We examined the optimal free energy and location of snRNA base pairing to mRNA, and also calculated the melting temperature of DNA. By discriminant analysis we can combine information processed by the perceptron algorithm with information obtained by other methods, e.g. free energy of snRNA and mRNA base pairing and thermal stability of DNA, and improve the degree of predictive ability in unknown sequences. We have applied this method to distinguish promoter sites, termination sites, exon/intron and intron/exon boundaries from merely fortuitous sequences, in eukaryotes and prokaryotes sequences, using the GenBank database. To asses the discriminatory power of these variables, we allocated additional sequences that have been newly included in the data base.

M-Pos174 ANALYSIS AND COMPARISON OF TWO FULLY SEQUENCED VIRAL DNA GENOMES USING H CURVES. Eugene Hamori and Bing Zhou, Department of Biochemistry, School of Medicine, Tulane University, New Orleans, LA 70112.

The method of H Curves was used to study the global characteristics of the nucleotide distribution in two large viral genomes that have been sequenced in toto recently; the 48,502 base-pairs lambda genome (Sanger, F. et al. J. Mol. Biol. 162, 729, 1982) and the 172,282 b.p. B95-8 Epstein-Barr genome (Baer, R. et al Nature 310, 207, 1984). The H-curve method (Hamori, E. and J. Ruskin, J. Biol. Chem. 258, 1318, 1983) is a graphic representation of the full information content of a DNA sequence which is particularly suitable for perusing long sequences. It involves the generation of 3-dimensional space curves by computer which serve as "fingerprints" of the DNA sequence. Unlike the customary letter-series representation, H-curves can be drastically reduced in size without obliterating the global features of the sequence information and thus their utility. The sequences used in this study were obtained from the GenBank database. In spite of the enormous reduction of resolution necessitated by the compression of the Epstein-Barr sequence information into a standard paper size, the global features of this H curve immediately reveal the two major characteristic regions of repeats, some locations at which the direction of reading frames changes, and some other functionally important regions of the sequence. The similarities and differences between the global nucleotide distribution pattern of this genome and that of the lambda genome studied earlier by this method (Hamori, E. Gene Anal. Techn. 1, 69-74, 1984) were noted. [Supported by grants from the NIH (GM 20008), BRSG of Tulane U. (533113) and BIONET (1U41RR-01685-02)].

M-Pos175 NUCLEOTIDE SEQUENCE OF AN ANTI-FLUORESCYL HAPTEN ANTIBODY. Z. Liu*, D. M. Reinitz**, E. W. Voss, Jr.**, C. Wood***, & T. T. Wu*. *Northwestern University, Evanston, IL 60201; **University of Illinois, Urbana, IL 61801; ***Abbott Laboratories, North Chicago, IL 60064.

We have sequenced the anti-fluorescyl hapten antibody heavy chain variable region gene from hybridoma 3-13. The nucleotide and translated amino acid sequences are as follows:

```
    GCTGCTGTCTTGTGAGTCCCCTGCTCTCATTATGGCAAATTACCTGAGTCTATGGTGATTAAAACAGGATGTCCACACCCTTAAATCAAC  90

    CGACGATCAGTGTCCTCTCCAAAGTCCCTGAACACACTGACTCTAACCATGGAATGGAGTTCCATATTTCTCTTTCTCCTGTCAGGAACT 180
                                                    MetGluTrpSerTrpIlePheLeuPheLeuLeuSerGlyThr
    GCAGGTAAGGGGCTCACCAGCTTCAAAATCTGAAGTGGAGACAGGACCTGAGGTGACAATGACATCTACTCTGACATTCTCTCCTCAGGT 270
 -5 AlaG                                                                                      ly
    GTCCACTCTGAGGTCCAGCTGCAGCAGTCTGGACCTGAGCTGGTAAAGCCTGGGGCTTCAGTGAAGATGTCCTGCAAGGCTTCTGGATAC 360
 -3 ValHisSerGluValGlnLeuGlnGlnSerGlyProGluLeuValLysProGlyAlaSerValLysMetSerCysLysAlaSerGlyTyr
    ACATTCTCTAGCTATGTTCTATACTGGGTGAAACAGAAGCCCTGGGCAGGGCTTGAGTGGATTGGCTTTATTTTTCCTTACAATGATGGT 450
 28 ThrPheSerSerTyrValLeuTyrTrpValLysGlnLysProTrpAlaGlyLeuGluTrpIleGlyPheIlePheProTyrAsnAspGly
    ACTAAGTACAATGAGAAGTTCAAACGGCAAGGCACACTGACTTCAGACAAATCCTCAAGCACAGCCTACATGGAACTCAGCAGCCTGACC 540
 57 ThrLysTyrAsnGlyLysPheLysArgGlnGlyThrLeuThrSerAspLysSerSerSerThrAlaTyrMetGluLeuSerSerLeuThr
    TCTGAGGACTCTGCGGTCTATTACTGTGCACGAACGGGCGCAGACAGCTCGGGCTACGTAAGGGCTATGGACTACTGGGGTCAAGGAACC 630
 84 SerGluAspSerAlaValTyrTyrCysAlaArgThrGlyAlaAspSerSerGlyTyrValArgAlaMetAspTyrTrpGlyGlnGlyThr
    TCAGTCACCGTCTCCTCAGGT
108 SerValThrValSerSer
```

(Supported by a grant from Leuk. Res. Found. of Chicago to TTW)

M-Pos176 AN "A"-LIKE DNA CONFORMATION AS AN INTERMEDIATE IN THE CONVERSION OF POLY(dGdC)·POLY(dGdC) FROM Z TO ψ. Y.A. Shin, R.P. Pillai, and G.L. Eichhorn, Gerontology Research Center, National Institute on Aging, National Institutes of Health, Baltimore, MD 21224 and W.C. Johnson, Jr., Department of Biochemistry and Biophysics, Oregon State University, Corvallis, OR 97331.

We have previously shown [Cold Spring Harbor Symp. 47, 125 (1983)] that the action of Co(III) on poly(dGdC)·poly(dGdC) brings about a series of transitions to the Z form, and then to an unknown (X) form, and finally to a chirally compacted ψ-structure. The Z-conformation is readily characterized by its typical CD-spectrum and its two-peak ^{31}P NMR spectrum, and the ψ structure by the highly intense magnitude of its CD spectrum. The structure of the intermediate is the most difficult to ascertain, but we have good evidence that it is an "A"-like structure. Its ^{31}P NMR spectrum has only one peak, in line with B or A and ruling out Z, and the CD spectrum rules out B, Z and ψ. The UV CD spectrum obtained under vacuum passes through zero ellipticity at 201 nm. This spectrum clearly rules out any Z-like structures and suggests an "A" type conformation. Such an "A" like structure is also obtained from the B conformer of poly(dGdC)·poly(dGdC) by the action of Ca(II), Ba(II), Co(II) and Zn(II).

M-Pos177 EVIDENCE FOR HETEROGENEITY OF SECONDARY STRUCTURE IN AQUEOUS DNA, DNA/RNA HYBRIDS, AND NUCLEOPROTEINS. James M. Benevides and George J. Thomas, Jr., Department of Chemistry, Southeastern Massachusetts University, North Dartmouth, MA 02747

The results of DNA structure determination from single crystal x-ray diffraction analysis at atomic resolution have been combined with the data of laser Raman spectroscopy to assign conformation-sensitive Raman marker bands of the DNA backbone and of different nucleosides in A, B and Z-DNA. Identification of distinct conformation markers is aided by the use of a recently developed Fourier deconvolution method for enhancement of spectral resolution. The transferability of single crystal Raman data among samples of different morphology, including fibers, gels and dilute solutions, is exploited to determine the preferred conformers of DNA for experimental conditions which vary significantly from those in the crystal and which may in certain cases more closely approximate those *in vivo*. The analysis is extended to RNA models and to DNA/RNA hybrid structures. Several new or unorthodox structures are revealed, including A-helical structures for poly(dA-dT)·poly(dA-dT) and poly(rA)·poly(dT). Oligonucleotide and polynucleotide hybrids can form "mixed" structures in which both A and B type conformers are present. Heterogeneity of secondary structure is indicated for both high and low molecular weight DNA in aqueous solution, including calf thymus DNA, the encapsidated DNA of bacteriophage P22 and the 17-base pair operator sequence, O_L1, which provides the tightest binding site for the phage lambda cI repressor.

Supported by N.I.H. Grant AI18758.

M-Pos178 THE INTERACTION OF DAUNOMYCIN WITH Z DNA. J. B. Chaires, Department of Biochemistry, The University of Mississippi Medical Center, Jackson, MS 39216-4505

Under ionic conditions favorable to the Z conformation, the anticancer drug daunomycin binds cooperatively to poly(dGdC). Binding isotherms may be fully accounted for by the allosteric model proposed by Crothers and co-workers (Dattagupta *et al.* (1980) Biochemistry *19*, 5998). The results of the analysis of binding data provides estimates for the equilibrium constant for the B to Z transition over a range of ionic conditions, in addition to estimates for the binding parameters for the interaction of the drugs with B and Z form DNA. Comparative studies show that adriamycin converts Z DNA to an intercalated B form more effectively than daunomycin. This arises solely from the fact that adriamycin has a higher affinity for B DNA. The temperature dependent transition of poly(dGm^{5}dC) from the B to the Z form has been characterized in detail. Addition of daunomycin results in an increase of the temperature at the midpoint of the B to Z transition, and a more complex, biphasic transition curve. This is analogous to the effect of intercalators on the melting transition of DNA and serves as an alternate experimental method for demonstrating the preference of the drug for B form DNA. Supported by U. S. Public Health Service Grant CA 35635.

M-Pos179 FLUORESCENCE AND ELECTRIC BIREFRINGENCE STUDIES OF THE BINDING OF ETHIDIUM BROMIDE TO TWO SMALL DNA RESTRICTION FRAGMENTS OF THE SAME MOLECULAR WEIGHT. John C. Stellwagen and Nancy C. Stellwagen, Department of Biochemistry, University of Iowa, Iowa City, IA 52242

Fluorescence anisotropies and lifetimes were measured for the binding of ethidium bromide to two 147 base pair DNA restriction fragments as a function of the dye/phosphate ratio, D/P. Emission spectra were recorded at 590 nm, using three different excitation wavelengths. The anisotropies observed by exciting at 300 or 325 nm were similar, exhibiting maxima at D/P ratios of 0.06-0.10. The anisotropies observed when exciting at 530 nm decreased monotonically with increasing D/P. The apparent lifetimes determined by phase retardation or by demodulation also decreased with increasing D/P.

The electric birefringence of the two fragments was also studied as a function of ethidium bromide concentration. The relaxation times increased with increasing D/P. For D/P ratios $\leq$ 0.06, the apparent length of the complex increased about 3.4 Å/bound dye molecule. At higher D/P ratios the calculated length increased more slowly than expected from the amount of added dye, consistent with outside binding as well as continued intercalation. No further increase in length was observed after D/P = 1.00. Supported by Grant No. 29690 of the National Institute of General Medical Sciences.

M-Pos180 FLUORESCENCE LIFETIMES OF 7,8-DIOL BENZO[A]PYRENE PHYSICALLY BOUND TO DNA. J.F. Becker, S.J. Strunk, K.G. Martinez, Dept. of Physics, San Jose State Univ., San Jose, CA 95192; T. Meehan, Dept. of Pharmaceutical Chemistry, Univ. of California, San Francisco, CA 94143.

We are using (±)7,8-diol-benzo[a]pyrene (diol) as a model compound to study the stereoselective physical binding of hydrocarbons to DNA. We have shown that the diol forms a physical complex with DNA and that this complex results from hydrocarbon intercalation. The fluorescence intensity of the diol is markedly quenched in the presence of DNA and the measured fluorescence lifetime (τ) is 29.8 ns for the free diol in solution, and 5.6 ns for the bound diol. The time resolved emission spectra of diol + DNA shows the spectrum of diol free in solution as well as that of diol bound to DNA. The emission spectrum, as well as the absorption spectrum, of diol bound to calf thymus DNA, is red shifted 10 nm, characteristic of an intercalated hydrocarbon. The physical binding of the diol is reversed by addition of $MgCl_2$ which reduces inter-base pair spacing. Fluorescence quenching experiments with iodide, an ion known not to reach the interior of DNA, give a similar bimolecular (dynamic) quenching constant, 1.2 $(10)^9$ $(Msec)^{-1}$, for both bound and free diol. This suggests that the emitted fluorescence is coming from a diol intercalated in such a way that at least part of the molecule is extended out of the DNA. Quenching with low concentrations of silver ions, which are known to bind predominantly to the guanine sites of DNA, results in reduced fluorescence intensity with τ (bound) remaining constant. This (static) quenching indicates that the fluorescence is emitted from diols bound at guanine sites. The results of quantum yield experiments have been used to calculate the fraction (~50%) of the bound diols which are totally quenched. These quenched molecules may be bound at adenine sites. Supported in part by NIH grant CA40598.

M-Pos181 **PROBING TRANSFER RNA ANTICODON LOOP STRUCTURE WITH A FLUORESCENT SPIN LABEL** Steve Seifried, John Hill and Barbara Wells, Chemistry Department, University of Wisconsin - Milwaukee, Milwaukee, WI 53201.

An EPR-active fluorescent label was designed in order to investigate anticodon loop motion across a wide range of lifetimes with a single probe at a defined location. A mixed anhydride of the spin label (SL) acid (2,2,5,5-tetramethyl-3-pyrroline-1-oxyl-3-carboxylic acid) was reacted with 3,6-diamino acridine (PF) to form the amide-linked nitroxyl proflavine (SL-PF). Isotropic and anisotropic correlation times of the fluorescent and non-fluorescent spin labels were different, with the rotation of the SL-PF faster and more anisotropic than the acid of the free spin label. Perrin plots and EPR glycerol titrations will be presented for each individual moiety, as well as for the SL-PF. Base 37 of yeast $tRNA^{Phe}$ (Y base) was acid excised (R. Thiebe and H.G. Zachau, *Eur.J.Biochem.* 5 (1968),546-555.) and replaced with the spin labelled proflavin. Fluorescence Polarization and lifetime experiments, and EPR correlation time determinations, will be discussed for labeled tRNA in terms of anticodon loop behavior under various buffer conditions. Supported by NIH grant GM 30300.

M-Pos182 SECONDARY AND TERTIARY INTERACTIONS IN M1 RNA AS DETERMINED BY PSORALEN CROSSLINKING

Samuel E. Lipson, George D. Cimino and John E. Hearst, Department of Chemistry, University of California, Berkeley, CA 94720.

The RNA moiety of ribonuclease P from *E. coli* (M1 RNA) has been photoreacted with 4'-hydroxymethyl-4,5',8-trimethylpsoralen and long wave UV light in a buffer containing 60 mM Mg^{2+}, where the RNA moiety acts as a true catalyst. Limited specific digestion and two dimensional gel electrophoresis yield fragments crosslinked by HMT. After photoreversal of the isolated crosslinked fragments and enzymatic sequencing of the fragments, the positions of the crosslinks have been elucidated. This method allows us to locate the crosslink to ±15 nucleotides. Further assignment of the exact location of the crosslinks has been made based on the known photoreactivity of the psoralen. Eight unique crosslinks have been isolated in the M1 RNA including 4 long range interactions. The short range interactions are discussed here in detail. A revised secondary structure of the M1 RNA is also presented. This study has been supported by NIH Grant #GM11180.

M-Pos183 INFLUENCE OF A CIS-SYN PHOTODIMER ON THE SECONDARY STRUCTURE OF POLY(dA)·POLY(dT). R.E. Rycyna and J.L. Alderfer, Biophysics Department, Roswell Park Memorial Institute, Buffalo, N.Y. 14263.

Cis-syn cyclobutane-type photodimers were induced into poly(dA)·poly(dT) using photosensitized UV-irradiation and the conformational changes investigated by H-1 and P-31 NMR spectroscopy. Non-exchangeable and imino proton, as well as phosphorus, resonance assignments were made unambiguously based on earlier work involving more simple thymine models containing cis-syn dimers such as poly(dT), d(TpTpTpT), d(TpTpT), and dTpdT. The non-exchangeable H-1 NMR spectra indicate: (1) 11% of the thymine bases are saturated with cis-syn cyclobutane rings, (2) the photodimers induce a 5°C destabilization into the polymer Tm, (3) some thymine bases presumably adjacent to the photodimer are not hydrogen-bonded in the duplex at low temperature, (4) downfield shifted AH2, AH8, TH1', and AH1' protons exist in the duplex state, and (5) poly(dA) maintains more duplex-like structure than poly(dT) with increasing temperature. Five imino proton resonances were observed in irradiated poly(dA)·poly(dT). At 1°C, both photodimer iminos (10.29 ppm) and adjacent nucleotide iminos (10.97 ppm) are not hydrogen-bonded. Next-nearest neighbor hydrogen-bonded iminos at 13.16 and 12.42 ppm are shifted upfield from the unmodified A·T imino (14.01 ppm) suggesting a weakened hydrogen bond. P-31 NMR also indicates a premature melting of the irradiated poly(dA)·poly(dT) compared with the unirradiated polymer. (Supported by SUNY/Buffalo GSA and N.I.H. CA39027).

M-Pos184 THE MAGNESIUM-INDUCED TRANSITION OF POLY(dG-dC).POLY(dG-dC). Yash P. Myer, Department of Chemistry, State University of New York, Albany, NY 12222

The Mg^{2+}-induced transition of poly(dG-dC) has been investigated using the concentration jump approach, baseline to baseline, in 20 mM cocadylate buffer, pH 6.6. The changes were monitored through circular dichroism measurements at 293 nm and spectra in the region 320-220 nm. Poly(dG-dC), 800 ± 100 base pairs, at $[MgCl_2]_f$ of 1.6 M, first undergoes CD changes typical of the B to Z transition with a biphasic decay profile. This is followed by another very slow process, $t_{1/2}$ = 5 hours, resulting in a form with a large positive Cotton effect at 273 nm. At $[MgCl_2]_f$ of 1.35 M, the B to Z transition profile remains unchanged, but the slow process yields another form with a large negative Cotton effect at 296 nm. Upon prolonged standing or centrifugation, the terminal forms sediment. These forms are insensitive to the lowering of the $[MgCl_2]$ by dilution, but removal by dialysis generates the normal B form. Reduction in size, $\leq$ 320 base pairs, eliminates the slowest of the processes, but the initial biphasic profile and the respective kinetic parameters remain unchanged. The biphasic nature and the observed magnitude of the two apparent rate constants, 2.5 ± 0.5 and 18 ± 4 s^{-1}, are also characteristic of the NaCl-induced transition, baseline to baseline jump (1.5 to 2.6 M). The simplest scheme is a two-step, three-species, process, B -> I -> Z . The Z form of poly(dG-dC) with more than 320 base pairs transforms to a super-helical, particulate Ψ form, positive or negative depending on the $[MgCl_2]_f$. These forms revert directly to the B form upon removal of $MgCl_2$. Kinetically the Mg^{2+}-induced B -> Z process appears to be indistinguishable from the Na^+-induced transition.

M-Pos185 CHARACTERISTICS OF B-TYPE DNA CONFORMATIONS IN SOLUTION: ANALYSIS OF RAMAN BAND INTENSITIES OF EIGHT DNAs. Roger M. Wartell and Juan T. Harrell, Georgia Institute of Technology, Atlanta, GA 30332

Raman spectra were obtained from four bacterial DNAs varying in GC content and four periodic DNA polymers in 0.1M NaCl. A curve fitting procedure was employed to quantify and compare Raman band characteristics (peak location, height and width) from 400-1600 cm^{-1}. This procedure allowed the determination of the minimum number of Raman bands in regions with overlapping peaks. A comparison of the Raman bands of the eight DNAs provided several new results. All of the DNAs examined required bands near 809 and 835 cm^{-1} to accurately reproduce the experimental spectra. Since these bands are associated with C3'-endo and C2'-endo sugar conformations, respectively, this result indicates that all DNAs in solution have a mixture of these sugar puckers on the time scale of the Raman scattering process. The intensities of these two bands in the poly d(A)·poly d(T) spectra were similar to intensities in the natural DNA spectra. This finding is not consistent with the heteronomous structure of this polymer observed in fibrous form. (Arnott et al., (1983) Nuc. Acids Res. 11, 4141). Three bands at 811, 823, and 841 cm^{-1} were required to reproduce the 800-850 cm^{-1} region of the poly d(A-T)·poly d(A-T) spectra. This may indicate the presence of three backbone conformations in this DNA polymer. Analysis of intensity vs. GC content for forty two Raman bands confirmed previous assignments of many base and backbone vibrations, and provided additional information on the assignments of a number of bands. (Supported by N.I.H. Grant GM33543.)

M-Pos186 **CD OF HOMOPOLYMER DNA·RNA HYBRIDS CONTAINING A·T OR A·U BASE-PAIRS.** H.T. Steely, D.M. Gray, and R.L. Ratliff(†) Program in Molecular Biology, University of Texas at Dallas, Richardson, Tx 75080 and (†)Genetics Group, Life Sciences Division, Los Alamos, NM 87545.

The CD spectra of 3 duplex hybrids (poly[r(A)·d(U)], poly[r(A)·d(T)], and poly[d(A)·r(T)]) possessed a negative CD band at ca. 208 nm of similar magnitude, and their spectra from 245-200 nm were most like that of a duplex RNA (poly[r(A)·r(U)]). Above 245 nm, the CD spectrum of the poly[r(A)·d(U)] hybrid most closely resembled that of the RNA, poly[r(A)·r(U)], while the spectrum of the poly[d(A)·r(T)] hybrid was similar to the spectra of 2 DNAs, poly[d(A)·d(U)] and poly-[d(A)·d(T)]. The spectrum of poly[r(A)·d(T)] was intermediate in shape and magnitude to those of the homopoymer RNA and DNAs. Thus, these DNA·RNA hybrids appear to differ considerably in their solution conformations. The CD spectrum at long wavelengths of poly[r(A)·d(T)] is consistent with X-ray diffraction data by Zimmerman and Pheipher [1981, PNAS (USA), *78*, 78] which show that the two strands may have different secondary conformations in wet fibers. A CD spectrum of a hybrid triplex (poly[r(U)·d(A)·r(U)]) was compared with spectra of 2 triplex DNAs (poly[d(U)·d(A)·d(U)] and poly[d(T)·d(A)·d(T)]) and a triplex RNA (poly[r(U)·r(A)·r(U)]). Except for poly-[d(T)·d(A)·d(T)], all the triplex molecules were spectrally similar to the spectrum of poly-[r(A)·r(U)] (A-form). While the spectrum of poly[d(T)·d(A)·d(T)] showed a CD band at 208 nm, at wavelengths > 250 nm it resembled the spectrum of its duplex analog in spectral shape and magnitude. All 4 triplexes had different magnitudes of their respective negative bands centered at 242-246 nm, with the hybrid and poly[d(T)·d(A)·d(T)] having intermediate intensities to those of poly-[d(U)·d(A)·d(U)] (maximal CD) and the triplex RNA (minimal CD). [This work was supported by Robert A. Welch Grant AT-503 and NIH Grant GM 19060.]

M-Pos187 CIRCULAR DICHROISM SCATTERING AND CIRCULAR DICHROISM ABSORPTION OF DNA-PROTEIN CONDENSATES AND OF DYES BOUND TO THE DNA-PROTEIN CONDENSATES. C. L. Phillips, Wm. Mickols, M. F. Maestre, I. Tinoco, Jr., Department of Chemistry, Univ. of California, Berkeley, CA, and Lawrence Berkeley Laboratory, Berkeley, CA.

DNA-protein condensates that give positive and negative Psi-type circular dichroism (CD) spectra (Psi-condensates) bind intercalative and non-intercalative dyes. The CD scattering and CD absorption patterns observed in the nucleic acid band of Psi-condensates is mimicked in the dye band of the Psi-condensates with bound dye. The large CD scattering and CD absorption bands are interpreted as resulting from long range chiral order, rather than nearest neighbor or next-nearest neighbor short range interactions. Our interpretation stems from the observation that the CD scattering and CD absorption signals in the dye band of the Psi-condensates depends only upon whether the CD in the nucleic acid spectral region gives a positive or negative Psi-type signal. However, CD absorption signals from dyes bound to uncondensed nucleic acids vary for different dyes and different nucleic acids. Calf thymus DNA, poly(dA-dT), and poly(dG-dC) result in positive Psi-type signals when condensed with poly(lysine-alanine), and negative Psi-type signals when condensed with polylysine. Five intercalative dyes and one non-intercalative dye were used in this investigation: ethidium, proflavine, tetrakis(4-N-methylpyridyl)porphine (H_2TMpyP-4), Cu(II)TMpyP-4, Ni(II)TMpyP-4, and Mu(II)TMpyP-4 (non-intercalative).

M-Pos188 THE ORIENTATION, RELAXATION AND REPTATION OF DNA IN ORTHOGONAL FIELD, ALTERNATELY-PULSED GEL ELECTROPHORESIS (OFAGE); A LINEAR DICHROISM STUDY

D.P. Moore, J.A. Schellman and W.A. Baase; Inst. of Mol. Biol., Univ. of Oregon, Eugene, OR 97403

The orientation and migration of DNA induced by alternately pulsed, perpendicular, inhomogeneous electric fields, when it is suspended in agarose gels, has recently become of practical and theoretical importance. This gel technique was discovered and developed for the separation of large double-stranded DNA molecules by Schwartz, et al. [D.C. Schwartz, W. Saffran, J. Welsh, R. Haas, M. Goldenberg, and C.R. Cantor, (1982) CSHSQB 47, 189-195.]. The molecular mechanism responsible for the behavior of DNA in this system is not yet clear. Stellwagen has, however, recently used electric birefringence techniques to measure relaxation times of DNA molecules oriented in 1.0% agarose gels by a single, homogeneous electric field [N.C. Stellwagen, (1985) Book of Absts. from Fourth Conv. Biomol. Stereody., ed. R.H. Sarma, SUNYA, p. 70]. These disorientation times were longer than those of similar DNAs in free solution. The pulse time for optimal resolution with orthogonal fields in gels was found by Carle and Olson to be longer yet [G.F. Carle and M.V. Olson, (1984) Nucleic Acids Research 12, 5647-64].

We have constructed an Olson style cell with UV transmitting windows on a vertical optical axis. This allows the direct visualization of DNA orientation in a horizontal gel. Linear dichroism at 253.7 nm is used to measure not only the steady state orientation of double-stranded DNAs but also the reorientation kinetics of the DNAs during field switching. Results of LD measurements in this system for DNA lengths ranging from T7 DNA (40 kilobases) to G DNA (about 750 kilobases) will be presented.

M-Pos189 STUDY OF DNA CONFORMATION BY VISCOELASTOMETRY

J.Y. Ostashevsky, C.S. Lange and M. Kapiszewska.
SUNY Downstate Medical Center, Brooklyn, New York 11203

Linear and circular DNA molecules of unknown molecular weight can be distinguished by their double strand break (DSB) response as observed by creep-recovery viscoelastometry. DSBs can be introduced by e.g., ionizing radiation. In the framework of the Zimm theory, we have developed a model which predicts that linear molecules should exhibit an exponential reduction in their principal recoil amplitude at constant retardation time as dose increases, while circular molecules should increase their retardation time about three times and their principal recoil dose-dependence should be a bell-shaped curve with a maximum. Experimental data with linear T4 DNA (Lange et al. Rad. Research **100**, 1 (1984)) and circular E. coli DNA (Bresler et al. Biophys. J. **45**, 749 (1984)) coincide very well with our calculated expectations.

In our experiments with mammalian DNA released from irradiated L5178Y-S mouse leukemia cells by 1% sarkcosyl (pH 7), we observed a 3-fold increase in retardation time and a bell-shaped dose-dependence of the principal recoil amplitude. Retardation time data consistent with our model have been obtained by Shafer and co-workers (Rad. Research **85**, 97 (1981); ibid. **90**, 310 (1982)) with irradiated 9L rat brain tumor cells lysed with sodium dodecyl sulfate. Comparing the model predictions for linear vs. circular DNA conformations, the data for both mouse and rat cells suggest a circular rather than a linear DNA conformation. This work is supported by grants from NSF (DMB 8416242), DHHS NCI (CA 39045), and the Mathers Charitable Foundation.

M-Pos190 SOLUTION STRUCTURE OF $[d\text{-}(AT)_5]_2$ VIA COMPLETE RELAXATION MATRIX ANALYSIS OF 2D NOE SPECTRA AND MOLECULAR MECHANICS CALCULATIONS. E.-I. Suzuki, N. Pattabiraman, G. Zon, T.L. James, Dept. Pharmaceutical Chemistry University of California, San Francisco, CA 94143

Knowledge of high-resolution molecular structures in solution has been an elusive goal for decades. The new NMR technique of two-dimensional nuclear Overhauser effect (2D NOE) spectroscopy has the potential for yielding a large number of internuclear distances which can be used in conjunction with other structural constraints to provide a detailed molecular structure via distance geometry and energy refinement calculations. To avoid the assumption of isolated spin pairs, commonly used for analysis of NOEs, and the consequent errors in distance determinations, we have been developing a full relaxation matrix analysis for 2D NOE spectra.

Pure absorption proton 2D NOE spectra at 500 MHz have been obtained for $[d\text{-}(AT)_5]_2$ in deuterium oxide solution using several mixing times. The 100 non-exchangeable proton resonances have been assigned. For smaller molecules it is possible to fit simultaneously all experimental 2D NOE spectra with theoretical 2D NOE yielding all internuclear distances <5 Å in the molecule. Such fitting of the 100 x 100 2D NOE matrices of the decamer is very time-consuming on the computer. Consequently, we have compared the experimental 2D NOE spectra with theoretical spectra calculated from x-ray crystallography-determined molecular coordinates of A, B, alternating B, left-handed B, C, D, and wrinkled D forms of DNA and of energy-minimized structures calculated from the most promising x-ray crystal structures using the molecular mechanics program AMBER.

M-Pos191 MEMBRANE FUSION AND CUBIC PHASE FORMATION VIA INTERMEDIATES IN $L_\alpha \rightarrow H_{II}$ PHASE TRANSITIONS.
D. P. Siegel, Procter & Gamble Co., P. O. Box 39175, Cincinnati, OH 45247

Originally it was thought [e.g., 1] that inverted micellar intermediates in the $L_\alpha \rightarrow H_{II}$ phase transition ("lipidic particles") mediated membrane fusion. However, theory indicates [2,3] and experiments have shown [4,5] that in systems with facile transitions only lipid mixing and vesicle leakage occur when vesicles aggregate above the transition temperature T_H. Here, a kinetic theory of the transition intermediates [2,3] is used to show that membrane fusion should occur in only a subset of systems that adopt the H_{II} phase. Fusion should occur only at $T \gtrsim T_H$ in systems with large H_{II} tube diameters, corresponding to values of the ratio {L_α phase head group area/H_{II} phase head group area} $\lesssim 1.2$. In such systems, the intermediates (IMI; [2,3]) that otherwise rapidly assemble into the H_{II} phase can instead decay into a second type of metastable intermediate (ILA), which causes membrane fusion. ILA are also shown to assemble into what have been called isotropic or cubic (C_{II}) phases [6]. The isotropic or cubic "phases" are thus metastable structures formed during slow and hysteretic $L_\alpha \rightarrow H_{II}$ transitions [7]. Therefore, vesicle fusion via intermediates in L/H_{II} transitions is only likely under circumstances in which multilamellar samples of the lipid form the isotropic or C_{II} phases. This agrees with observations of fusion in isotropic (but not H_{II}) phase regions by Bentz, Ellens, et al. [4,5, and this volume], who suggested a very similar model, and by others [8].

(1) Verkleij, et al., BBA 555:358; (2,3) D. P. Siegel, Biophys. J. (in press); (4,5) Ellens, Bentz & Szoka, Biochemistry (to appear); (6) Boni & Hui; BBA 731: 177; (7) D. P. Siegel, (submitted); (8) Gagne, et al., Biochem. 24: 4400.

M-Pos192 FUSION OF PHOSPHATIDYLETHANOLAMINE-CONTAINING LIPOSOMES AND THE MECHANISM OF THE L_α- H_{II} PHASE TRANSITION.
Harma Ellens, Joe Bentz and Francis C. Szoka. Department of Pharmacy and Pharmaceutical Chemistry, University of California, San Francisco, CA 94143.

N-methylated dioleoylphosphatidylethanolamine (DOPE-Me) is in the lamellar phase (L_α) at and below 20°C, in the hexagonal phase (H_{II}) above 70°C and shows isotropic ^{31}P-NMR signals at intermediate temperatures (Gagné et al., 1985, Biochemistry, in press). We have correlated the initial kinetics of fusion and leakage of DOPE-Me liposomes with the phase behaviour of this lipid. Aggregation, fusion and leakage were induced upon reduction of the pH to 4.5 and were monitored kinetically between 20 and 80°C. At 20°C (L_α phase) there is little aggregation or destabilization. Between 30-60°C (isotropic or intermediate state) the liposomes aggregate and show fusion (mixing of contents) and leakage. After some time delay the aggregated and fused liposomes collapse and rapidly eject their contents into the medium. This collapse is accompanied by a sudden change in the scattered light intensity and an increase in the quantum efficiency of NBD-PE fluorescence. At higher temperatures the initial rates and extents of fusion decrease, whereas leakage is enhanced. At 80°C fusion is abolished. Similar results were obtained with DOPE/DOPC 2:1. Liposome fusion occurs only in the temperature range of the intermediate state (see also Bentz et al., this volume). At higher temperatures, where the H_{II} phase is observed calorimetrically, these liposomes undergo contact-mediated lysis. Nevertheless, we propose that the collapse of the aggregated and fused liposomes in the intermediate state represents the extensive formation of H_{II}-phase domains. If so, the intermediate state reflects a kinetic bottleneck of the L_α- H_{II} phase transition. In fact it would imply that the L_α- H_{II} phase transition occurs at about 40°C, albeit slowly. Supported by NIH grants GM-31506 (J.B.) and GM-29514 (F.C.S.).

M-Pos193 SPONTANEOUS FUSION OF PHOSPHATIDYLCHOLINE SMALL, UNILAMELLAR VESICLES IN THE FLUID PHASE.
BR Lentz, TJ Carpenter, DR Alford; Dept. Biochemistry, Univ. North Carolina, Chapel Hill
Using a differential scanning microcalorimeter capable of performing cooling scans, the phase behavior of small, unilamellar vesicles (SUV) has been examined as a function of time of storage above their order-disorder phase transition. Vesicles composed of dipalmitoylphosphatidylcholine (DPPC) and dimyristoylphosphatidylcholine (DMPC) were examined. Cooling scans on fresh (5 to 7 hours post sonication) samples revealed broad, relatively simple heat capacity peaks (19.9°C for DMPC, 37.8°C for DPPC) free of high temperature spikes or shoulders. Not surprisingly, subsequent heating scans displayed a sharp peak characteristic of fusion products formed below the phase transition. For SUV samples stored for one or more days above their phase transition, a moderately broad high-temperature shoulder (23.8°C for DMPC and 40.2°C for DPPC) appeared in the cooling profile. The enthalpy associated with this peak increased in a first order fashion with time. Hydrolysis products were not detected until 12 to 20 days of storage. Both the rate and extent of shoulder appearance increased with temperature ($k_+ = 0.0009$ hr^{-1}, $k_- = 0.008$ hr^{-1}, $K_{eq} = 0.11$ at 36°C; $k_+ = 0.0027$ hr^{-1}, $k_- = 0.010$ hr^{-1}, $K_{eq} = 0.26$ at 42°C). Freeze fracture electron micrographs confirmed that a larger vesicle population appeared in SUV samples stored above their phase transition in conjunction with development of the high temperature heat capacity shoulder. Finally, to rule out the possibility that esterolytic hydrolysis products might be responsible for inducing membrane fusion, the experiments were repeated with ditetradecylphosphorylcholine (DTPC), an ether lipid analogue of DMPC. Comparable results were obtained ($k_+ = 0.0012$ hr^{-1}, $k_- = 0.0035$ hr^{-1}, $K_{eq} = 0.34$ at 41.5°C). Our results demonstrate that at least a subpopulation of a normal SUV preparation is unstable even above the SUV phase transition. (USPHS grant GM32707)

M-Pos194 LONG-LIVED FUSOGENIC MEMBRANE SITES INDUCED BY ELECTRIC FIELD PULSES ARE NOT FREE TO DIFFUSE LATERALLY IN THE PLANE OF THE MEMBRANE. Arthur E. Sowers, Cell Biology Laboratory, American Red Cross, Bethesda, MD 20814.

High strength (700 V/mm) electric field (EF) pulses (0.8 ms decay halftime) induce a long-lived (minutes) fusogenic state in a suspension of randomly positioned spherical-shaped erythrocyte ghost membranes (J.C.B. 99:1989 (1984); B.J. 47:171a (1985)). The fusogenicity is measured in terms of the fusion yeild in a population of fusogenic membranes when the membranes are brought into close membrane-membrane contact (accomplished by inducing a low strength alternating EF in the suspension) after EF pulse treatment. An EF should induce a transmembrane potential in a spherical shaped membrane which is a maximum at two places - the poles - where the membrane plane is perpendicular to the EF vector. In contrast, the transmembrane potential at the equator should be zero. We have utilized a four electrode chamber in which the angle between the pulse EF vector and the membrane contact-inducing EF vector can be varied between 0-90°. Thus membrane-membrane contact in a population of membranes could be induced at any location on a membrane with respect to the poles. Results show that induced fusogenicity falls off gradually from poles to equator. However, the time dependent decay in fusogenicity shows up as a set of parallel curves. This result indicates that the lateral distribution of fusogenic sites does not change with time and that these sites are essentially immobile. This implies that the nature of fusogenic sites cannot be solely due to pores in the lipid bilayer portions of membranes.

M-Pos195 MICROMANIPULATION OF ELECTRICALLY-FUSED HUMAN ERYTHROCYTES. Donna M. Miles, Robert M. Hochmuth. Department of Biomedical Engineering, Duke University, Durham, North Carolina 27706.

A system has been developed to electrically fuse red cells and to allow manipulation of the fused cells in order to study the elastic and viscous properties of the membrane and the structural properties of the lumen between the two fused cells. The fusion process involves an AC field of 5KHz and 9V/mm rms to induce "chaining" of the cells and several DC pulses of 250V/mm and 50μs duration to produce the membrane defects that initiate membrane fusion. Platinum electrodes are inserted into a $5mm^3$ glass chamber sealed with a 250μm thick parafilm gasket. The cells are suspended in an isotonic solution of 30mM phosphate buffer, 30mM NaCl, 160mM sucrose, and 20gm/l albumin. Application of the DC pulses causes the cells to crenate, slowly sphere and form a cell doublet with an expanding lumen. A slow resealing process causes the fused cells to return to a flaccid state with a stiff, tunnel-like structure joining them. Aspiration of a portion of the fused cells into a 1μm diameter pipette increases the size of the lumen. Pressures as high as 15,000 dyn/cm^2 (which correspond to a membrane tension of approximately 0.5 dyn/cm) are required to transform the cell doublet into a single spherical cell. However, the lumen has a memory, and upon removal of the aspiration pressure, it rapidly recovers its original diameter. Thus, electrofusion of erythrocyte membrane is not a compelete process. Remaining at the junction between fused cells is a sphincter or veil with an apparent elastic stiffness more than an order of magnitude greater than the elastic shear modulus of normal erythrocyte membrane.

We gratefully acknowledge the help and advice of Art Sowers, American Red Cross and Shiro Takashima, University of Pennsylvania. (Supported by NHLBI Grant HL 23728)

M-Pos196 CORRELATION OF CHANNEL INCORPORATION AND CONTENT RELEASE DURING FUSION OF UNILAMELLAR VESICLES WITH A PLANAR BILAYER. Dixon J. Woodbury. Dept. of Physiology and Biophysics, University of California, Irvine, CA 92717.

The conductance increase due to channel transfer from vesicle to bilayer and appearance of vesicular contents on the side of the membrane trans to vesicle addition have been used separately as indicators that vesicle fusion has occurred. This study tests if channel incorporation is correlated with release of vesicular contents. To measure correlation between content release and channel incorporation, large (0.3-3 micrometer) unilamellar vesicles containing the ion channel porin and a self-quenching (100mM) concentration of the fluorescent dye, calcein are made. A fluorescent microscope with a sensitive TV camera is used to detect the adhering vesicles and the fluorescent flash caused by release of the quenched dye from the vesicles. The degree of correlation (at a time resolution of 17 millisec.) appears to depend on the vesicle preparation. Experiments with vesicles made in the presence of porin and dye showed three types of event: 1) conductance increase with no visible release, 2) release with no conductance increase, and 3) correlated release and conductance increase. Porin containing vesicles leak calcein with a half time of several hours, therefore the first type of event is likely due to porin-containing vesicles that have leaked most of their dye. The second type of event may be due to vesicles containing dye but without porin channels. To reduce these possibilities, vesicles formed in the presence of porin channels are soaked in dye. Those with functional porin channels take up dye and are isolated by centrifugation. Thus each dye-filled vesicle must also contain porin channels. Preliminary experiments with these vesicles show only correlated events. This work supported by NIH grant EY 05661.

M-Pos197 OSMOTIC INFLUENCES ON FUSION OF SYNAPTIC VESICLES TO PLANAR BILAYERS. M. S. Perin and R. C. MacDonald, Dept. Neurobiology & Physiology. Northwestern University, Evanston, IL 60201

We have shown previously that by freeze-thawing, synaptic vesicles can entrap high concentrations (200 mM) of the fluorescent dye calcein. These freeze-thawed synaptic vesicles (FTSV's) adhere via divalent ions to solvent-free PS-PE planar bilayers. In buffered 400 mM KCl (isosmotic to 200 mM calcein), bound FTSV's spontaneously release their contents as bright flashes of fluorescence, this release resulting mostly from fusion of FTSV's to the planar bilayer but also from lysis of bound FTSV's. Various solutes (KCl, LiCl, choline chloride, choline nitrate, glucose and glucose plus urea) at iso-, hypo-, and hyper-osmotic concentrations were tested for their effects on this spontaneous release. Release of contents (as flashes) persisted in all solutions that did not contain calcium chloride. Flashes were eliminated in 800 mM glucose 15 mM calcium chloride, but could be elicited by reperfusion with KCl soluion or by addition of urea (membrane permeant solute) to the glucose solution. Flash numbers were reduced in choline salt solutions. Hyposmotic solute solutions increased only leakage (background fluorescence). Leakage of external solute and accompanying water into FTSV's appears to generate an osmotic stress that results in fusion and lysis of adhering FTSV's. A sub-class of small FTSV's (<300 nm) bind to the planar bilayers at low, possibly physiological, calcium concentrations (100 μM). These FTSV's bleach in 1-2 sec. although they continue to release their contents in flashes. Furthermore, they fuse to PS-PE LUV's containing sucrose, resulting in tranfer of fluorescence to, and release of sucrose from LUV's. This suggests that the fusion event is leaky.

M-Pos198 SENDAI VIRUS INTERACTION AT LOW pH WITH ACIDIC PHOSPHOLIPID VESICLES LACKING VIRUS RECEPTOR. Ruby I. MacDonald, Dept. Biochem., Mol. Biol. and Cell Biol., Northwestern University, Evanston, IL 60201.

On exposure to Sendai virus, vesicles composed almost entirely of acidic phospholipids (e.g., phosphatidylserine, phosphatidylinositol or cardiolipin) but without sialic acid-bearing receptors release calcein trapped at self-quenched concentrations and/or undergo lipid mixing with Sendai virus, measured as dequenching of NBD-PE fluorescence by Rhodamine-PE in the target membrane. In contrast, vesicles with a lower acidic phospholipid content have been shown to require a sialic acid-bearing receptor for their fusion with and/or destabilization by Sendai virus (Oku et al., 1982; Kundrot et al., 1983; Tsao and Huang, 1985). Also unlike receptor bearing target vesicles, the responsiveness to Sendai virus of the liposomes containing predominantly acidic phospholipids increases markedly as the pH is decreased from neutral to 4-5. The occurrence of no lipid mixing following the exposure of Sendai virus alone to low pH, prior to raising of the pH to near 7 and the subsequent addition of acidic phospholipid vesicles, conforms with the known pH independence of the biological activity of Sendai virus and may indicate that low pH affects the ability of the acidic phospholipids to respond to the virus, rather than the fusogenic activity of the virus. Nor does lipid mixing occur between NBD-PE + Rhodamine-PE labeled, acidic phospholipid vesicles and unlabeled vesicles composed either of acidic or neutral phospholipids in the absence of Sendai virus. A low pH dependent association of fluorescent, acidic phospholipid vesicles with Sendai virus is also seen on sucrose gradient centrifugation of the virus-phospholipid mixtures.

Supported by NIH Grant AI20421.

M-Pos199 A CLUE TO THE LOCATION OF THE CA-BINDING SITE(S) RESPONSIBLE FOR EXOCYTOSIS AND PHOSPHATIDYLINOSITOL 4,5-BISPHOSPHATE (PIP_2) HYDROLYSIS IN AN ISOLATED PLASMA MEMBRANE PREPARATION FROM SEA URCHIN EGGS. Stuart McLaughlin and Michael Whitaker. Dept. Physiology & Biophysics, SUNY Stony Brook, NY 11794 & Dept. Physiology, University College London, Gower Street, London WC1E 6BT.

High concentrations of Mg increase the free [Ca] required for half maximal stimulation of (i) exocytosis of cortical granules and (ii) PIP_2 hydrolysis (Whitaker and Aitchison, 1985). In the presence of 1, 5 or 50 mM Mg, a free [Ca] of 0.5, 2 or 20 μM produces half maximal exocytosis (Whitaker and Baker, 1983). One simple interpretation of these results is that Mg decreases the magnitude of the negative electrostatic potential, ψ , and thus the [Ca], adjacent to the Ca-binding site(s) responsible for exocytosis and PIP_2 hydrolysis. We examined this possibility experimentally by measuring the effect of Mg on the zeta potential of bilayer membranes containing 50% phosphatidylinositol (PI), which should mimic the composition of the cytoplasmic surface of the egg membrane (Kinsey et al., 1980). Mg reduces the surface potential of these membranes as predicted by the Gouy-Chapman-Stern theory: the intrinsic Mg-PI association constant is 10 M^{-1}. Thus we can account quantitatively for the biological effects of Mg if we postulate the Ca-binding site(s) are located at the membrane-solution interface. Consider one corollary of our postulate: any cation that adsorbs hydrophobically to a bilayer membrane should reduce the ψ of the plasma membrane and, therefore, the local [Ca] and the ability of Ca to induce exocytosis. For example, 6 μM trifluoperazine (TFP) significantly reduces both the ψ of bilayer membranes containing 50% PI and the exocytosis of cortical granules produced by 2 μM Ca; 100 μM TFP reverses the charge on the bilayer membranes and completely inhibits the exocytosis produced by 2 μM Ca. NIH grant GM 24971.

M-Pos200 SYNTHESIS AND CHARACTERIZATION OF AN AMPHIPHILIC PEPTIDE THAT UNDERGOES A pH TRIGGERED RANDOM COIL - α-HELICAL TRANSITION. Nanda Subbarao,* Laszlo Nadasdi,** and Francis C. Szoka, Jr.*. *School of Pharmacy, Depts. of Pharmacy and Pharmaceutical Chemistry and **Brain Tumor Research Center, Univ. of California, San Francisco.

We have synthesized a 30 amino acid amphipathic peptide (P 100) that undergoes a random coil to α-helical conformational change as the pH is lowered from 7.6 to 4.2. P-100 has the following sequence: H-Trp-Glu-Ala-Ala-Leu-Ala-Glu-Ala-Leu-Ala-Glu-Ala-Leu-Ala-Glu-His-Leu-Ala-Glu-Ala-Leu-Ala-Glu-Ala-Leu-Glu-Ala-Leu-Ala-Ala-OH. It was synthesized by the Merrifield solid phase method using symmetrical anhydrides. Following cleavage from the resin the crude product was chromatographed over Sephadex G10 and then on a DEAE cellulose column. The purified material gave a single peak on reverse phase HPLC which had the expected amino acid composition. Circular dichroism measurement on the peptide as a function of pH indicated that the α-helical content increased from about 25% in pH 7.6 to 100% in pH 4.2. Model building studies show that in the α-helical conformation, the glutamic acid residues are mainly on one side of the helix, leaving one face completely hydrophobic. Thus, it is reminiscent of Apo-AI. When added to egg phosphatidylcholine liposomes containing ANTS-DPX, it caused them to leak both at neutral and low pH at all the peptide to lipid molar ratios studied. When added to negatively charged liposomes (egg phosphatidylglycerol:egg phosphatidylcholine 1:4) complete leakage of liposomal contents occurred at pH 4.5 in less than 2 min, whereas virtually no leakage occurred at pH 7.6. The role of amino acid substitutions in the sequence on bilayer destabilization is being studied. Supported by NIH grant GM-29514 (F.C.S.).

M-Pos201

WITHDRAWN

M-Pos202 SYNEXIN-LIKE PROTEINS FROM THE CYTOSOL OF HUMAN NEUTROPHILS MEDIATE AGGREGATION AND APPARENT FUSION OF SPECIFIC GRANULES AND LIPOSOMES. Paul Meers, Joel Ernst, Keelung Hong, Nejat Düzgünes, Ira M. Goldstein and Demetrios Papahadjopoulos; Cancer Research Institute and Rosalind Russell Arthritis Institute, University of California, San Francisco.

Synexin is a protein thought to be involved in the aggregation and fusion of intracellular membranes. We have isolated synexin-like proteins from the 25% NH_4SO_4 precipitate of the cytosol of human neutrophils. Purification was achieved by Ca^{2+}-dependent binding to a liposome affinity column. Four major proteins were obtained with molecular weights of about 67, 48, 37 and 29 kilodaltons. Rabbit antibodies raised to bovine liver synexin reacted with the 48 kilodalton neutrophil protein. The isoelectric point of this protein was also the same as that of synexin. Aggregation of granules, as measured by the turbidity change at 400 nm, did not occur in the absence of added protein at Ca^{2+} concentrations up to 10 mM. In the presence of bovine liver synexin or the neutrophil proteins, aggregation of granules could be observed at 0.5 mM Ca^{2+}. Fusion of liposomes was monitored by the Tb^{3+}/dipicolinic acid fluorescence assay for the intermixing of aqueous contents of the liposomes. It was found that neutrophil proteins, like bovine liver synexin, increased the overall rate of Ca^{2+}-induced fusion for phosphatidate(PA)/phosphatidylehtanolamine(PE) (1/3) and phosphatidylserine(PS)/PE (1/3) liposomes but decreased the rate of spermine-induced fusion of PA/PE liposomes. The apparent fusion of liposomes with granules was observed using PA/PE (1/3) liposomes with the fluorescence energy transfer probes N-7-nitro-2,1,3-benzoxadiazol-4-yl PE (NBD-PE) and rhodamine-PE incorporated into the liposome membranes. Dilution of the probes into the granule membranes by fusion leads to a decrease of the efficiency of energy transfer and hence an increase of the NBD fluorescence. This occured when 1 mM Ca^{2+} was added and when both synexin-like proteins (about 5-10 μg/ml) and free arachidonic acid (about 10 μM) were present at a total lipid concentration of 5 μM. Lack of one of the components precluded the observed probe dilution. (supported by NIH grant # GM 28117 and American Cancer Society # PF 2398)

M-Pos203 THE EFFECTS OF DOLICHOL ON THE PERMEABILITY OF PE/PC LIPOSOMES. J. A. Monti(1,3), S.T. Christian(1,3), and J.S. Schutzbach(2). Depts. of Psychiatry(1), Microbiology(2), and the Neurosciences Program(3), U. of Alabama at Birmingham, Birmingham, AL 35294.

Fluorescence measurements indicate that dolichols affect the permeability properties of sonically dispersed vesicles composed of phosphatidylethanolamine (PE) and phosphatidylcholine (PC). Membrane permeability was determined by fluorescence quenching of the tetra-anionic dye calcein by Co^{+2}. Vesicles were prepared from PE/PC and PE/PC/dolichol in the presence of either 40 or 0.5 mM Calcein. Following centrifugation and column chromatography on Sephadex G-50, these vesicles were impermeant to the tetra-anionic fluorophore. Ca^{+2} and Mg^{+2} had no effect on the permeability of calcein. However, addition of Co^{+2} to PE/PC/dolichol vesicles containing entrapped calcein resulted in the quenching of the calcein fluorescence, suggesting increased permeability to Co^{+2}. The rate of quenching was dependent on temperature, dolichol concentration, and PE concentration. A sharp transition in the rate of permeability of PE/PC/dolichol vesicles to Co^{+2} was noted between 25 and 35°C. Under these conditions PE/PC vesicles were no more permeable to Co^{+2} than control vesicles composed of only PC, nor did dolichol affect the permeability of PC vesicles to Co^{+2}. A similar temperature-dependent transition was noted in PE/PC/dolicol vesicles when turbidity was measured, suggesting that dolichol might enhance vesicle-vesicle aggregation and/or fusion. Column chromatography and measurement of trapped volume indicated that the average size of PE/PC/dolichol vesicles increased upon incubation at 35°C, which would also be consistent with vesicle-vesicle fusion. Resonance energy transfer measurements may yield more information on the mechanism(s) involved in the increase in vesicle size. Since all of these effects of dolichol were observed only in the presence of PE, it is possible that the mechanism by which the polyisoprenoid affects membrane permeability involves the formation of hexagonal II phases in these mixed phospholipid bilayers.

M-Pos204 EFFECTS OF PHOSPHATIDYLINOSITOL METABOLITES ON MEMBRANE FUSION OF LIPOSOMES. Paul Meers, Keelung Hong, Joe Bentz and Demetrios Papahadjopoulos, Cancer Research Institute and Department of Pharmacy, University of California, San Francisco.

The turnover of phosphatidylinositol (PI) has been observed in many cell types upon stimulation of secretion by exocytosis. One possible function of these metabolites could be to promote the membrane fusion accompanying exocytosis. An increase in the rate of Ca^{2+}-induced membrane fusion was demonstrated when PI was replaced by PA by previous studies in this laboratory. We now have investigated the effects of phosphatidylinositol 4,5 diphosphate (PIP_2), free fatty acids and diacylglycerol on the rate of Ca^{2+}-induced fusion of large unilamellar liposomes using fluorescent assays for the mixing of liposome contents upon fusion (Tb^{3+} with dipicolinic acid or 1-aminonaphthalene 6,8-trisulfonate with p-xylyl-bis-pyridinium bromide). Replacement of PI by PIP_2 had a marked effect on the rate of Ca^{2+}-induced membrane fusion especially in the presence of spermine, a ubiquitious cytosolic polycation. At 200 μM spermine the rate of fusion induced by 1 mM Ca^{2+} increased about 10-fold when liposomes containing 10 mole % PI or PA were replaced by liposomes containing 10 mole % PIP_2 instead. The effect of spermine on fusion of PIP_2-containing liposomes was observed even at only 20 μM spermine. These data indicate a strong specific interaction of spermine with PIP_2. Free fatty acids had large effects on overall rates of Ca^{2+}-induced fusion at levels of only 1-20 mole % of the lipid in the membrane when fusion rate limiting conditions are in effect. Under aggregation rate limiting conditions promoters of liposome aggregation acted synergistically with the fatty acids. The specificity for various fatty acids and their analogs was not very high. Molecules which would be expected to be most fluidizing or occupy the most space in the bilayer, such as cis-unsaturated fatty acids, had the greatest effects. Dioleolylglycerol incorporated into PS liposomes at only 2 mole % moderately increased the rate of Ca^{2+}-induced fusion as compared to PS alone. This result suggests that small amounts of diacylglycerols generated physiologically can have an effect on the propensity of membranes to fuse in the absence of proteins. (supported by NIH grants # GM 28117 and GM 31506 and American Cancer Society # PF 2398)

M-Pos205 pH-SENSITIVE IMMUNOLIPOSOME-MEDIATED DELIVERY OF DIPHTHERIA TOXIN A TO THE CYTOPLASM OF TOXIN-RESISTANT CELLS. David Collins and Leaf Huang, Department of Biochemistry, University of Tennessee, Knoxville, TN 37996-0840.

Liposomes composed of phosphatidylethanolamine and oleic acid become unstable and fusion-active at the weakly acidic pH of 5-6.5. These pH-sensitive liposomes can be coated with fatty acid-derivatized antibody to enhance the cytoplasmic delivery of encapsulated molecules to antigen-expressing cells (Connor and Huang, J. Cell Biol. 101, 582). Cytoplasmic delivery is thought to be achieved through receptor-mediated endocytosis of the immunoliposomes. The liposomes then encounter the acidic pH of the endosome and are thought to fuse with the endosome membrane from within, thus releasing the encapsulated contents into the cytoplasm. To test this hypothesis we have used the A fragment of diphtheria toxin (DTA) as a marker for cytoplasmic delivery. It has been shown that diphtheria toxin (DT) resistant mouse L-929 cells bind and internalize DT normally, and possess a DT-sensitive elongation factor 2 (intracellular target of DTA). Thus, DT resistance in L-929 cells seems to result from a block in the translocation of DTA from the endosomes into the cytoplasm. In the present work we have prepared pH-sensitive immunoliposomes to contain DTA and measured the cytoplasmic delivery of DTA by the inhibition of protein synthesis. The most effective delivery of DTA was via the pH-sensitive immunoliposomes; non-targeted pH-sensitive liposomes and pH-insensitive liposomes were not effective. Free DTA and DT were non-toxic to the cells as were empty liposomes. These results indicate that pH-sensitive immunoliposomes are able to release DTA from an acidic cellular compartment, probably by fusion with the endosome membrane, thus bypassing the block which prevents the translocation of DTA into the cytoplasm. Supported by NIH grant CA 24553.

M-Pos206 RATE AND EXTENT OF POLY(ETHYLENE GLYCOL) INDUCED LARGE VESICLE FUSION. Roberta A. Parente and Barry R. Lentz, Biochemistry Dept., University of North Carolina, Chapel Hill, NC 27514.

Poly(ethylene glycol) (PEG) of average molecular weight 8000, was used to mediate the fusion of large, unilamellar vesicles composed of dipalmitoyl phosphatidylcholine. For the first time, PEG-induced fusion was demonstrated by use of fluorescence assays of lipid mixing and aqueous contents mixing. Assays were chosen such that PEG did not interfere with the properties of the fluorophores used. The extent of lipid mixing, monitored by the fluorescence lifetime of DPHpPC showed that large, unilamellar vesicles underwent a single fusion cycle regardless of the PEG concentration of the incubation mixture. The ANTS/DPX assay for contents mixing indicated that both addition and dilution of PEG were accompanied by extensive contents leakage. However leakage was not coincident with fusion. The initial rate of fusion was a continuous function of PEG concentration from 0 to 35 wt %, with substantially enhanced fusion efficiency occurring above 26 wt %. Results showed that fusion preceded dilution of vesicle-PEG mixtures. Both the rate and extent of fusion were unaffected by impurities in the PEG. In fact, another dehydrating polymer, dextran (average molecular weight 9000), was capable of promoting fusion, though at a much slower rate than PEG. Also, osmotic swelling of vesicles after contact with PEG had no influence on the extent or rate of fusion. Thus, neither bilayer destabilizing impurities, nor osmotic stress, nor any unique properties of PEG appear to be crucial in the fusion process. Rather, our results tentatively suggest that even partial bilayer dehydration, presumably accompanying close interbilayer contact may be sufficient to increase the probability of a fusion event. *Supported by NIH grant GM32707.*